

N 70 29 85 9

NASA CR 110365

DESIGN, FABRICATION, AND TEST OF A
BREADBOARD HYBRID
PRESSURIZATION SYSTEM

FINAL REPORT

NOR 69-129

May 1970

BY

WALTER F. KELLER

PREPARED FOR

NATIONAL AERONAUTICS AND SPACE ADMINISTRATION

CONTRACT NAS 7-714

CASE FILE
COPY

NORTHROP CORPORATION

DESIGN, FABRICATION, AND TEST OF A
BREADBOARD HYBRID
PRESSURIZATION SYSTEM

FINAL REPORT

NOR 69-129

May 1970

BY

WALTER F. KELLER

PREPARED FOR

NATIONAL AERONAUTICS AND SPACE ADMINISTRATION

CONTRACT NAS 7-714

NORTHROP CORPORATION

TABLE OF CONTENTS

SECTION		PAGE
	FOREWORD	iii
	ABSTRACT	iv
I	INTRODUCTION	1
II	REVIEW OF AVAILABLE INFORMATION	3
III	SELECTION OF PROPELLANT COMBINATION	6
	Analytical Studies	7
	Acceptable Hot Gas Constituents	7
	Methodology	8
	Initial Fuel Selection	9
	Results of First Elimination	9
	Improvement Study	10
	Experimental Studies	14
	Hypergolicity Tests	14
	Sterilizability Test	15
	Oxidizer/Fuel Selection and Preparation	16
IV	COMBUSTION STUDIES	19
	Combustion Chamber Design	19
	Test Setup	21
	Instrumentation	23
	Test Program and Results	24
	Initial Tests	24
	Combustion Tests	26
V	BREADBOARD SYSTEM DESIGN AND TESTING	33
	System Design	33
	Test Program and Results	35
	Group A Test Results	36
	Groups B and C Test Results	39

TABLE OF CONTENTS (Continued)

SECTION		PAGE
VI	ANALYSIS	46
	Data Reduction Analysis	46
	Nomenclature	46
	Procedure	46
	Correlation of Results	51
	Optimum Gas Temperatures Study	53
	Theoretical Background	53
	Results	54
VII	SUMMARY AND CONCLUSIONS	59
VIII	RECOMMENDATIONS FOR FURTHER STUDY	61
IX	COMPARISONS	64
APPENDIX		
I	BIBLIOGRAPHY	I-1
II	OPTIMUM GAS TEMPERATURE STUDY	II-1
III	DISTRIBUTION LIST	III-1

FOREWORD

Results of an approximately 6000 manhour, one year contract to design, build, and test a breadboard hybrid pressurization system are presented herein.

Sponsorship of this work was by the Jet Propulsion Laboratory for the NASA Office of Advanced Research and Technology. Technical Manager was Wolfgang Simon, JPL; Program Manager was Frank E. Compitello, NASA. Northrop personnel were: Walter F. Keller, Principal Investigator; Joseph A. Bogdanovic, Analyst; Victor B. Manire, Chemist; and John H. Rudy, Test Engineer.

ABSTRACT

Results are reported on a NASA-sponsored, JPL-managed program to design, build, and test a breadboard hybrid pressurization system. The system makes use of liquid chlorine trifluoride and solid sodium azide to generate hot nitrogen suitable for direct contact pressurization of both fuels and oxidizers of typical earth and space storable propellants.

The program included a survey, analysis, and test of candidate oxidizer/fuel combinations, development of components, combustion studies, analysis of the selected combination and study of optimum hot gas temperatures, and design, fabrication and test of the breadboard system.

Sodium azide was selected as the fuel on the basis of its high yield of nitrogen and separability of impurities, physical properties, and availability. Other potential compounds were rejected due to reactivity of combustion products, lack of hypergolicity, or unavailability. Testing was conducted on both shell grain and pellet bed configurations of 1-1/4 to 1-1/2 inch diameter and 1 to 8 inches in length. The final breadboard configuration was a 1-1/2 inch OD by 5/8 inch ID by 7 inch long shell grain.

Contractually specified gas weight flows and pressures, expelling both water and liquid nitrogen, were demonstrated. All of the major impurity, liquid sodium, was trapped in a Demister; no CTF was detected in the sampled gas. Burning durations of 60 seconds, with only 10% fuel residuals, were also demonstrated along with stop-restart and pressure controlled operation.

CTF/sodium azide represents a suitable combination for a hybrid pressurization system which will generate hot non-reactive nitrogen gas in a controllable manner. The concept is ideal for direct contact pressurization of propellant tanks on restart and/or throttling rocket applications.

SECTION I

INTRODUCTION

The need exists to minimize weight and volume of spacecraft and upper booster stage propulsion systems while maintaining high reliability. The pressurization system is a worth while target, since it represents a significant fraction of total weight in pressure fed propulsion systems, and a method of generating hot, inert gas represents a worthwhile approach. In comparison with nitrogen stored at high pressure and ambient temperature, a suitable hot gas pressurization system has the potential of reducing weight and volume to 25 to 10 percent, respectively. Providing inert gas permits direct contact expulsion of highly reactive propellant or, when positive expulsion is required by the mission, protects against catastrophic total loss due to minor leakage and subsequent reaction between propellant and pressurizing gas.

Prior to award of this contract, Northrop had studied and demonstrated the feasibility of applying the hybrid principle, shown in schematic form in Figure 1, to the generation of hot nitrogen gas.

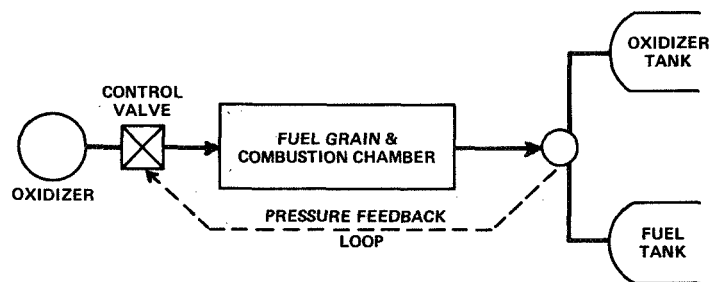
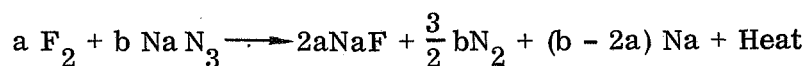


FIGURE 1. SCHEMATIC OF THE HYBRID PRESSURIZATION SYSTEM CONCEPT

This work was based on the use of fluorine gas as the oxidizer and pressed pellets of sodium azide as the fuel. Fluorine gas ignites hypergolically with sodium azide (formula, NaN_3), according to the following equation:



An oxidizer/fuel ratio of 0.02 produces approximately 63.5 percent nitrogen, 32.3 percent sodium, and 4.2 percent sodium fluoride. It was demonstrated that this theoretical yield of nitrogen could be approached, with suitable temperatures (600-2000R) and low oxidizer fuel ratios. The sodium is produced in liquid form, readily trapped by a Demister*. Another feature of the hybrid principle is that the reaction ceases upon termination of oxidizer flow. Thus the pressure feedback loop shown in the schematic controls propellant tank pressure and permits operation in a demand mode.

A contract was awarded by NASA/JPL to design, build, and test a breadboard system based on the hybrid concept and work begun in July 1968. The goal was to demonstrate delivery of an equivalent gas flow of 6.6 ± 1.6 SCFM of hot nitrogen at 200 ± 20 PSIA, expelling water and liquid nitrogen for 30 seconds. Specific tasks, to be discussed in the text which follows, were:

- I Review Available Information
- II Select Propellant Combination
- III Design Breadboard System
- IV Fabricate and Test Breadboard System.

*A patented device, consisting essentially of fine mesh screening, which collects and stores entrained liquid droplets from a gas stream.

SECTION II

REVIEW OF AVAILABLE INFORMATION

A review was conducted of available information in the areas of: hybrid systems (pressurization systems specifically, and hybrid rockets, generally), solid propellant fuels, pressurization and expulsion, properties of earth and space storable propulsion systems, and of injector design*. The following actions were taken in conducting this review:

1. A search was conducted in the Northrop library, including Chemical Propulsion Information Agency Abstracts, U. S. Government Research and Development Reports, and National Aeronautics and Space Administration Scientific and Technical Aerospace Reports.
2. A search was requested and conducted by the Chemical Propulsion Information Agency. **
3. Searches of various areas were requested and received from Defense Documentation Center.
4. Personal contacts, through letter and telephone, were made with fuels researchers at various government agencies and private industrial concerns.

The reports obtained have been listed and annotated in a bibliography, contained in Appendix I. No references other than those generated by Northrop were found pertaining to hybrid pressurization systems.

The replies to Northrop's inquiries regarding potential fuels by the following individuals, representing the organizations noted, are most appreciated:

Capt. R. Bargmeyer, Air Force Rocket Propulsion Laboratory
V. P. Wystrach, R. B. Wainright, American Cyanamid Co.
R. G. Rhoades, Army Missile Command
A. T. Maasberg, T. E. Niles, Dow Chemical Co.

* Injector design was included because the anticipated low oxidizer flow rates are not state of the art.

** With special thanks to Mr. T. L. Reedy for his prompt, thorough action.

F. Marsh, E.I. DuPont DeNemours & Co.
M. Visnov, Frankford Arsenal
J.W. Morton, Allegany Ballistics Lab., Hercules Inc.
E.C. Draley, NASA Langley Research Center
R.A. Mitsch, Minnesota Mining and Manufacturing Co.
G.L. McKenzie, Naval Propellant Plant
D.H. Couch, Naval Weapons Center
I. Forsten, Picatinny Arsenal
A.J.L. Toombs, Shell Development Co.

Several of those responding reported that they had nothing directly to contribute or provided references to other work; the following significant information was obtained:

V.P. Wystrach

Suggested triaminoguanidinium nitrate, and volunteered further data if required.

R.G. Rhoades

Described status of his work with CTF/sodium azide. He has successfully operated a boiler plate gas generator, designed on the basis of the Northrop concept, with essentially qualitative results measured; further tests are planned.

A.T. Maasberg

Discussed the availability (or lack thereof) of high nitrogen compounds formerly produced by Dow (TAG, TAZ, THA, and DB-27).

F. Marsh

Discussed two compounds he has worked with: cyanogen azide and $\text{NH}_4 \text{CN}_7$.

M. Visnov

Discussed type of work done at Frankford Arsenal, provided many contacts at other agencies and recommended consideration of the tetrazoles.

J.W. Morton

Suggested nitramines and nitramine azides. Provided references and offered his cooperation.

G.L. McKenzie

Described work in progress at the Naval Propellant Plant, including azides and tetrazoles. Provided references and extended an invitation to visit his facility for further discussions.

D.H. Couch

Also suggested the tetrazoles as a source of nitrogen.

Further results of the review have been fed into the study topics and are discussed under the appropriate headings.

SECTION III

SELECTION OF PROPELLANT COMBINATION

The approach to selection of a propellant combination was to seek compounds which improved upon the characteristics of fluorine/sodium azide, the combination previously used at Northrop with success. It was decided that storable liquid oxidizers such as nitrogen tetroxide or chlorine trifluoride would be preferable to gaseous fluorine. Thus, this study was essentially concerned with finding a fuel which would combine satisfactorily with one of these oxidizers and, if possible, exceed the gas generating capability of sodium azide. If none were found, then sodium azide would be used for the breadboard system.

Analytical Studies

Candidate propellants were studied with the aid of a thermochemical computer program which calculates theoretical equilibrium flame temperature and combustion products.

ACCEPTABLE HOT GAS CONSTITUENTS

The computer program was also utilized to first determine acceptable amounts and constituents of typical, chemically generated hot gas for direct contact with oxidizers. This was done by studying the reaction of small quantities of typical constituents (diluted with nitrogen) with two oxidizers, nitrogen tetroxide (NTO) and chlorine trifluoride (CTF). The validity of this technique has been verified experimentally by previous studies at Northrop.*

Since it is unlikely that the gas generated will be oxidizer rich, and even if it were, the reaction is not likely to be as severe, reactivity with fuels was not investigated.**

Figure 2 plots theoretical combustion temperature versus percent of combustion product for the reaction of individual combustion products with nitrogen tetroxide. Similar plots are available from the previous reference for chlorine trifluoride. Assuming a maximum permissible theoretical reaction temperature of 2000F (actual values should be lower) allowable percentages by weight of products are tabulated below:

CONSTITUENT	ALLOWABLE PERCENT	
	w/CTF	w/NTO
Hydrogen	0	1.5
Carbon	10	4.5
Carbon Monoxide	20	14.0
Methane	0	3.0
Water	18	14.0

* Northrop Report NOR-66-257, "Preliminary Investigation of Liquid Propellant Reactivity," August 1966.

** The assumption was made, however, that no amount of hot solid particles would be acceptable with diborane.

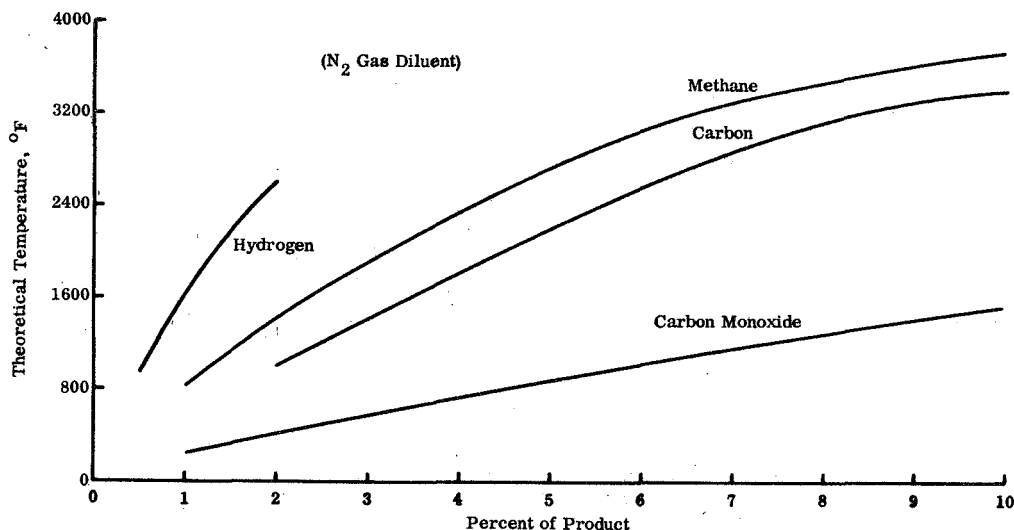


FIGURE 2. REACTION OF INDIVIDUAL COMBUSTION PRODUCTS WITH NITROGEN TETROXIDE

Obviously these amounts are not permissible in combination, without exceeding the allowable temperature, but they do provide a rough standard for screening purposes. The amount of carbon allowable with CTF exceeded 10 percent, based on temperature considerations but was arbitrarily limited due to potential propellant contamination problems. The allowable amount of water (steam) also exceeded the value noted with NTO but was limited due to possible condensation problems (reaction temperatures with NTO were very low).

METHODOLOGY

Methodology of the analytical study of fuels is diagrammed in Figure 3. Fuels for initial study were selected on the basis of recommendations from the respondents to Northrop's fuels inquiries, including Dr. Clyde Alley of Northrop Carolina, and from review of the published literature; many were obtained from Reference 35. Reactions at an oxidizer/fuel ratio of 0.02 were run on the computer and the resulting information used to eliminate fuels on the basis of extreme temperature and undesirable products. The remaining fuels were studied with various additives and oxidizer changes to seek improvements in temperature and products. Comparisons were next made with the sodium azide system. A final screening of remaining compounds for availability and favorable chemical properties was made in preparation for a review with the Technical Manager.

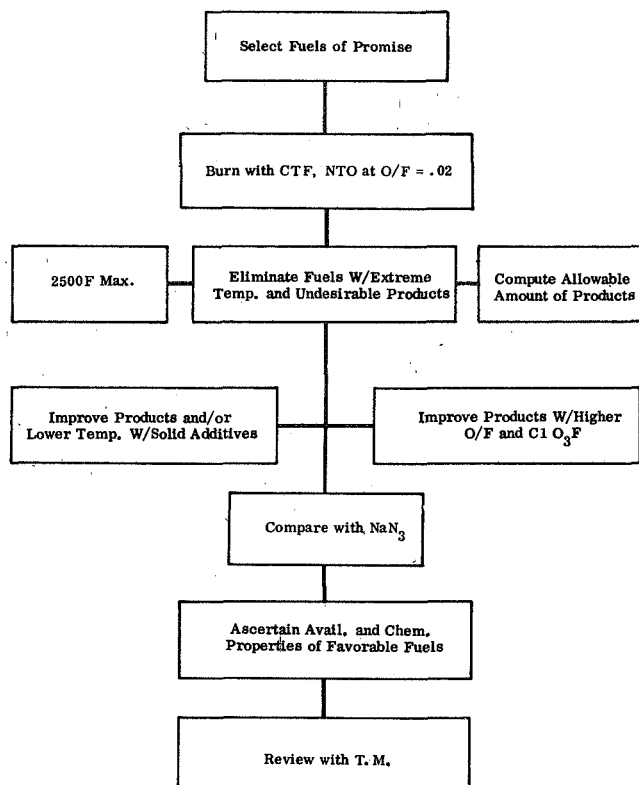


FIGURE 3. METHODOLOGY OF ANALYTICAL FUEL STUDY

Initial Fuel Selection

The initial fuels selected for study are shown in Table 1. Properties of other azides were reviewed but none were found to be significantly more suitable. They were selected primarily on the basis of their potential yield of inert gas, without regard for hypergolicity, self-extinguishment, stability, or availability. It was decided to investigate these characteristics after the list had been reduced for other reasons.

Results of First Elimination

Eliminating those compounds whose temperature and amounts of reactive constituents appeared beyond reduction, reduced the list considerably, as shown by Table 2. Temperatures in excess of 2500F were deemed excessive (from the viewpoint of tank material limitations).^{*} An immediate conclusion which may be reached

^{*} Hydrazine azide, with a reaction temperature of 2816F, was also carried on in the study because of the absence of solid combustion products and potential of temperature reduction.

is that very low oxidizer/fuel ratios are necessary to prevent excessive temperature. It was also found that the amount of oxidizer used is so slight that the kind of oxidizer used will not significantly influence the products formed.

TABLE 1. INITIAL FUEL SELECTION

COMPOUND	FORMULA	MOL. WEIGHT	ΔH_f Kcal/100g	PERCENT		
				C	H	N
Tetrazole	CH_2N_4	70.06	+ 80.87	17.144	2.878	80.0
5-Hydroxytetrazole	$\text{CH}_2\text{N}_4\text{O}$	86.06	+ 1.76	13.957	2.343	65.0
5-Nitraminetetrazole	$\text{CH}_2\text{N}_6\text{O}_2$	130.08	+ 46.3	9.233	1.55	64.7
5-Aminotetrazole	CH_3N_5	85.075	+ 58.39	14.117	3.555	82.2
Guanylazide Nitrate	$\text{CH}_4\text{N}_6\text{O}_3$	148.09	+ 2.56	8.11	2.723	56.8
5-Cyanotetrazole	C_2HN_5	95.07	+ 101.07	25.268	1.060	73.5
Cyanoguanyl Azide	$\text{C}_2\text{H}_2\text{N}_6$	110.09	+ 88.09	21.820	1.831	76.3
Dicyandiamide	$\text{C}_2\text{H}_4\text{N}_4$	84.09	+ 8.49	28.567	4.795	66.6
5,5'-Hydrazotetrazole	$\text{C}_2\text{H}_4\text{N}_{10}$	168.13	+ 80.38	14.288	2.398	83.2
2-Methyl-5-Aminotetrazole	$\text{C}_2\text{H}_5\text{N}_5$	99.10	+ 48.85	24.240	5.086	71.0
5-Guanylaminetetrazole	$\text{C}_2\text{H}_5\text{N}_7$	127.12	+ 31.91	18.897	3.965	77.1
DAZAL	$\text{C}_2\text{H}_8\text{N}_8$	144.15	+ 74.1	16.665	5.594	78.0
5-Tricyanotriazine	C_6N_6	156.11	+ 100.69	46.164	0	53.836
Hydrazine Azide	N_5H_5	75.08	+ 73.4	0	6.713	93.287
BTU	$\text{C}_3\text{H}_2\text{F}_{12}\text{N}_8\text{O}$	394.11	- 20.3	9.143	.512	28.5
1-(5-Tetrazolyl)-4-Guanyltetrazene Hydrate	$\text{C}_2\text{H}_8\text{N}_{10}\text{O}$	188.17	+ 24.03	12.8	4.25	74.7
Viton	$\text{C}_{11}\text{H}_8\text{F}_{14}$	406.1	- 179.0	32.5	1.97	0
Teflon	$(\text{CF}_2)_n$	50.01	- 193	24.0	0	0

TABLE 2. FUELS WITH COMBUSTION TEMPERATURES BELOW 2500°F
(burned with CTF, O/F = 0.02)

FUEL	COMB TEMP°F	MAJOR PRODUCTS, PERCENT							
		N ₂	H ₂	H ₂ O	C	CO	CO ₂	CH ₄	Other
5-Hydroxytetrazole/CTF	2006	63.8	2.1	0.3	0.1	30.9	0.4	0.3	
Dicyandiamide/CTF	1199	65.3	1.8	0	19.8	0	0	11.0	
2-Methyl-5-Aminotetrazole/CTF	2144	69.3	4.7	0	23	0	0	0.8	
5-Guanylaminetetrazole/CTF	1730	75.6	3.3	0	17.1	0	0	1.8	
BTU/CTF	2145	27.9	0	0	0	0.1	5.4	0	+ free F ₂ + HF
Tetrazine Hydrate/CTF	1954	73.0	3.9	0.3	5.8	14.0	0.1	0.9	
Viton/NTD	1851	0	0	0	26.5	2.1	0	0	+31.5% CF ₄
									+38.6% HF
Teflon/CTF	2086	0	0	0	10.8	0	0	0	+87% CF ₄
									+1% CClF ₃

Improvement Study

The family of compounds, lithium nitrate, lithium carbonate, and lithium perchlorate, was chosen as typical additives potentially useful in reducing fuel-rich combustion products and/or reaction temperature; others such as oxalates and oximides were eliminated due to excessive hydrogen and carbon. Mixtures of perchlorylfluoride (PCF) and chlorine trifluoride were also considered in higher O/F ratios for the same purpose.

The results of studies with lithium nitrate and PCF are shown in Table 3. Much of this study was conducted with dicyandiamide, selected somewhat arbitrarily. It may be seen that addition of lithium nitrate reduces the quantities of hydrogen, methane, and carbon in the combustion products at the cost of slightly increased temperature, increased carbon monoxide and a significant quantity of lithium hydroxide. Increasing the amount of oxidizer raises the temperature, decreases the carbon and methane content while increasing carbon monoxide and hydrogen (slightly). Changing oxidizers had negligible influence. Similar trends occur with other fuels on the list. Addition of 25 percent lithium nitrate to hydrazine azide reduced hydrogen content from 6.5 percent to 3 percent but increased temperature greater than the already excessive value of 2816F.

The results of studies with lithium carbonate are shown in Table 4. The cooling effect on hydrazine azide may be noted, percent hydrogen is also reduced but it does not appear possible to bring it within acceptable limits. In the case of 5-guanylamino-tetrazole, percent hydrogen can be successfully dropped but at the cost of excessive methane formation and low temperatures. Similar effects occur with other fuels. The result of adding lithium perchlorate to the fuels, Table 5, is an increase in temperature and carbon monoxide, with an accompanying reduction in carbon and methane. In the case of dicyandiamide, the amount of hydrogen in the combustion products actually increases (probably due to decomposition of methane); in all cases, the perchlorate does not appear sufficiently useful in reducing hydrogen content.

Table 6 shows the effect of adding the compound BTU to 5-guanylamintetrazole. It may be seen that the additive is not sufficiently effective in removing the hydrogen and carbon.

TABLE 3. EFFECT OF LITHIUM NITRATE + PCF AS ADDITIVE

FUEL	OXIDIZER	O/F	% LiNO ₃	TEMP (°F)	PERCENT BY WEIGHT OF COMB. PRODUCTS							
					N ₂	H ₂	H ₂ O	C	CO	CO ₂	CH ₄	OTHER
Dicyandiamide	1/3 CTF + 2/3 PCF	.02	0	1206	65.2	1.85	0.6	19.8	0	0	10.7	0.7 HF
		.02	25	1337	54.0	1.67	4.9	13.8	7.0	5.4	3.8	7.6 LiOH
		.02	50	1403	43.2	.98	4.1	2.4	16.3	14.9	.9	16.5 LiOH
		.06	0	1333	62.8	2.3	1.2	20.9	0	0	7.4	
		.06	25	1447	52.6	2.0	4.2	11.8	12.3	5.1	2.0	5.6 LiOH
	1/3 CTF + 2/3 PCF	.06	50	1465	42.2	1.1	3.5	0.6	21.2	13.0	0	14.9 LiOH
Dicyandiamide	CTF	.04	25	1414	53.2	1.9	4.4	12.7	10.0	4.9	3.1	5.4 LiOH
Viton	1/3 CTF + 2/3 PCF	.02	0	1851	0	0	0	26.5	2.1	0	0	38.6 HF + 31.5CF ₄
"	"	.02	25	1384	5.0	0	0	5.6	12.5	14.4	0	23.5 C ₂ F ₂ + 29 HF + 9.3 Li ₂ F ₂
Viton	1/3 CTF + 2/3 PCF	.02	40	2277	8.0	0	0	0	24.4	19.2	0	8.8 C ₂ F ₂ + 23.4 HF + 9.3 Li ₂ F ₂

TABLE 4. EFFECT OF USING LITHIUM CARBONATE AS ADDITIVE
(CTF OXIDIZER)

FUEL	O/F	% LiCO ₃	TEMP °F	PERCENT BY WEIGHT OF COMB. PRODUCTS								OTHER
				N ₂	H ₂	C	CO	CO ₂	CH ₄	H ₂ O		
Hyd. Azide	.02	0	2816	91.5	6.5	0	0	0	0	0		
↑	.02	25	1269	68.6	2.5	0	2.3	2.9	3.0	10.7		+7.4% LiOH
↓	.04	25	1351	67.5	2.8	0	3.8	3.4	2.5	10.3		+5.8% LiOH + 2.4% Li ₂ F ₂
Hyd. Azide	.04	15	2141	78.3	4.9	0	5.0	.5	0	5.8		+2.6% Li ₂ F ₂
5-Guanylamino- tetrazole	.02	0	1718	75.6	3.3	16.7	0.9	0	1.9	0		+ .6% HF
↑	.02	25	260	57.0	0	14.5	0	2.0	4.5	12.5*		* includes H ₂ O liq.
5-Guanylamino- tetrazole	.06	15	1333	63.7	1.7	11.7	5.1	3.1	4.1	4.1		

TABLE 5. EFFECT OF USING LITHIUM PERCHLORATE AS AN ADDITIVE
(OXIDIZER: 1/3 CTF + 2/3 PCT)

FUEL	O/F	% LiClO ₄	TEMP °F	PERCENT BY WEIGHT OF COMB. PRODUCTS								OTHER
				N ₂	H ₂	C	CO	CO ₂	CH ₄	H ₂ O		
Dicyandiamide	.02	0	1199	65.3	1.8	19.8	0	0	11.0	0		
Dicyandiamide	.02	25	1698	49.2	2.88	10.0	22.0	1.7	1.6	1.7		+ 8.7% Li ₂ Cl ₂
Dicyandiamide	.06	25	1702	49.2	2.89	10.3	21.5	1.5	1.6	1.6		
2-Methyl-5Aminotetrazole	.02	0	2144	69.7	4.7	28.2	0	0	.8	0		
2-Methyl-5Aminotetrazole	.02	25	2526	52.2	3.7	6.4	26.6	0	.2	.1		+ 2.8% Li ₂ Cl ₂ + .9% HCl + 6.5% LiCl
Viton	.02	0	1851	0	0	26.5	2.1	0	0	0		+31.5% CF ₄ + 38.6% HF
Viton	.02	25	1466	0	0	4.4	15.1	9.2	0	0		+ 8.6% Cl ₂ + 27.6% C ₂ F ₂ * + 29.0% HF + 6.0% Li ₂ F ₂
Viton	.06	25	1449	0	0	4.5	14.0	9.4	0	0		+ 8.6% Cl ₂ + 28.3% C ₂ F ₂ * + 6.0% Li ₂ F ₂ + 29% HF

* Should actually be CF₄; due to limitation in number of species considered (encountered with addition of lithium perchlorate to viton), CF₄ could not be considered by computer program without modification. Actual result is probably higher temperature and more carbon.

TABLE 6. EFFECT OF USING BTU AS ADDITIVE
(WITH 5-GUANYLAMINOTETRAZOLE (C₂H₅N₇)/CTF, O/F = .02)

	No BTU	10% BTU	20% BTU	100% BTU
Tc	1736	2317	3013	2145
% N ₂	75.3	70.8	66.1	27.9
% C	17.1	17.1	16.0	0
% H ₂	3.3	3.1	2.5	0
% CH ₄	1.8	0	0	0

It may be concluded that none of the fuels studied are suitable replacements for sodium azide on the basis of excessive combustion temperatures or reactive products. A few, such as the dicyandamide/lithium nitrate combination, might be acceptable for direct pressurization of NTO if the lithium hydroxide combustion product does not prove troublesome; teflon has some possibility for use in a CTF pressurization system, however an excessive amount of carbon and a heavy gas may be formed.

Experimental Studies

In view of the results of the analytical study, only a limited amount of experimental studies were conducted. These consisted of laboratory hypergolicity tests (1/4-inch diameter by 1/2-inch long pellets at ambient pressure and temperature) and of a space sterilizability test.

HYPERGOLICITY TESTS

Chlorine trifluoride/sodium azide was found to be smoothly hypergolic. Since nitrogen tetroxide would be a desirable oxidizer with sodium azide, from the standpoint of a slightly higher nitrogen yield and logistics (on NTO/hydrazine propulsion systems), hypergolicity with the following fuels was tested: sodium azide, sodium azide + 5 percent magnesium, copper, silver, and polyvinyl acetate. When hypergolic ignition did not occur, 100 percent quantities of potentially hypergolic powders were tested - in all cases no reaction occurred. A test at 100 psia was also conducted without obtaining ignition.

It is not certain whether teflon will form C_2F_4 or CF_4 plus carbon when burned fuel rich with chlorine trifluoride; since the former reaction would provide a suitable pressurizing gas, hypergolicity was tested. Neither teflon, teflon with 5 percent magnesium, or 100 percent magnesium was found to react with CTF. Kel-F and viton were also tested with similar results.

During the literature search, a compound was found referenced which was reputed to be extremely reactive with CTF and IRFNA.* Small powdered samples of this chemical, tetramethylammonium hydrotriborate (QMB-3) obtained from Callery Chemical Company, were subjected to gaseous chlorine trifluoride and nitrogen tetroxide. The QMB-3 ignited and burned with CTF but no reaction was observed with the N_2O_4 even after two minutes continuous exposure. Bar stock of TFE was filed to produce a fine powder. This powder was mixed with QMB-3 and pressed into 1/4-inch pellets. These were exposed to gaseous CTF. The QMB-3 reacted but the TFE appeared unaffected, except for some sooty carbon-like deposits in the combustion tube.

* Reference 57.

STERILIZABILITY TEST

A space sterilizability test was conducted using a Parr pressure reactor. A 4.7202g pressed azide slug was placed in the reactor and cycled three times to 135C for 22 hours at that temperature. After the third cycle the slug was removed, inspected and weighed. No evidence of reaction was detected; weight loss was insignificant (0.63 percent).

Oxidizer/Fuel Selection and Preparation

Based on the results of analytical and experimental studies, the combination chlorine trifluoride/sodium azide was selected as the hybrid liquid oxidizer/solid fuel for the breadboard system development. Theoretical performance is shown in Figure 4. It may be seen that good yields of nitrogen can be obtained with suitable temperatures at oxidizer fuel ratios of 0.02 to 0.10. For example, at an O/F ratio of 0.04 the theoretical combustion temperature is 1575F and the percentages of combustion products are:

Nitrogen Gas	62.2 percent
Liquid Sodium	30.2 percent
Liquid Sodium Chloride	2.4 percent
Solid Sodium Fluoride	5.2 percent

The oxidizer was obtained in one-pound containers from the Matheson Company (97 percent purity). The fuel was obtained in one-pound containers from Alpha Inorganics (reputedly 99 percent pure).

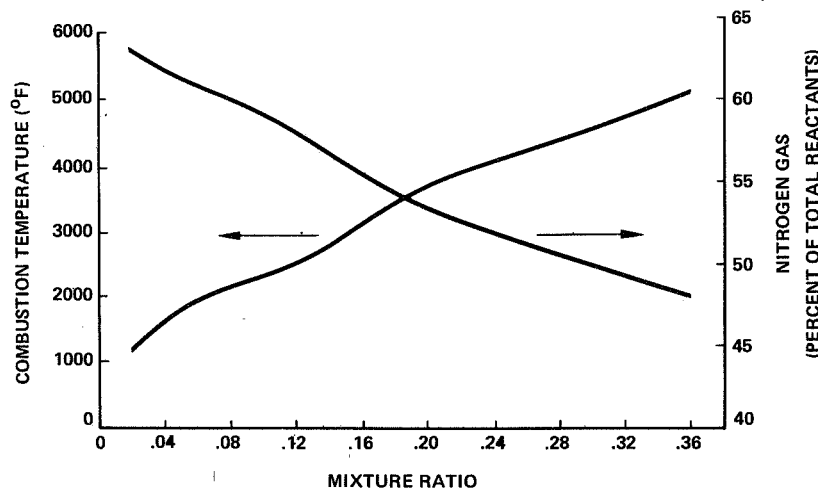


FIGURE 4. THEORETICAL COMBUSTION TEMPERATURE AND NITROGEN GENERATED VERSUS MIXTURE RATIO

Physical/chemical properties of sodium azide are as follows:

Formula	NaN_3
Density, pound/inch ³	0.0666

Decomposition Temperature, R	1060
Heat of Formation, BTU/pound	141
Specific Heat, BTU/pound R	0.249
Impact Sensitivity, cm/kg	200 (with 10 percent Viton A binder)

Sodium azide does not decompose in the absence of heat, or below its decomposition temperature. Although heat is liberated upon decomposition, it is not sufficient to sustain the process; thus, the compound may be used as a coolant for gases hotter than 1060R.

Steel dies were fabricated for production of both pellets, in 1/4-inch, 3/8-inch, and 1/2-inch diameters of various lengths, and perforated slugs in 1-3/16-inch to 1-1/2-inch outside diameter by 3/8-inch to 5/8-inch inside diameter, by 1-inch to 1-7/16-inch lengths. Grains were pressed with no difficulty at pressures of 120,000 to 150,000 psi with excellent physical properties. Typical grains and dies are shown in Figures 5 and 6. No binders were used. The pellets were used in various packed bed configurations; the perforated grains were used both singly and in lengths up to 8 inches long. The pellets were tacked together with a small amount of adhesive for convenience in handling. While the perforated grains were initially cemented together end-wise, or wrapped with aluminum tape, the practice was found unnecessary and eliminated from later tests.

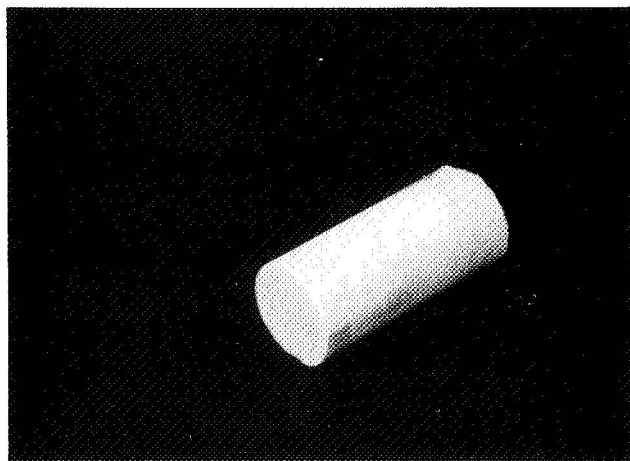
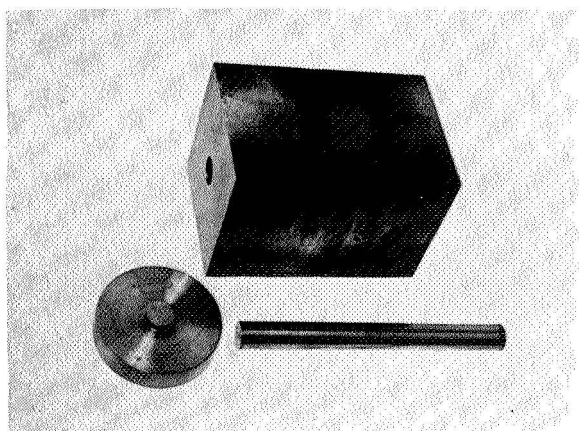


FIGURE 5. 1/2" DIAMETER FUEL DIE AND TYPICAL GRAIN

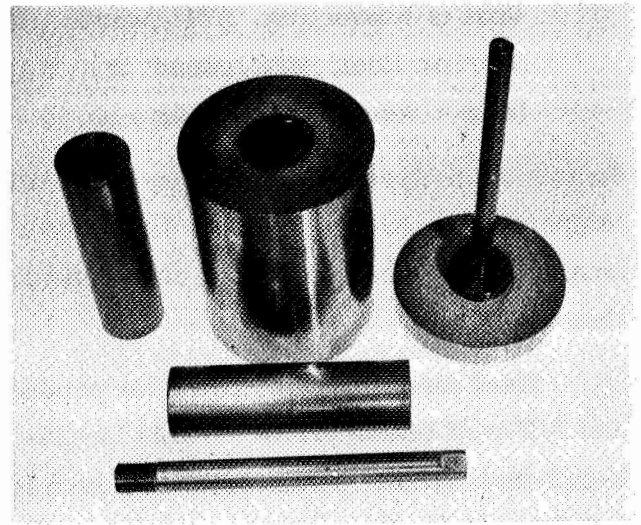
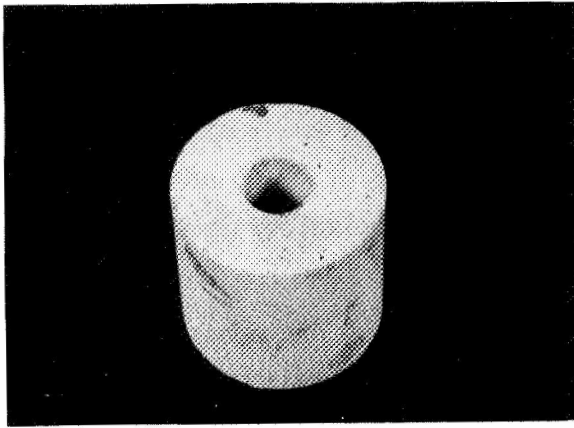


FIGURE 6. 1-3/16" DIAMETER FUEL DIE AND TYPICAL GRAIN

SECTION IV

COMBUSTION STUDIES

The purpose of the combustion studies was to provide an approximate measure of system operating limits while exhausting to ambient pressure, and to provide design information for the breadboard system.

Combustion Chamber Design

The test chamber, which is suitable for testing either 1/2-inch diameter by 1-inch long slugs, small pellets, or 1-3/16-inch diameter perforated grains of fuels, is shown in cut-away in Figure 7 and photographed disassembled in Figure 8. Center-bodies of various lengths were available to permit variation in grain length. The chamber is fabricated from 316 stainless steel, the exit orifices (of several interchangeable sizes to vary pressure and flow rate) and support plate are of nickel. Internal surfaces were flame sprayed with aluminum oxide to reduce heat losses.

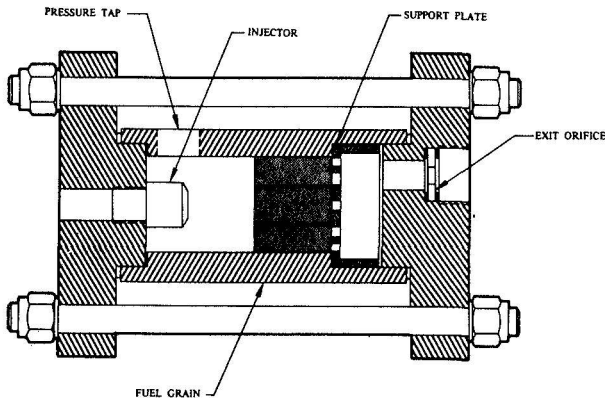


FIGURE 7. COMBUSTION
TEST CHAMBER

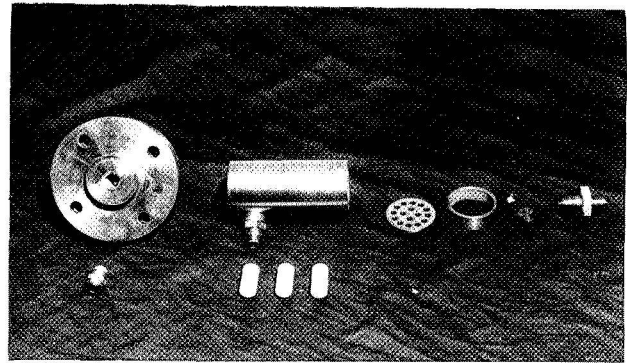


FIGURE 8. COMBUSTION TEST
CHAMBER DISASSEMBLED

A commercial stainless steel hollow-cone spray nozzle was selected for the injector. The internal flow passages were modified to reduce dribble volume and permit addition of a 20-micron filter. Several designs were tested before one was obtained

which met the extremely low flow requirements without plugging. Flow characteristics of the standard injector, used in both combustion and breadboard chambers are shown on Figure 9.

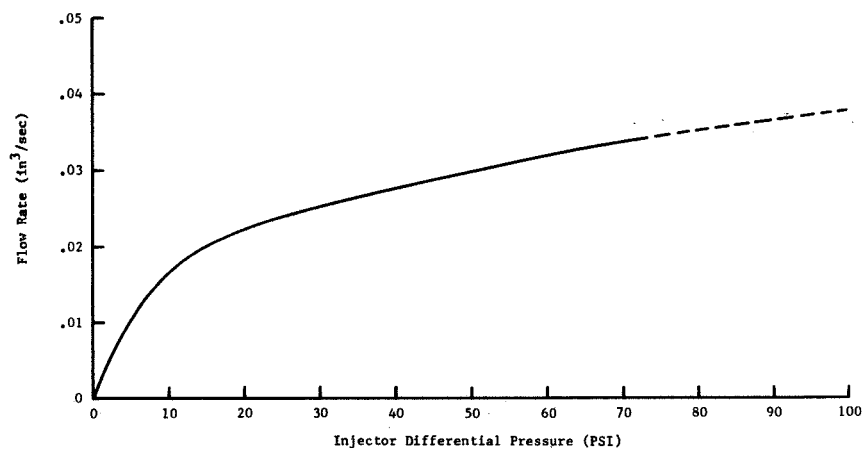


FIGURE 9. WATER FLOW CALIBRATION FOR STANDARD INJECTOR

Test Setup

A schematic of the combustion test setup is shown in Figure 10. Figure 11 is a photograph of the actual installation in the exhaust duct of the Northrop engine test

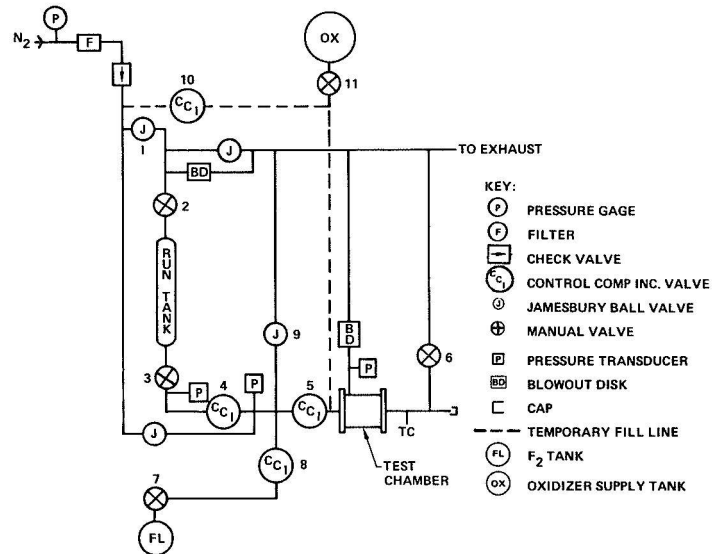


FIGURE 10. COMBUSTION TEST SETUP SCHEMATIC

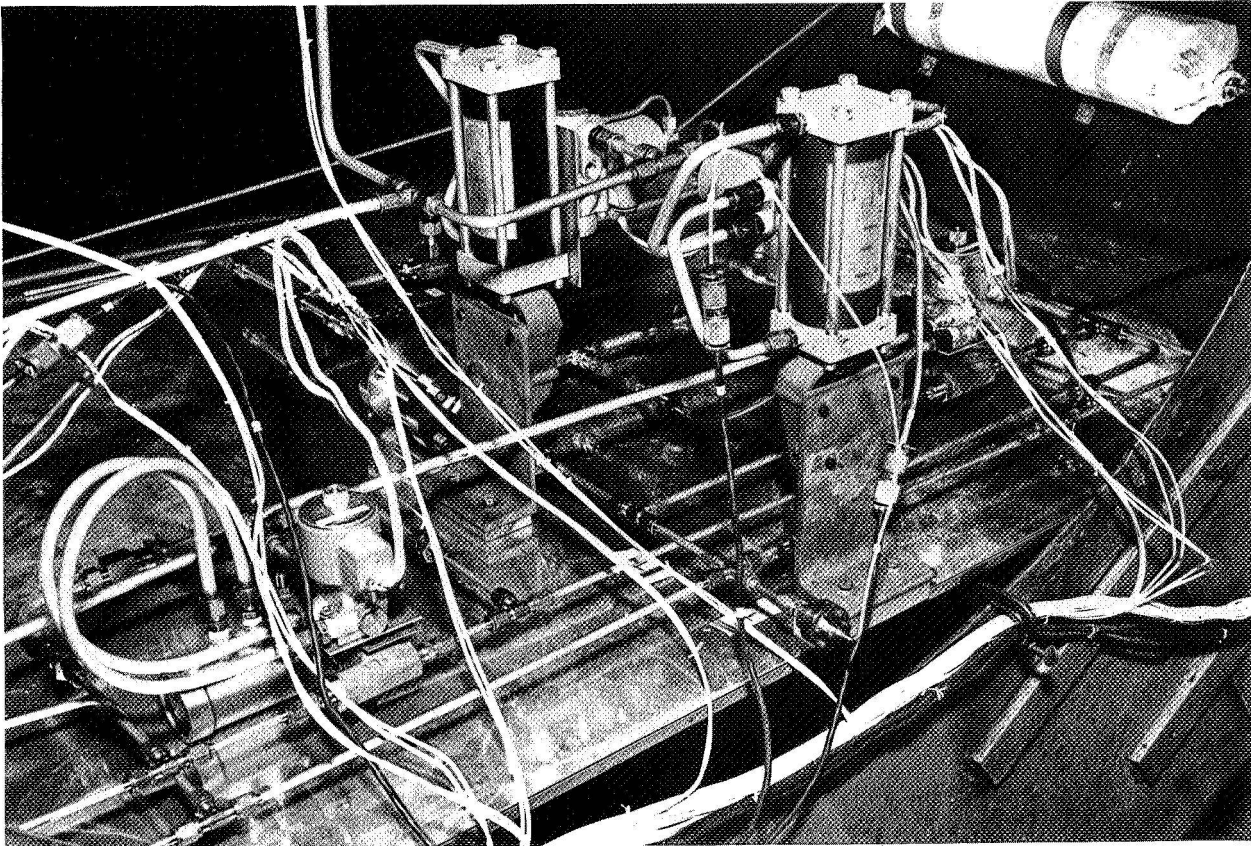


FIGURE 11. COMBUSTION TEST SETUP

cell. The oxidizer tanks are mounted behind the heavy steel plate at the mouth of the duct for personnel safety. A 1/2-pound bottle of fluorine gas was plumbed into the system for use in system passivation and checkout. The oxidizer run tank holds sufficient CTF for several tests. The run valve (No. 5) was a 1/4-inch Control Components valve specially modified to minimize dribble volume and to accept 1/8-inch fittings. The on time of the run valve is controlled by a timer.

It is necessary to transfer the oxidizer from the single-opening container in which it is delivered to the double-opening run tank to permit ready variation in feed pressure. The dashed lines in the schematic indicate the temporary hookup which is used during pressurized transfer. Figure 12 is a photograph of the control panel which has been designed to provide rapid, accurate control of the valving; it has been found to be very helpful.

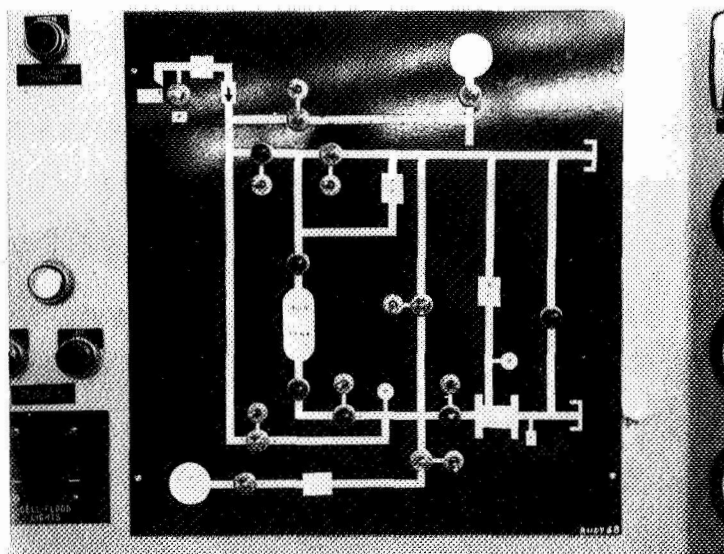


FIGURE 12. TEST CONTROL PANEL

Instrumentation

The test measurements include time, pressures, and temperature. The pressures measured are: oxidizer tank, oxidizer line, and combustion chamber pressure. The pressure sensors are CEC, type 4-311, 0-500 psig. Their response rate is 1000 cps and accuracy is 0.5 percent full scale. The temperature sensor is installed to measure combustion chamber exhaust temperature. The probe used is a Conac K-INC12-G-PJFC. The response time is 0.6 seconds to indicate 63 percent of the temperature change. Accuracy is ± 2 percent.

Because existing flowmeters capable of measuring the design flow rates were either of questionable performance or excessively expensive, a flow meter was designed, built, and calibrated by Northrop. The unit made use of a CEC model 4-351 0-50 psi differential pressure transducer and four feet of 0.0385" capillary tubing. The capillary tubing provided laminar flow, and thus a linear pressure drop versus flow rate relation. Nonlinearity introduced by the end fittings was accounted for by analysis and calibration.

The flowmeter was calibrated and installed between valves 4 and 5. It was found to be quite useful in providing a sufficiently accurate measure of oxidizer flow rate; the device also provided a clearcut indication of flow media phase change (sharp drop in pressure) useful during propellant transfer and in indicating oxidizer depletion. Unfortunately, water hammer effects damaged the differential pressure transducer during the test program (a replacement was not available), subsequent oxidizer flow rates were obtained from calculations which made use of injector differential pressure and the curve of Figure 9.

All pressures and temperatures are recorded on a Sanborn, Model 3914, 14-channel tape recorder. The tape recorder has a response rate of 10,000 cps at 60 in/sec. and 2500 cps at 15 in/sec. After the run the recorded signal is fed into a CEC Model 5-124 Recording Oscillograph, for reproduction of data on a visible trace. Various combinations of tape recorder and oscillograph speeds can be used to obtain desired time scale traces.

Test Program and Results

As stated previously, the purpose of this phase of testing was to provide a measure of system operating limits and to provide information for design of the bread-board system.

INITIAL TESTS

Two initial tests were conducted using fluorine gas to check out the set-up and provide a relationship with previous Northrop work. The remote actuated valves and instrumentation operated satisfactorily. The CCI valve controlling flow into the chamber requires 100-120 msec. from signal to full flow, and closes in approximately 75 msec. The fluorine injector consisted simply of a 0.013 inch diameter hole drilled in a 0.093 inch thick nickel disc which was mounted within a recessed 1/2-inch diameter hole at the head end of the chamber. A 0.050 inch exit orifice was used. Test parameters and measured results are tabulated below.

Test No.	Ox. Supply Pres (psia)	Fuel Form	Fuel Wt. (grams)	Run Time (sec)	Max. Chamb. Pres. (psia)	Max. Temp (°F)	Time, Valve open to 10 psi rise (sec)	Fuel Wt Consumed (grams)
1a	140	4-1/2" dia x 1" pellets	23.37	3.20	128	230	0.17	11.14
1b	139	Restart		3.25	131	270	0.36	
2	130	Perf. grain 3/8" ID x 1" long	29.01	5.36	112	180	2.12	6.05

The first test was similar in design (a circular nesting of fuel pellets) and in results to previous tests conducted by Northrop; combustion was smooth and stabilized at the maximum pressures noted. The restart was also smooth and actually exhibited a more rapid build-up of pressure than the first firing. Reproduction of the oscillograph record is presented in Figure 13.

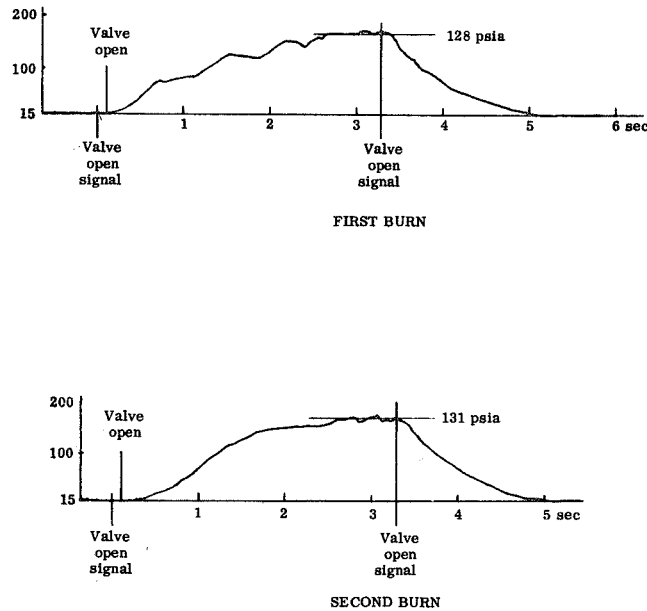


FIGURE 13. INITIAL COMBUSTION TEST WITH FLUORINE/SODIUM AZIDE PELLETS

Based on the measured weight of azide consumed and the calculated flow of fluorine, the average oxidizer/fuel ratio for this test is 0.086. The corresponding theoretical temperature is 2900 R. Calculating temperature of the gas flowing out of the chamber on the basis of measured pressure and orifice diameter results in a temperature of 1490 R. The difference from theoretical is due primarily to combustion inefficiencies and heat loss to the heavy walled chamber. The thermocouple installed in the exit tube recorded a maximum temperature of 730 R, indicating significant error. In view of these results, two steps were taken. Portions of the chamber were flame-sprayed with aluminum oxide as an insulation. In addition, a Nanmac Model AA-455 thermocouple with an exposed junction was ordered.

The second test utilized a 1-inch long grain with a 3/8-inch ID perforation. The reason for the abnormally long ignition delay is not clear. When ignition finally did occur, it was followed by a very slow straight line build up, without spiking, to the pressure noted. The reason postulated is that the regression rate of sodium azide with gaseous fluorine is extremely low and that the reduced grain area exposed to fluorine flow, coupled with the heat sink provided by the grain, retarded ignition.

Initial tests (Runs 3 - 18) conducted with CTF at a feed pressure of 300 psia and a 1-inch long by 3/8-inch ID grain produced a smooth and much more rapid build-up of pressure than with fluorine; however a spike and a rather long tail-off occurred at shut-down.

The spike was found to be caused by an excessive dribble volume (estimated to be 0.188 in^3) and the characteristic plunger action of the valve; the dribble volume also was the prime contributor to the tail-off along with some residual decomposition of the fuel caused by contact with hot molten sodium remaining in the chamber. It was at this point that the modifications previously noted were made to the valve and injector to reduce dribble volume. It was also decided to conduct future tests on larger (longer) grains to minimize the influence of tail-off on results.

During these initial tests a problem was also encountered with injector plugging with internal corrosion products. When addition of a filter at the injector failed to remedy the problem, a procedure of soaking the injector parts in 70 percent nitric acid for 20-30 minutes prior to each test was adapted; no further difficulty with corrosion was experienced.

COMBUSTION TESTS

The results of successful tests conducted during this phase are summarized in Table 7. The omitted runs were unsuccessful. Information computed by the analytical technique, described in a later section, is contained in the columns denoted by asterisks. Figures 14 to 23 are tracings of typical data tapes. The following general comments can be made:

1. Measured pressures and temperatures noted in the table are average, steady state values.
2. Run 27 is a repeat of 26 (Figures 14 and 15) with the forward face of the grain an inch further from the injector. Results indicate good repeatability of steady state pressure and temperature operation; build-up to pressure was much slower with the increased spacing, but the injector face was cleaner. The small peak at valve closure is characteristic of the plunger action of the valve.
3. The system appears to run stably at very low injector ΔP 's (note runs 25, 26, 27, 32, and 34). Run 32 (Figure 19) actually operated in a self-limiting mode, at times, when chamber pressure cycled about a value equal to supply pressure.
4. Inspection of shell grain remainders indicated that a good deal of the burning occurred in an end burning mode.

5. Run 32 is especially encouraging, in that design duration was almost achieved with four inches of grain at 275 psia and a gas generation rate of probably half of the design value. Run 32 also included a rapid stop-start transient.
6. Many of the lower gas temperature readings are suspect, due to the tendency for sodium chloride and fluoride to accumulate and form an insulating barrier on the protruding thermocouple.
7. Runs 33-39 (Figures 20-23) are pellet bed configurations which may be seen to operate just as stably as perforated slugs. Also included, are two mixed configurations (Runs 36 and 40) which exhibit somewhat more rapid start-up.

TABLE 7. SUMMARY OF COMBUSTION TESTS RESULTS

RUN NO.	FUEL FORM	SUPPLY PRES. (PSIA)	EXIT I.D. (IN.)	DURATION (SEC.)	CHAMBER PRES. (PSIA)	INJ. ΔP (PSI)	GAS TEMP (°R)	\dot{W}_{CTF}^* (LB/SEC)	$\dot{W}_{N_2}^*$ (LB/SEC)	O/F*
19	4-1/2" dia x 1" slugs	295	0.063	3.00	120	175	520	N. A.	0.00397	N. A.
20	2 layers of 1/4" dia x 1/2" pellets	245	0.063	3.00	175	70	1010	0.00162	0.00582	0.18
21	4-3/8" ID x 1" slugs	295	0.063	3.01	235	60	1080	0.00157	N. A.	N. A.
25	2-3/8" ID x 1" slugs	296	0.046	3.03	291	5	930	0.00050	0.00633	0.050
26	2-3/8" ID x 1" slugs	295	0.046	3.10	287	8	1080	0.00069	0.00498	0.091
27	2-3/8" ID x 1" slugs	295	0.045	3.10	285	10	1130	0.00079	0.00522	0.097
29	3-3/8" ID x 1" slugs	274	0.055	3.03	220	52	980	0.00145	0.00807	0.116
30	3-3/8" ID x 1" slugs	275	0.055	6.06	255	20	1010	0.00106	0.00463	0.129
31	4-3/8" ID x 1" slugs	274	0.063	15.65	258	16	1235	0.00098	0.00558	0.114
32	4-3/8" ID x 1" slugs	280	0.063	25.01	278	0 - 5	1470	0-0.00048	0.00488	0-0.064
33	3 layers of 1/4" dia x 1/2" pellets	270	0.063	3.05	220	50	1100	0.00149	0.00840	0.114
34	5 layers of 1/4" dia x 1/2" pellets	275	0.063	6.08	275	0 - 5	1260	0-0.00048	0.00305	0-0.101
35	7 layers of 1/4" dia x 1/2" pellets	275	0.080	3.06	260	15	1485	0.00096	0.00838	0.074
36	2-3/8" ID x 1" slugs + 2 layers of 1/4" pellets	275	0.063	6.09	240	35	1160	0.00127	0.00898	0.091
37	3 layers of 3/8" dia x 1/2" pellets	275	0.046	3.04	212	63	860	**	0.00382	**
38	5 layers of 3/8" dia x 1/2" pellets	275	0.055	3.04	225	50	745	0.00197	0.00748	0.170
39	7 layers of 3/8" dia x 1/2" pellets	275	0.063	10.08	255	20	690	0.00145	0.00826	0.113
40	3-3/8" ID x 1" slugs + 2 layers of 3/8" pellets	278	0.063	10.05	261	17	1320	0.00101	0.00782	0.083
41	4-3/8" ID x 1" slugs	272	0.080	25.25	245	27	1240	0.00116	0.00875	0.086

*Calculated Values

**Injector partially plugged

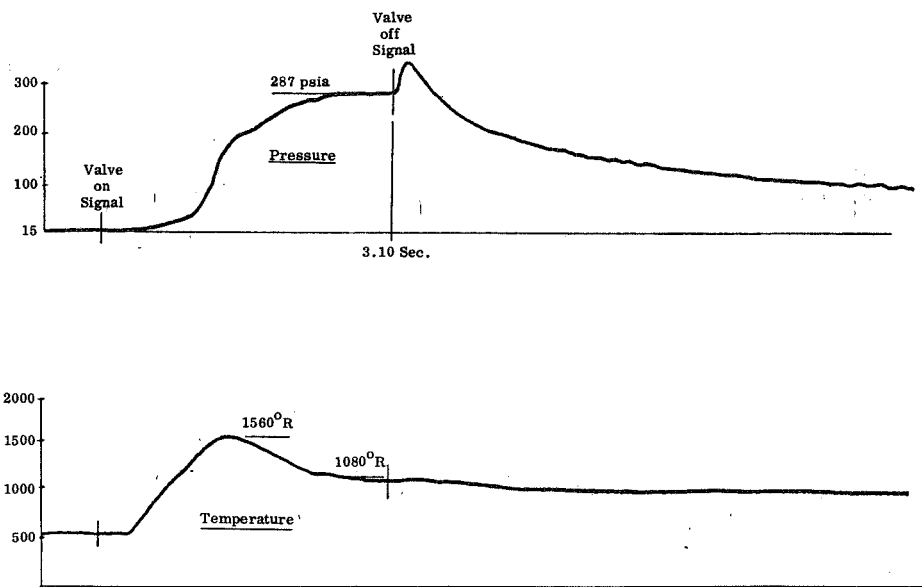


FIGURE 14. RUN 26: 2-3/8" ID x 1" SLUGS
(NORMAL INJECTOR SPACING)

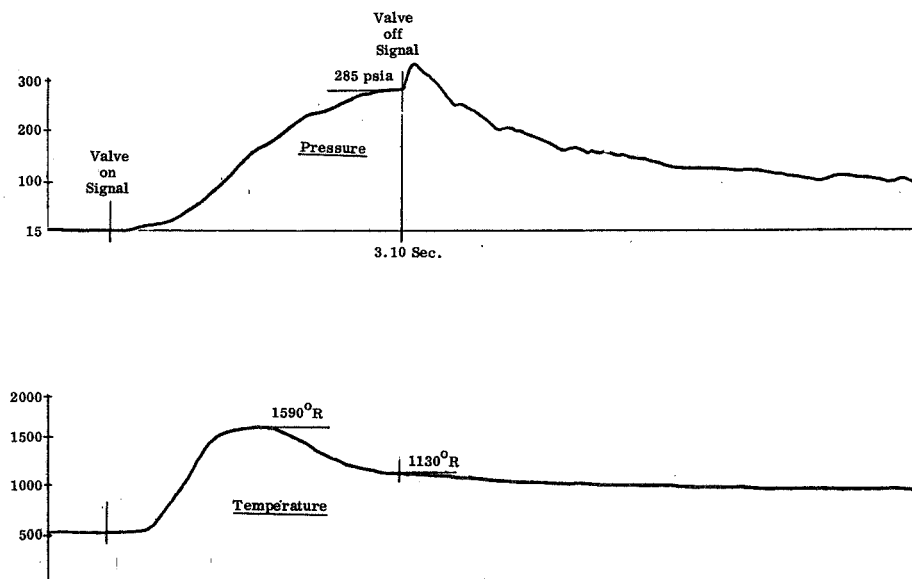


FIGURE 15. RUN 27: 2-3/8" ID x 1" SLUGS
(1-INCH ADDITIONAL INJECTOR SPACING)

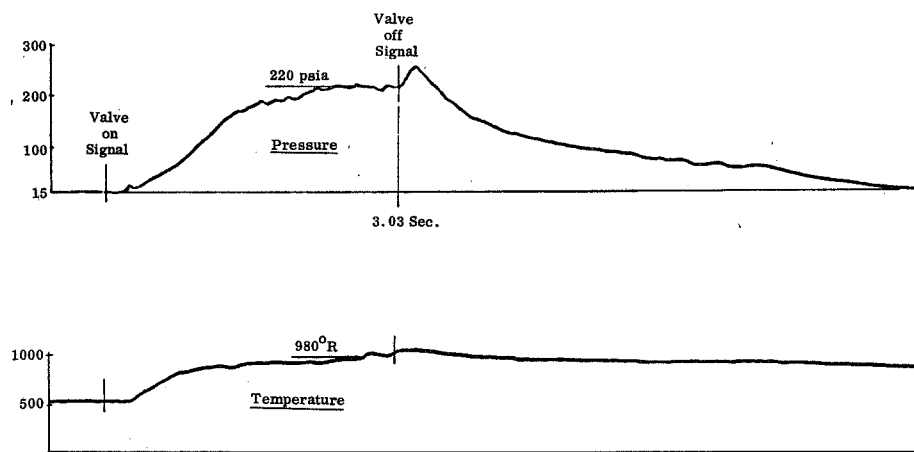


FIGURE 16. RUN 29: 3-3/8" ID x 1" SLUGS

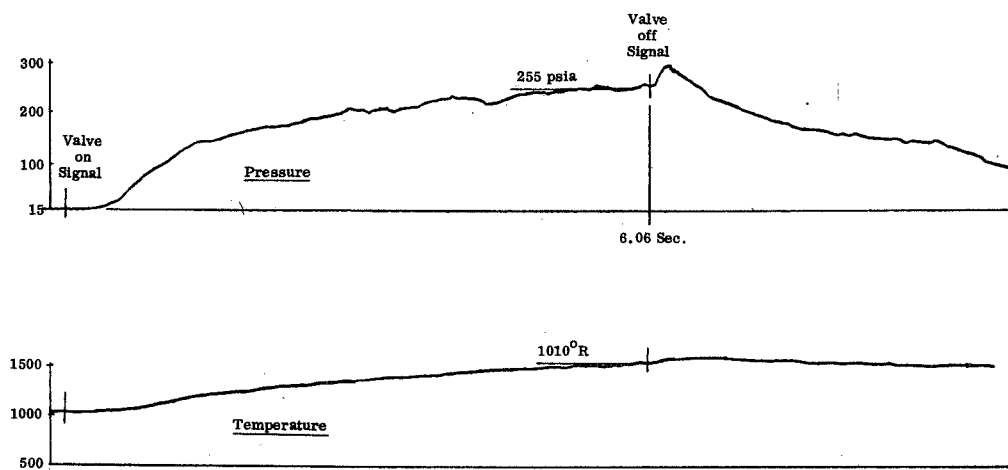


FIGURE 17. RUN 30: 3-3/8" ID x 1" SLUGS

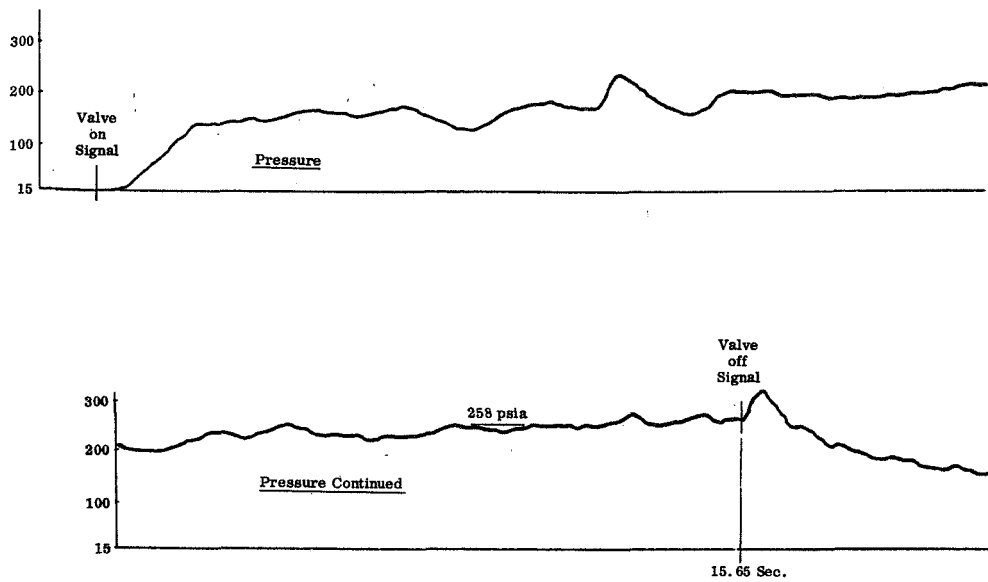


FIGURE 18. RUN 31: 4-3/8" ID x 1" SLUGS

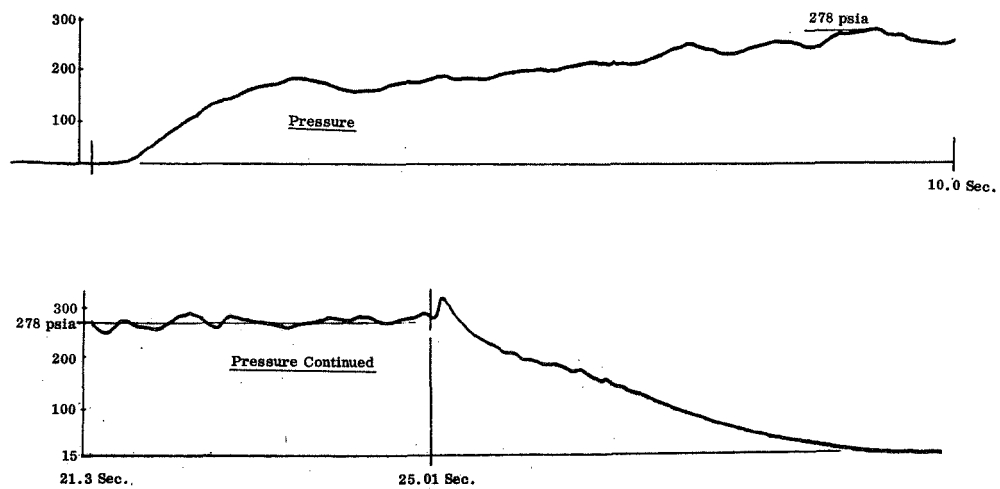


FIGURE 19. RUN 32: 4-3/8" ID x 1" SLUGS

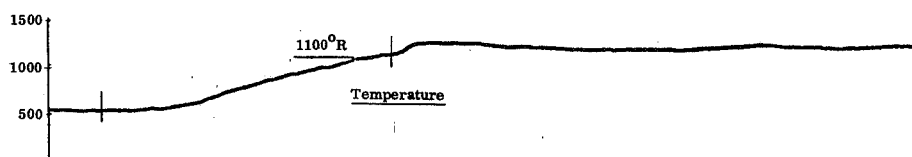
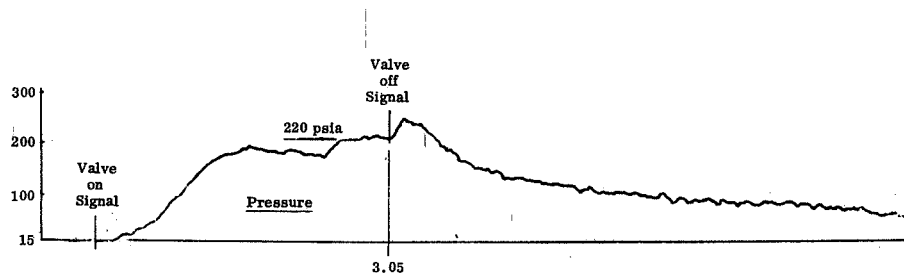


FIGURE 20. RUN 33: 3 LAYERS OF 1/4" DIA. x 1/2" PELLETS

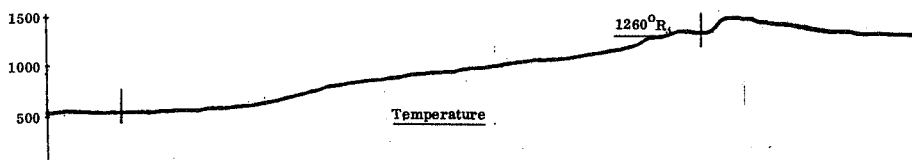
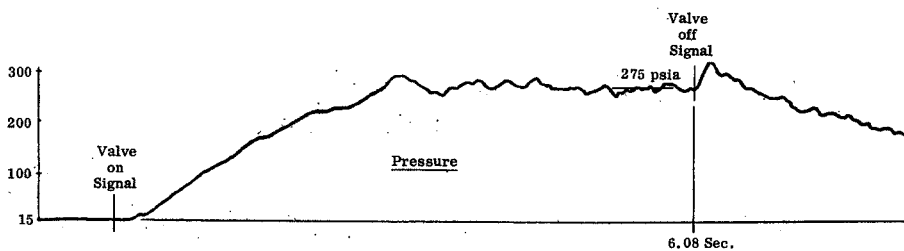


FIGURE 21. RUN 34: 5 LAYERS OF 1/4" DIA. x 1/2" PELLETS

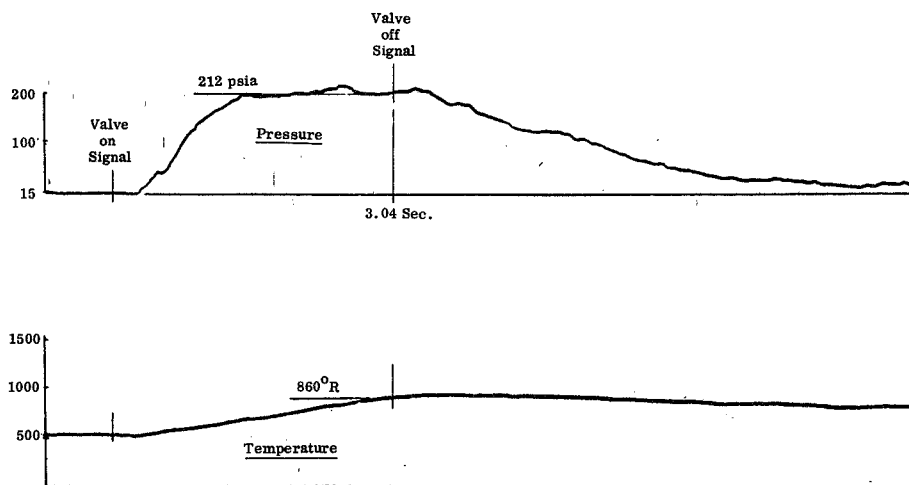


FIGURE 22. RUN 37: 3 LAYERS OF 3/8" DIA. x 1/2" PELLETS

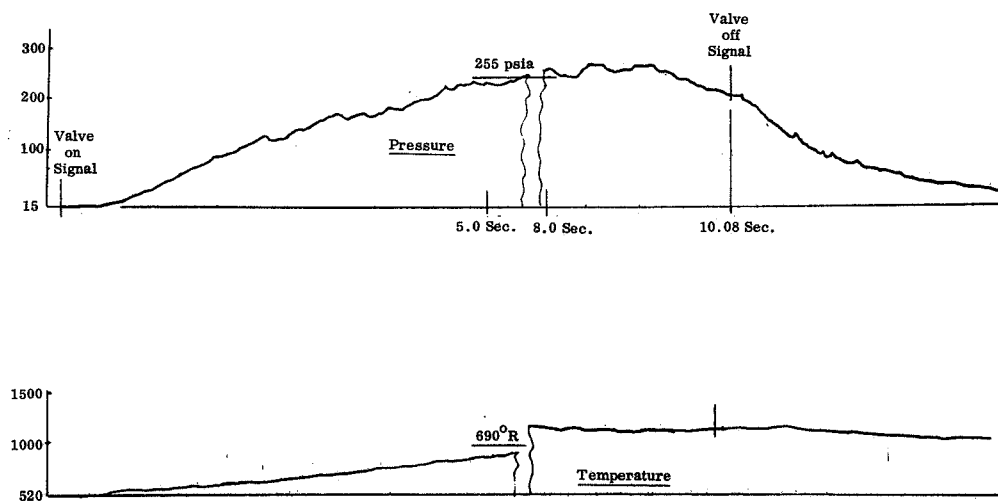


FIGURE 23. RUN 39: 7 LAYERS OF 3/8" DIA. x 1/2" PELLETS

SECTION V

BREADBOARD SYSTEM DESIGN AND TESTING

Breadboard system design and testing were based on the information obtained from the previous phase of testing and upon addition to the previous test setup.

System Design

Grain design is based on a perforated slug, or shell-type grain, since tests indicated quite satisfactory performance. The pellet bed configuration also performed satisfactorily, but was relegated to back-up status due to the expense and time involved with pellet manufacture in the available hand mold. Suitable automatic machines are available; however, their use would have required coordination and possible delay in the program.

The design flow rate was calculated from the original RFP requirement (6.6 ± 1.6 SCFM of equivalent nitrogen flow) and found to equal $.008 \pm .002$ lbs/sec. Assuming an average ullage gas temperature of 960R results in a volumetric flow rate of $25.3 \text{ in}^3/\text{sec}$. A flow duration of 30 seconds requires an expellant tank of approximately 750 in^3 .

Weight of sodium azide required to provide the above flows at the specified pressure of 200 psia was computed to be approximately 0.4 pounds. Study of the combustion test data indicated that seven of the 1-1/4-inch OD (nominal) by 3/8-inch ID by 1-inch long grains would closely approximate both the desired fuel weight and flow rate. Each pressed grain weighs approximately 28 grams, which is very close to theoretical density. Test data indicated that an oxidizer/fuel ratio of 0.075 ± 0.025 , with the above fuel grain, would result in the desired flows and temperatures.

The chamber design is shown in Figure 24. The design uses the flanges and injector from the combustion study chamber; the 0.125-inch thick ceramic liner may be removed to permit an increase in grain OD (or a second liner added for a reduction) and its length may be varied to change location of the support plate. A volume was reserved in the Demister for the sodium which will be formed during combustion.

The Demister is a patented device made by the York Company for removal of entrained liquids from gas flows and was added to trap the liquid sodium formed during combustion. It consists essentially of a length of 1-1/2-inch pipe containing a plug of coarse steel wool. A plug of fine steel wool was added by Northrop to trap the fluoride and chloride powder which is also formed during combustion.

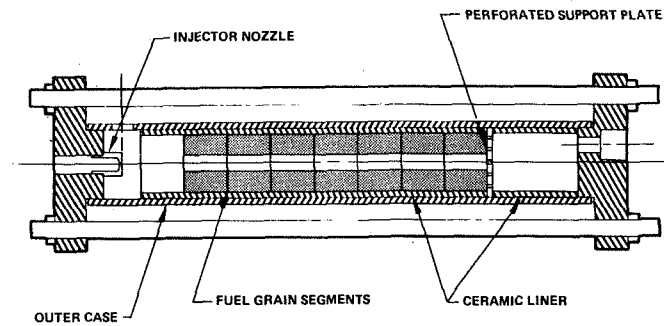


FIGURE 24. BREADBOARD COMBUSTION CHAMBER

A complete schematic of the breadboard system is shown in Figure 25. It may be seen to be an extension of the combustion test setup. The CCI valve used to control oxidizer flow is controlled, after initial opening, by a signal from the pressure transducer located near the expellant tank which is intended to hold tank pressure at 200 ± 20 psia.

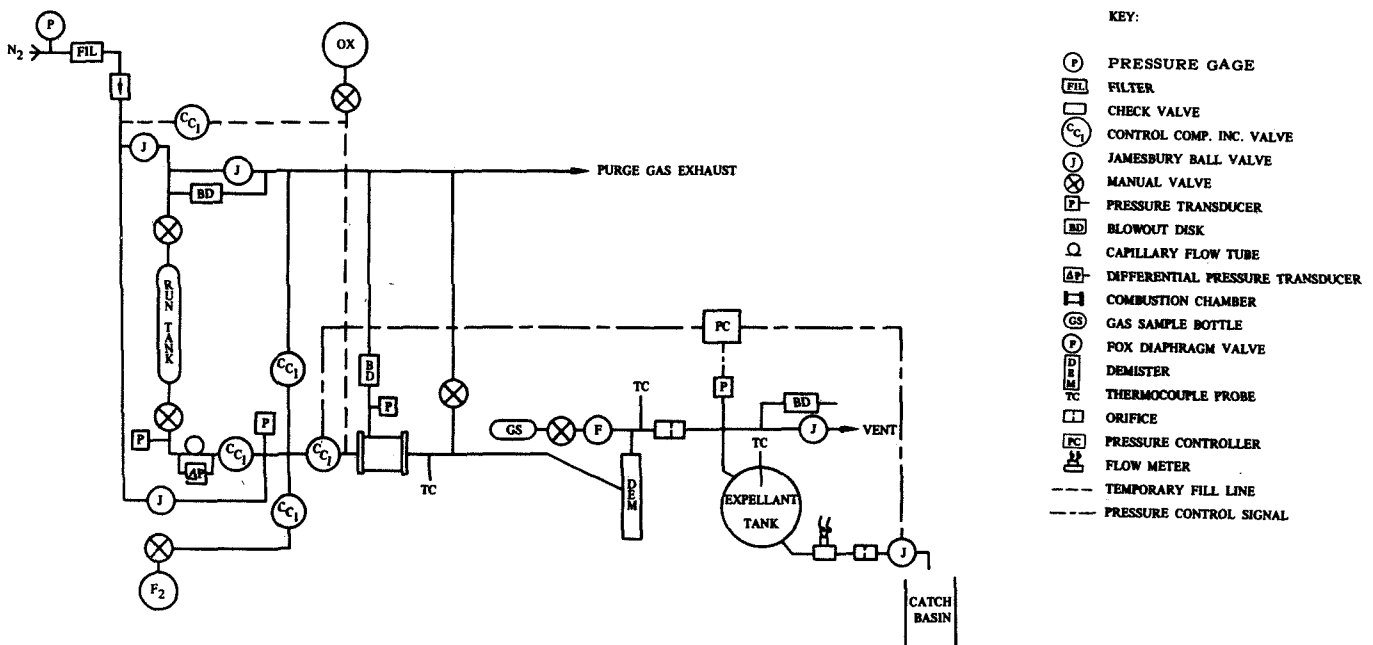


FIGURE 25. BREADBOARD SYSTEM SCHEMATIC

The expellant tank is a 10-liter vacuum-jacketed oxygen converter obtained on loan from the Bendix Corporation. The pressure transducer which controls oxidizer flow is also being used to provide the opening signal to the expellant tank flow control valve (set to open as tank pressure approaches 200 psia). A flow meter is installed in the expellant tank exit line along with an adjustable orifice to measure and obtain desired flows. A thermocouple is installed at the top of the expellant tank. A thermocouple was also installed downstream of the Demister along with a gas sample valve and bottle.

Test Program and Results

Testing was conducted in three phases, distinguished as follows:

Group A: Tests with Demister only

Group B: Preliminary expulsion tests with water and LN_2

Group C: Demonstration expulsion tests per contract

Additional tests were interspaced to calibrate oxidizer injector and expellant tank flow rates, and to achieve proper operation of the expellant tank pressure control.

The test plan is shown in Table 8. Group A tests were for the purpose of final characterization and sizing of the system. If necessary, fuel grain inside and outside diameters and length were to be varied. The target stable operating pressure was 200 psia. System gas generating capability was to be evaluated in terms of capability of generating the desired weight flow rate at target pressure. Gas was to be sampled at various time points of the runs (once per test) and purity determined. Pressure control was to be added and checked out during Group B tests. These tests were also to include final modifications to the fuel grain dimensions, if necessary. The objective was to insure that the system was operating properly and repeatably for the final demonstration. Group C tests represent the formal demonstration of the breadboard system per contract specifications.

Instrumentation is similar to that described for combustion studies. The following measurements were made:

1. Oxidizer run tank pressure
2. Oxidizer valve supply pressure
3. Expellant tank pressure
4. Combustion chamber pressure
5. Combustion chamber gas temperature
6. Demister gas temperature (later, expellant tank inlet)
7. Demister wall temperature
8. Expellant tank gas temperature
9. Expellant flow rate
10. Gas purity
11. Oxidizer and expellant valve positions.

TABLE 8. BREADBOARD PRESSURIZATION SYSTEM TEST PLAN

TEST GROUP	NO. OF TESTS PLANNED	VARIABLES	INFORMATION TO BE OBTAINED
A	10-20	Duration Grain Dimensions Oxidizer Flow Rate	1. System gas generating capability 2. Generated gas purity 3. Liquid and solid removal efficiency
B	10-20	Duration Expellant Grain Dimension	1. System response 2. Delivered gas temperature 3. Pressure control and stability 4. Effect of cryogenic expellant
C	3-6	Expellant Expellant flow	1. Capability of system to deliver hot, clean N ₂ gas at spec. pres. 2. Capability of system to expel water and liquid nitrogen 3. Capability of system to restart

GROUP A TEST RESULTS

Results of tests conducted, with the grain designs previously described, and with the Demister installed (but without the expellant tank) are shown in Table 9. Pressures and temperatures are steady-state values.

TABLE 9. SUMMARY OF TEST RESULTS

RUN NO.	FUEL FORM	SUPPLY PRES. (PSIA)	EXIT I.D. (IN.)	DURATION (SEC.)	CHAMBER PRES. (PSIA)	INJ. 4P (PSI)	GAS TEMPERATURE (°R)		\dot{W}_{CHF} (LB/SEC)	\dot{W}_{N_2} (LB/SEC)	O/F*	REMARKS
							CHAMBER	DEMISTER				
42	2-3/8 ID	280	.0487	4.07	109	171	940	517	.00182	.0036	.326	Had restart
43	4-3/8 ID	285	.0487	20.3	240	45	1090	640	.00152	.00547	.179	P. went up in steps
44	3-3/8 ID	235	.0487	10.75	215	20	1195	700	.00107	.00612	.113	Steady after 18 seconds
45	3-3/8 ID	237	.0487	10.77	137	100	1020	560	.00107	.0019	.364	Ch. exit partially plugged
48	3-3/8 ID	232	.0487	15.16	137	95	-	-	-	-	-	Inj. orifice partially plugged
49	3-3/8 ID	245	.0487	-	245	0-5	1480	1210	.00230	.00329	.045	Demister insulated
50	3-3/8 ID	272	.0563	10.1	189	83	950	860	.0012	.00242	.32	Demister insulated and heated to 960°R
51	4-3/8 ID	227	.0563	15.3	215	12	1130	860	-	-	-	
52	3-3/8 ID	219	.0532	10.0	212	7	1880	840	.00087	.0048	.117	
53	4-1/2 ID	226	.0563	10.05	219	7	910	700	.00064	.00310	.133	
54	7-3/8 ID	231	.080	20.2	115	116	910	760	.00064	.00117	.352	Exit/Inj. partially plugged
55	7-3/8 ID	234-232	.0570	20.2	155	77	2460	1610	.0019	.00837	.146	Changed to large hole sup. plated
56	7-3/8 ID	234-232	.0570	21.66	210	22	1260	875	.00167	.0064	.167	
57	7-3/8 ID	240-235	.0570	34.8	165	70	1275	1345	.00109	.0064	.110	Returned to perforated sup. plate
58	7-3/8 ID	227	.0533	35.0	227	0-5	990	960	.00194	.0050	.207	
59	7-3/8 ID	238	.0533	15.25	128	110	660	820	-	-	-	Inj. and exit orifice partially plugged
60	7-3/8 ID	232-226.5	.0533	15.0	133.5	93	740	745	.00189	.00543	.225	
61	7-3/8 ID	225	.0533	30.0	153	72	780	937	.00178	.0077	.150	Stop - restart
62	7-3/8 ID	230	.0533	30.2	195	35	940	940	.00163	.0062	.169	Add graphite spacer
63	8-1/2 ID	231	.0533	30.0	199	32	1235	811	.00126	.00892	.091	
64	7-3/8 ID	228	.0533	30.2	180	48	1360	837	.00124	.00780	.103	
65	7-3/8 ID	210	.0533	30.2	194	16	1190	811	.00138	.0063	.140	Drop exit - reduce line length (move cham. T.C. from exit line to chamber)
66	8-3/8 ID	228	.0533	30.5	197	31	890	890	.00098	.0069	.091	Return to large hole sup. plate
67	8-1/2 ID	238	.0533	29.8	153	85	910	744	.00122	.0028	.282	
68	8-1/2 ID	235	.0533	30.0	173	62	940	803	.00172	.0044	.252	
69	7-1/2 ID	Injector burned out					990	803	.00154	.00651	.163	Incr. exit to 1/2"
70	7-1/2 ID	234	.0533	26.4	123	111	1170	786	.00189	.00538	.221	

* Computed Values

Generated gas purity was measured on Runs 50-54 by bubbling the gas through a solution of potassium iodide. The resultant solution can be chemically analyzed for total chlorine trifluoride. Small amounts of chlorine trifluoride, ranging from 0 to 3.8 grams, were detected. There appeared to be no direct correlation between the amount of chlorine trifluoride detected and test parameters such as supply pressure, steady state injector ΔP , or run duration. However, it is suspected that: (a) most of the CTF passes through during the high injector ΔP ignition phase, and (b) when sodium remains on the Demister screen from a previous run, it serves to react CTF which has passed through the chamber (the Demister screen was found partially burned after Run 52).

The essential purpose of Runs 55 through 70 was to check out the full-scale 7-grain configuration and make whatever modifications were necessary to meet design requirements. The following observations and comments are appropriate:

1. Large quantities of sodium were found in various portions of the chamber after many of the tests. While this might not constitute a problem in a pellet bed configuration, it was feared that the sodium deposited near the injector could spatter and plug the injector, and that sodium on the surface of the grain would interfere with the combustion process. The combustion chamber is mounted horizontally and thus operates without the assistance of gravity to remove sodium. Although tipping the chamber would very likely remove the sodium, it appeared useful to try to operate under simulated "zero G." The following modifications noted in Table 9 were, however, progressively made: The thermocouple was removed from the exit line (where it trapped sodium) and inserted in the chamber (Run 58 and after); a graphite spacer, 1-1/4-inches long was inserted around the injector; the chamber exit port was rotated from its position near the top of the chamber to a position near the bottom; lines and fittings between the chamber and Demister were increased in size from 3/8 inch to 1/2 inch. Later tests indicated that the modifications were successful.
2. Inspection of the chamber after a test indicates that a combination of end-plus-internal burning occurs.. Most of the internal burning occurs on the three forward most grains at any given time. This appears to be an ideal arrangement for long duration operation.
3. Grains with 1/2-inch ports may result in slightly higher flow rates, but require an additional inch of length to obtain sufficient fuel weight. Addition

of one more grain in the existing chamber reduces space available at the aft end for sodium storage.

4. Calculations indicated that nitrogen gas weight flow within the specification should be obtained with the 7-inch by 3/8-inch ID grain configuration.
5. Chamber pressure was considered of secondary importance to gas weight flow during these tests, since analysis indicates low sensitivity of burning characteristics to pressure. With satisfactory gas weight flow generation and proper orificing of liquid expellant flow, proper chamber pressure should result.
6. Addition of fine mesh steel wool in the Demister trapped sodium chloride and fluoride dust.
7. Typical results of analysis of a gas sample on a Perkin-Elmer Gas Chromatograph are shown in Figure 26. No evidence of CTF or its elements was found in this or any other samples analyzed (samples were taken intermittently from Runs 56 through 89).

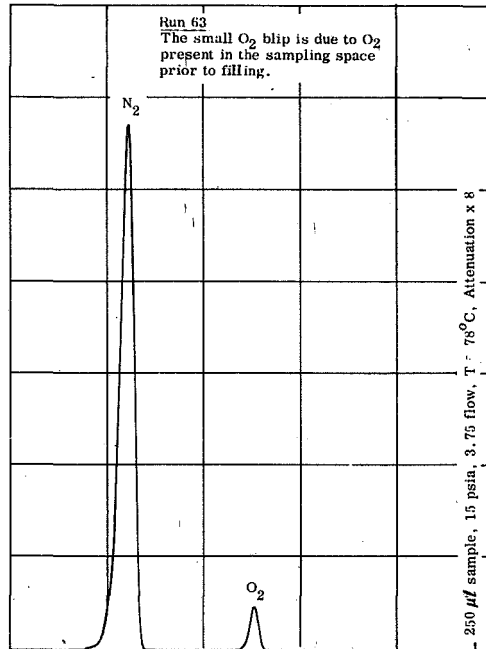


FIGURE 26. RESULTS OF GAS CHROMATOGRAPH ANALYSIS OF RUN 63 GAS SAMPLE

GROUPS B AND C TEST RESULTS

The expellant tank was added for this series of tests (per Fig. 25). An adjustable orifice (a needle valve) was installed in the exit line along with a flowmeter, to match liquid volumetric flow rate to gas flow rate in order to obtain the desired tank pressure; they were later replaced by calibrated fixed orifices (one sized for water expulsion and one for liquid nitrogen).

Steady-state test results are summarized in Table 10. CTF weight flow rate is computed from a steady-state value of injector ΔP and the injector flow calibration curve. Nitrogen weight flow rate is computed from measured steady-state values of tank expellant volumetric flow rate, pressure, and temperature when data are available. Oxidizer/fuel ratio is based on the computed values of \dot{W}_{CTF} and \dot{W}_{N_2} (assuming $\dot{W}_{FUEL} = \frac{\dot{W}_{N_2}}{.646}$). Portions of the three temperature columns are blank because only two channels were available for recording these values at any one time. The thermocouple measuring Demister outlet gas temperature was relocated closer to the expellant tank prior to Run 88. Values noted under the "GPM" heading represent water expulsion flow rates in gallons per minute; tests in which values are not provided were conducted with a 0.057-inch diameter orifice in place of the expellant tank.

TABLE 10. SUMMARY OF TEST RESULTS

RUN NO.	FUEL FORM	SUPPLY PRES. (PSIA)	DURATION (SEC.)	CHAMBER PRES. (PSIA)	INJ. Δ P (PSI)	GAS TEMPERATURE (°R)				\dot{W}_{CTF} (LB/SEC)	\dot{W}_{N_2} (LB/SEC)	O/F	REMARKS
						CHAMBER	DEMISTER	TANK	GPM				
71	7" x 1 1/4" OD x 3/8" ID	205	29.8	135	70	910	1240	-	4.15	.00162	.0046**	.228	
72	7" x 1 1/4" OD x 3/8" ID	205	30.5	133	72	880	1490	-	4.2	-	NA	NA	Burned grain weight not recorded
73	7" x 1 1/4" OD x 1/2" ID 8-1/4" pellets	205	29.9	100	105	660	1480	-	3.7	.00183	.0025	.384	
74	7" x 1 1/4" OD x 3/8" ID	213	30.0	127	86	795	750	-	3.8	.00173	.0035**	.339	100 psig pre-pressure
75	7" x 1 1/4" OD x 1/2" ID 7-3/8" pellets	225	29.9	106	119	860	-	660	3.8	.00192	.00355	.335	50 psig pre-pressure
76	6" x 1 1/4" OD x 3/8" ID	231	29.7	105	126	740	-	690	3.8	.00195	.00336	.350	46 psig pre-pressure
77	7" x 1 1/4" OD x 3/8" ID	225	29.9	105	120	760	-	660	3.25	.00192	.00301	.412	92 psig pre-pressure Restart - poor ignition Could be CTF almost gone
79	7" x 1 1/4" OD x 3/8" ID	209	29.9	135	74	820	1810	-	-	.00166	.0028**	.383	Exit partial plug
80	7" x 1 1/4" OD x 3/8" ID	209	29.9	157	52	1025	1240	-	-	.00145	.0047**	.1995	Grain dried at 110°C and surface roughed up
81	5 3/4" x 1 1/2" OD x 1/2" ID	213	28.0	167	46	950	760	-	-	.00142	.0044**	.209	Exit partial plug
82	5 3/4" x 1 1/2" OD x 1/2" ID	212	13.0	212	0	710	1050	-	-	-	-	-	Shut down early due to orifice plug
83	5 3/4" x 1 1/2" OD x 1/2" ID	212	30.0	182	30	860	820	-	-	.00125	.007**	.115	
84	5 3/4" x 1 1/2" OD x 1/2" ID	215	30.0	165	50	880	-	610	4.1	.00143	.00646	.143	Bore roughed up
85	5 3/4" x 1 1/2" OD x 1/2" ID	228	4.5	176	52	570	-	NC	-	-	-	-	Expel. tank burst disc failed at 4.5 seconds
86	5 3/4" x 1 1/2" PD x 1/2" ID	230	31.5 22.75*	181	49	-	-	625	4.23	.00142	.00711	.129	Restart
87	5 3/4" x 1 1/2" OD x 9/16" ID	235	30.0 30.8*	170	65	-	---	580	4.2	.001575	.0072	.141	Restart
88	5 3/4" x 1 1/2" OD x 5/8" ID	230	30.0 9.7* 28.7*	200	30	-	1150	610	3.75	.00120	.00713	.109	Restart
89	5 3/4" x 1 1/2" OD x 5/8" ID	231	41.0	180	51	-	1210	610	3.63	.00144	.00621	.150	Limits on press. control reduced
90	7 3/16" x 1 1/2" OD x 5/8" ID	230	43.8	170	60	-	1310	620	3.75	.00153	.00596	.166	
91L	5 3/4" x 1 1/2" OD x 5/8" ID	226	60.0	185	41	-	580	260	2.14	.00133	.00882	.097	LN ₂ expul.
92L	5 3/4" x 1 1/2" OD x 5/8" ID	232	42.9	195	37	-	970	340	N.A.	.00128	.00469**	.176	LN ₂ expul., 25% ullage; bad leak at tank fill
93L	5 3/4" x 1 1/2" OD x 5/8" ID	218	44.8	187	31	-	930	260	N.A.	.0122	.00614	.128	Diffuser added
94	5 3/4" x 1 1/2" OD x 5/8" ID	225	37.3	192	33	-	780	660	3.80	.00125	.00642	.125	15% ullage
95	7 3/16" x 1 1/2" OD x 5/8" ID	238	42.55	203	35	-	1210	650	4.20	.00127	.00761	.108	
96L	7 3/16" x 1 1/2" OD x 5/8" ID	234	38.75	185	49	-	1010	260	N.A.	.00143	.00885	.104	Flowmeter failed
97L	7 3/16" x 1 1/2" OD x 5/8" ID	240	34.4 29.4*	203	37	-	1210	490	3.56	.00130	.00876	.096	Restart: P _{tank} stabilized at 145 psia between starts
98L	7 3/16" x 1 1/2" OD x 5/8" ID	237 234 228	24.6 32.1* 12.9*	195 199 190	42 35 38	- - -	610 640 710	385 390 375	2.14 2.16 2.11	.00135 .00127 .00130	.00629 .00658 .00620	.139 .125 .136	Multiple start
98L	7 3/16" x 1 1/2" OD x 5/8" ID	-	-	-	-	-	-	-	-	-	-	-	Burst diaphragm in tank leaked
100	7 1/2" of 3/8" Pellets	228	23.67	182	46	935	590	780	3.65	.001391	.00538**	.25	Low ullage - Appears that some reaction occurred in tank diffuser produced abnormal temp. Most sodium trapped in bed
101L	7 3/16" x 1 1/2" OD x 5/8" ID	228 225 223	22.0 21.3* 17.0*	185 189 185	43 36 38	N.A. N.A. N.A.	1350 920 870	200 210 235	N.A. N.A. N.A.	.00136 .00128 .00130	N.A. N.A. N.A.	- - -	

* Restart

** Based on $\frac{.65W}{t \text{ run}}$ Azide Burned, all others based on measured P, V, T.

*** Thermocouple moved closer to tank inlet.

L Denotes Liquid Nitrogen Test.

Test runs 71 through 77 represent experiments with the grain configuration which was expected to provide the desired nitrogen gas weight flow (0.008 ± 0.002 lbs/sec). Although runs 60-65, conducted with a similar grain configuration but without the expellant tank, delivered the desired weight flow, it may be seen that tests with the expellant tank added failed to do so. Operation in all cases was smooth and stable, with the expellant tank liquid flow valve opening automatically after pressure had built up to 190 psia; pressure usually fell off somewhat after valve opening, followed by a gradual build-up to the values noted. The sodium trapped by the Demister occasionally ignites, in turn igniting the Demister screening and causing it to burn for 5-15 seconds, as evidenced by an increase in measured gas temperature at the Demister (which may be noted in the table) and a charring of approximately the lower quarter of the screening. It is postulated that traces of CTF, sufficient to cause this, pass into the Demister — probably during ignition. Gas samples taken during these runs have never indicated the presence of measurable CTF downstream of the Demister.

Runs 71 through 77 include various modifications, as noted in the table under "Fuel Form" and "Remarks", made to improve performance; they were without significant success. Run 78 was aborted due to oxidizer depletion. Runs 79 and 80 were repeats of previously successful tests (60-64) without the expellant tank. Since they failed to deliver the required gas flow also, it has been concluded that a change in the properties of the fuel and/or oxidizer supplies had occurred and caused the change in performance (the injector flow pattern was also checked with water and found satisfactory). The CTF supply is several months old and may have reacted sufficiently with the container material to significantly reduce the purity. The sodium azide supply is also several months old and in two batches.

Since two to four weeks are required to obtain new supplies and an additional delay in the program was deemed highly undesirable, it was decided to first try a change in grain configuration as an attempt to adapt to the variation (the chamber was originally designed to permit such flexibility). A new mold was fabricated and grains of 1-1/2-inches OD by 1/2-inch ID by approximately 1-7/16-inches long pressed. These grains were also dried at 110 C for a minimum of 24 hours. Test runs 81-85, made with these grains, indicated satisfactory results and this basic grain configuration was therefore adapted.

Runs 86 to 90 were conducted expelling water; the grain bore was increased in two steps (Runs 87, 88) to remedy a slight drop-off in nitrogen generation which occurred shortly after the expellant flow valve opened; an additional grain was also

added (Run 90), but did not appear to help. Expellant flow rate was decreased to bring tank pressure within specification (Run 88 and thereafter) and the limits on the pressure controller were changed to reduce pressure variation (Oxidizer valve open at 195 psia, close at 210 psia).

Runs 91-93 were conducted with liquid nitrogen. It was necessary to further reduce expellant flow rate to compensate for the marked reduction in tank bulk gas temperature. A diffuser was added to prevent direct impingement of the gas into the liquid nitrogen (Run 93). The design, shown in Figure 27, was dictated by tank inlet dimensions and is definitely not optimum. The lower end extended to the level of the fluid with 15 percent ullage. Drawings of the interior of the expellant tank were obtained from the manufacturer after Run 93, and it was determined that an excessive amount of initial ullage volume has been used; 10 percent to 15 percent ullage was used in all subsequent tests.

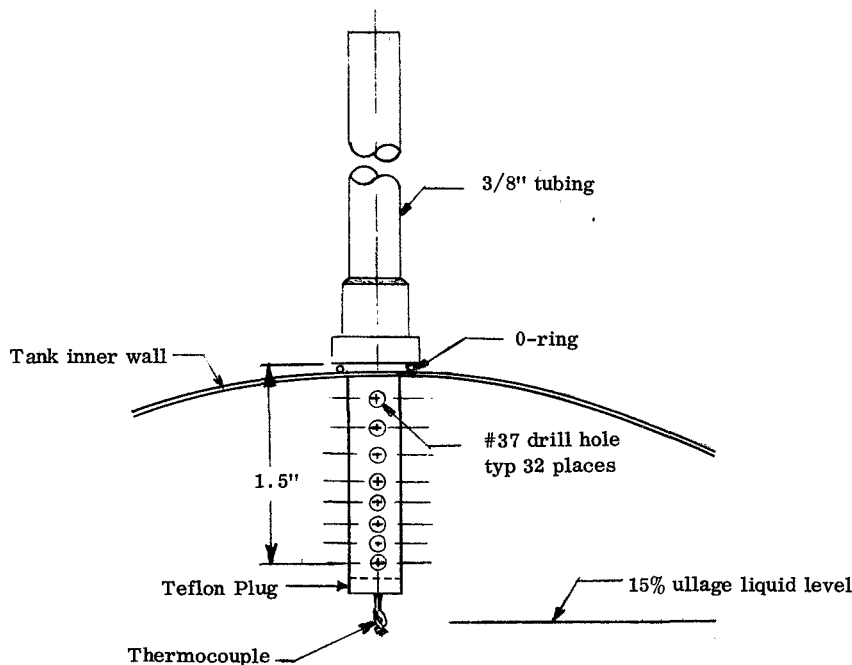


FIGURE 27. EXPELLANT TANK DIFFUSER DESIGN

Run 95 was a repeat of Run 90 with slightly higher oxidizer flow; the additional grain length improved operation sufficiently to merit its use on all further tests. A tape of this run is reproduced as Figure 28. Operation was as follows: At time zero, the oxidizer valve is manually signaled to open, causing generation of gas and pressurization of the lines and tank ullage; at a tank pressure of 165 psig, a signal from the pressure transducer opens the expellant tank valve permitting flow to occur (11.2

seconds); operation continued until the oxidizer valve and expellant valve were manually signaled to close at 42.55 seconds. Pressure ranged from 170 to 188 psig. with a peak after shutdown of 193 psig. Tank ullage gas temperature increased gradually to 230F at shutdown. With an optimum diffuser and full-scale operation, it is expected that ullage gas temperature would more closely approximate the Demister outlet gas temperature (measured at a point no more than 12 inches from the tank).

Run 97, a data tape of which is shown in Figure 29, represented a demonstration of liquid nitrogen expulsion. The flowmeter was replaced with a calibrated orifice at this time. Operation was similar to Run 95 but included a restart. The first expulsion may be seen to have remained within very tight pressure limits (180 to 184 psig) with very little overshoot at shutdown. The expellant tank required approximately 45 minutes to chill down and fill with liquid nitrogen at ambient pressure; thus heat transfer from the gas to tank wall as well as to liquid could be expected to be significant. Approximately 10 percent of the fuel grain remained after the second burn, indicating excellent fuel utilization.

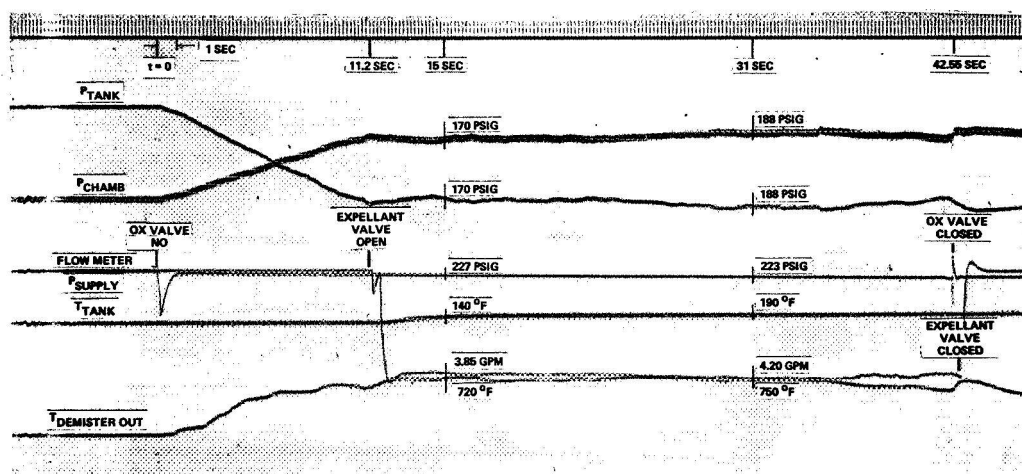


FIGURE 28. RUN 95: WATER EXPULSION

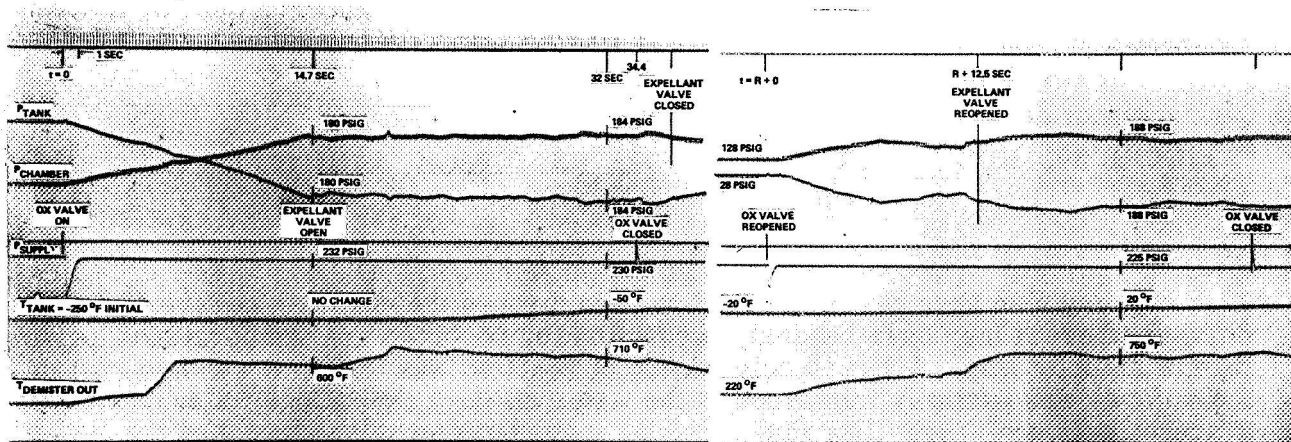


FIGURE 29. RUN 97: LIQUID NITROGEN EXPULSION

Run 98 represents expulsion of liquid nitrogen in three events of 10 ± 5 , 60 ± 10 percent of liquid, and the remainder. Between expulsions, this particular system thermally stabilizes at about 100 psig. The second restart (Figure 30) shows operation of the pressure feedback loop in holding tank pressure within the specified range. Again, slightly less than 10 percent of the fuel grain remained after the test.

Run 99 was aborted due to a severe tank fitting leak. Run 100 was conducted with a 7-1/2-inch long bed of 3/8-inch diameter by 1/2-inch long pellets expelling water. The expellant valve opened in 9.2 seconds; however, burning appears to have been regressive, with pressure falling gradually from 182 psig at 9.2 seconds, to 167 psig at 15 seconds, and 140 psig at 23 seconds. Inspection of the residual indicates that a gap existed between the pellets and the top of the chamber (operation was horizontal) and burning occurred on the forward face and along the top of the bed. *

Run 101, conducted as a demonstration to the Technical Manager, was similar to Run 98 in procedure and resulting appearance. Pressure remained within specified limits at all times.

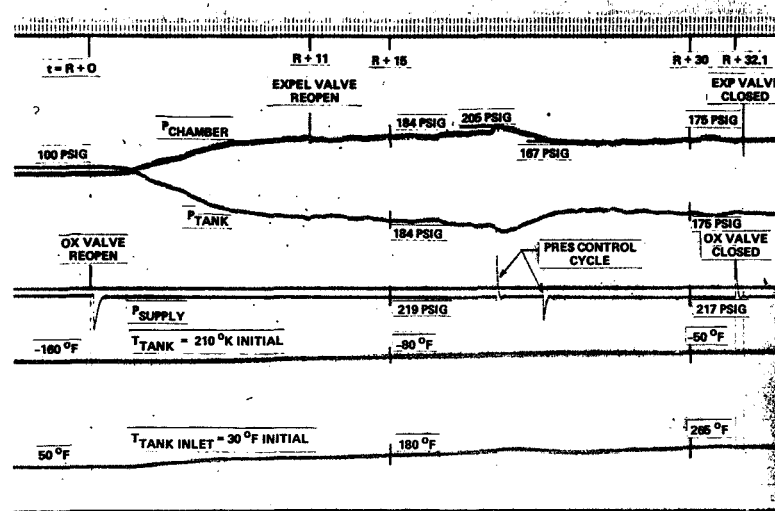


FIGURE 30. RUN 98: LIQUID NITROGEN EXPULSION, MULTIPLE EVENTS

*This gap may also have permitted CTF to pass through the chamber and into the tank diffuser where it may have reacted, accounting for recorded gas temperatures higher than in the inlet line. Although no evidence of reaction was found, it was known that the diffuser was partially immersed in the water initially (low ullage); also, time averaged nitrogen weight flow rate exceeded instantaneous values based on these temperatures thus indicating them to be artificially high and not representative.

Runs 95, 97, and 98 may be considered as having approximated the three types of demonstrations contractually specified: (1) continuous expulsion of water; (2) continuous expulsion of liquid nitrogen; (3) expulsion of liquid nitrogen in three events.

SECTION VI

ANALYSIS

Contained in this section are discussions of the analytical techniques utilized for data reduction and correlation studies plus the results of a study of optimum hot gas temperatures.

Data Reduction Analysis

The analytical techniques used in reducing the test data from the combustion tests and Group A of the breadboard tests are presented below. They are based on measured data, while compensating for the effects of dribble volume, heat losses, and thermocouple error. The analysis provides nitrogen flow rate, oxidizer flow rate, oxidizer/fuel ratio, and corrected temperature of the nitrogen gas when expelled through a sonic orifice.

NOMENCLATURE

A_t	Exit area — in ²
C_D	Discharge coefficient
P_C	Chamber pressure — lbs/in ²
ΔW_{N_2}	Weight of nitrogen — lbs
\bar{T}_{cal}	Calculated average temperature — R
\bar{T}_{meas}	Average measured temperature — R
t	Time — sec
\dot{W}_{ox}	Oxidizer flow rate — lbs/sec
\dot{W}_{N_2}	Nitrogen flow rate — lbs/sec
P_s	Supply pressure — lbs/in ²
λ	Flow function

PROCEDURE

The following steps were used to obtain the above quantities.

1. The run tapes are reduced to numerical values of pressures, temperature, and differential pressure versus time.

2. Chamber temperature based on the flow is calculated by (a) integrating the chamber pressure with time (by trapezoidal rule), (b) measuring total azide consumed (initial azide weight less final azide weight after reacting free sodium in methyl alcohol) and, (c) calculating temperature from the time integration of the flow equation

$$\int_0^t \dot{W} dt = \frac{\lambda A_t}{\sqrt{\bar{T}_{cal}}} \int_0^t P_c dt$$

$$\bar{T}_{cal} = \left(\frac{\lambda A_t \Sigma P_c \Delta t}{\Delta W_{N_2}} \right)^2 \quad (1)$$

where:

$$\Delta W_{N_2} = 0.646 \Delta W \text{ azide consumed}$$

\bar{T}_{cal} = the average chamber temperature

$$\lambda = C_D \left[\frac{g\gamma}{R} \left(\frac{2}{\gamma+1} \right)^{\frac{\gamma+1}{\gamma-1}} \right]^{1/2}$$

C_D = Discharge coefficient ≈ 0.83

3. The average measured temperature is calculated by integrating the time history and dividing by the total time.

$$\bar{T}_{meas} = \frac{\Sigma T \Delta t}{t_f - t_i} \quad (2)$$

4. Comparing the average calculated and measured temperatures provides a measure of the error due to losses. Ratioing the values:

$$\frac{\bar{T}_{cal}}{\bar{T}_{meas}} = K_1 \quad (3)$$

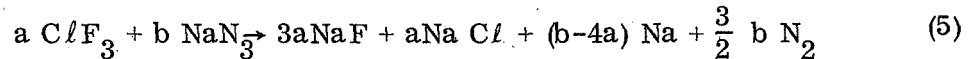
5. Instantaneous oxidizer/fuel ratio is calculated as follows: (a) the oxidizer flow rate is obtained from the differential pressure measurement and injector calibration data; (b) the instantaneous nitrogen flow is calculated from the chamber pressure and corrected temperature.

$$\dot{W}_{N_2} = \frac{\lambda A_t P_c}{\sqrt{T_{cor}}} \quad (4)$$

where $T_{cor} = K_1 \bar{T}_{meas}$

The reasons for using the corrected temperature in equation (4) are:

- 1) The measured temperature is not a true reading due to thermocouple lag and error because of installation losses (i.e., heat transfer due to conduction and radiation).
- 2) The corrected temperature is based on the total flow of nitrogen and forces the calculated total nitrogen produced ($\Delta W_{N_2} = \int_0^t \dot{W}_{N_2} dt$) to equal the measured nitrogen produced ($\Delta W_{N_2} = .646 \Delta W_{azide}$). By doing this it is assumed the reaction in equation (5) produces only nitrogen gas and all the other products of combustion stay in the combustion chamber or the Demister.



- 3) Forcing the calculated total nitrogen produced to be correct makes the correction factor on temperature self-compensating. For example, if the orifice should partially plug during the run, the corrected temperature will be higher causing the calculated nitrogen flow rate to be lower in a proportional amount.
- (c) the azide (fuel) flow rate is a ratio of the nitrogen flow rate

$$\dot{W}_{azide} = \frac{1}{.646} \dot{W}_{N_2}$$

- (d) The oxidizer fuel ratio is then

$$O/F = \dot{W}_{ox} / \dot{W}_{azide} \quad (6)$$

When the gas generator was used to pressurize the expellant tank, the nitrogen flow rate was calculated from the perfect gas law using measured tank pressure and temperature and expellant volumetric flow rate:

$$P_T \dot{V} = \dot{W}_{N_2} R T_T \quad (7)$$

$$\therefore \dot{W}_{N_2} = \frac{P_T \dot{V}}{R T_T} \quad (8)$$

Example

Using data from Run 65:

a. Calculated average temperature:

$$\lambda \cong 0.53 \text{ for nitrogen gas}$$

$$C_D = 0.83 \text{ (this is an assumed value for a sharp edged orifice)}$$

$$A_t = \frac{\pi}{4} D_t^2 = \frac{\pi}{4} (0.057^2) = 0.00255 \text{ in}^2$$

$$\Delta W_{N_2} = 0.216 \text{ lbs of nitrogen (obtained from the weight of azide consumed during the run).}$$

$$\Sigma P_c \Delta t = 5210 \text{ psia-sec}$$

Using these values in equation (1)

$$\bar{T}_{cal} = \left(\frac{0.53 \times 0.83 \times 0.00255 \times 5210}{.216} \right)^2$$

$$\bar{T}_{cal} = 734 \text{ R}$$

b. Average measured temperature:

$$\Sigma T \Delta t = 14754 \text{ F-sec}$$

$$t_i = 0$$

$$t_f = 46 \text{ sec}$$

from equation (2)

$$\bar{T}_{meas} = \frac{14754}{46} = 321 \text{ F}$$

c. Temperature correction factor:

$$K_1 = \frac{734 \text{ R}}{781 \text{ R}} = 0.94$$

d. Instantaneous nitrogen flow rate:

taken from run 65 at 20 sec

$$P_c = 189.4 \text{ psia}$$

$$P_s = 210.9 \text{ psia}$$

$$T_{\text{meas}} = 879\text{R}$$

and using them in equation (4).

$$T_{\text{cor}} = 0.940 \times 879 = 836\text{R}$$

$$\dot{W}_{N_2} = \frac{0.53 \times 0.83 \times 0.00255 \times 189.4}{\sqrt{836}} = 0.00736 \text{ lbs/sec}$$

e. Oxidizer flow rate:

$$\Delta P_{\text{inj}} = 210.9 - 189.4 = 21.5 \text{ psi}$$

$$\dot{W}_{\text{ox}} = 0.001089 \text{ lbs/sec}$$

f. Oxidizer/fuel ratio: from equation (6)

$$\frac{\dot{W}_{\text{ox}}}{\dot{W}_{\text{f}}} = \frac{0.001089}{0.00736} \times 0.646 = 0.0957$$

Correlation of Results

While no attempt was made to determine regression rates, per se, a correlation was made with a quantity proportional to the regression rate, nitrogen flow per unit area (\dot{W}_{N_2}/A_G). The relationship between regression rate and (\dot{W}_{N_2}/A_G) is as follows.

$$\text{Assuming } r_f = f(G_{ox}, L/D_p) \quad (9)$$

then $\dot{W}_f = r_f A_G \rho_f$

$$\therefore \frac{\dot{W}_{N_2}}{A_G} = r_f K_2 \quad (10)$$

where $K_2 = \left(\dot{W}_{N_2}/\dot{W}_f\right) \rho_f$

Figure 31 shows that gas produced per unit area is not only a function of the oxidizer mass flow velocity, but length to diameter ratio also. The final regression rate correlation, or \dot{W}_{N_2}/A_G , has the form

$$\frac{\dot{W}_{N_2}}{A_G} = K G_{ox}^n (L/D_p)^m \quad (11)$$

where $K = 0.0505$

$$n = 0.6$$

$$m = -0.61$$

The lines drawn through the data in Figure 31 are from the above equation and are within ± 10 percent of the data points.

With the large percentage of condensables (35 percent by weight) in the products of combustion, it was felt that at the size tested there may be radiation heat transfer effects; however, no correlation could be found.

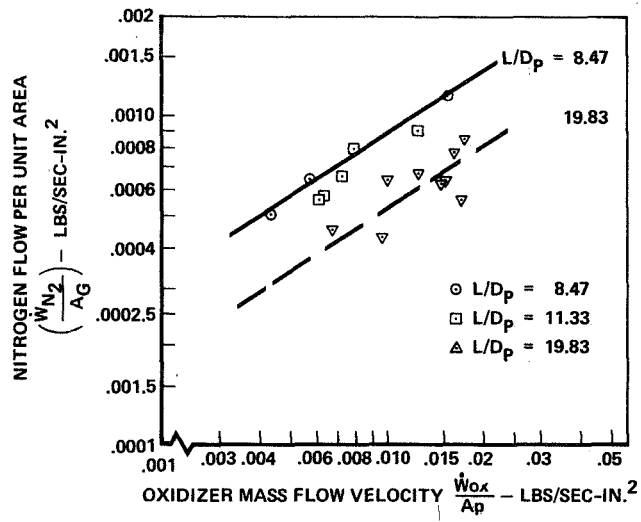


FIGURE 31. BURNING RATE CORRELATION

Optimum Gas Temperatures Study

A study was conducted as part of Task II to estimate optimum gas temperature for the various propellant and expulsion combinations of interest, as presented by the following cases:

1. Gas impinging directly on mild cryogenics of the $\text{OF}_2 - \text{B}_2\text{H}_6$ class.
2. Gas impinging directly on earth storable propellants of the $\text{N}_2\text{O}_4 - \text{N}_2\text{H}_4$ class.
3. Gas impinging on Teflon bladder.
4. Gas impinging on metal diaphragms.

Each case is further subdivided into: (1) single pulse — continuous expulsion to depletion, and (2) multiple pulses — expelling 10 percent, 80 percent, and 10 percent of propellant per event with thermal equilibrium established between events.

Background and results of the study are summarized in the paragraphs which follow. Details are provided in Appendix II.

THEORETICAL BACKGROUND

After review of existing thermodynamic computer programs generated by Northrop, NASA Lewis and NASA Marshall, it was decided that it would be more efficient to generate a new program for this study. Optimization is on the basis of minimum system weight, i.e., pressurant, propellant evaporated, plus tankage weight increments. The tradeoff which occurs, then, is between weight of pressurant gas, which decreases with increasing temperature, and weights of propellant evaporated and tank wall, which increase with gas temperature.

The thermodynamic analysis, using a "lumped system" approach, closely follows the work of Gluck and Kline.* In addition, the model for heat transfer to the tank wall assumes well diffused gas, i.e., "gentle" injection with temperature varying vertically and linearly from the inlet valve to liquid saturation temperature at any instant in time. Further, mass transfer resistance at the interface is neglected.

The thermodynamic analysis also assumes flat-ended cylindrical tankage. Results were converted to spherical tankage on the basis of equivalent tank wall mass and enclosed volume; conversion to cylindrical tankage with hemispherical ends was on the basis of equal diameters and enclosed volume.

*Reference 78

RESULTS

Results are based on the following uniform assumptions:

- Spherical tankage, 20 inches to 40 inches in diameter
- Cylindrical tankage of equivalent volume with hemispherical ends and $L/D = 2$
- Titanium tank wall material (0.02 inch minimum gage)
- Tank wall factor of safety of 2.0
- Operating pressure of 200 psia
- Nitrogen gas pressurant
- Typical earth storable propellant thermodynamic properties represented by N_2H_4
- Typical space storable propellant thermodynamic properties represented by B_2H_6
- Nominal heat transfer coefficient between gas and wall of 8.0 BTU/HR Ft^2F
- Nominal expulsion time of 500 sec (maximum 1000 sec)
- Nominal formula for tank wall heat loss to environment given by:
$$\dot{q} = \sigma \epsilon \left(\frac{T_{\text{gas inlet}} + T_{\text{liq}}}{4} \right)^4$$
- Multiple pulse case expels 10 percent, 80 percent, and 10 percent of propellant per event.

Figure 32a shows the influence of tank volume and shape on optimum gas temperature for earth storable propellants. The following conclusions may be drawn from this figure:

1. The optimum temperatures for single pulse cylindrical and spherical tankage are approximately 900 and 1300F, respectively, with volume having negligible influence.
2. Optimum temperatures vary with volume for multiple pulse cylindrical and spherical tankage, from 1800 to 1500 and 2400 to 1930R, respectively.
3. Optimum temperatures are probably higher for spherical tankage than for cylindrical tankage due to the higher structural efficiency of spherical tanks.

4. Optimum temperatures are probably higher for multiple pulse operation due to the need to heat cool ullage gas injected during the previous pulse.

Figure 32b indicates similar trends for space storable propellants, with a bit more sensitivity to tankage volume in the single pulse case.

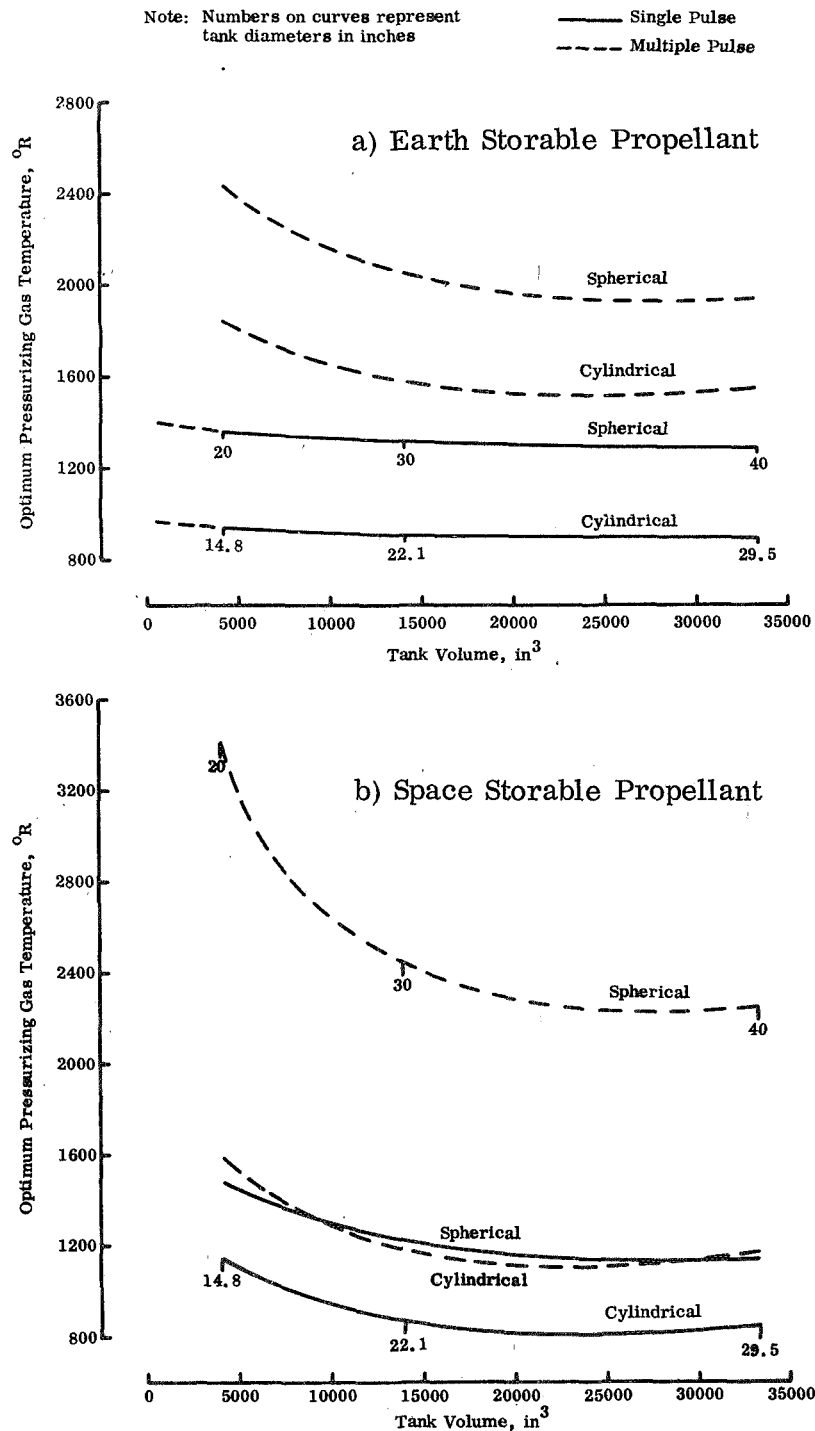


FIGURE 32. INFLUENCE OF TANK VOLUME AND SHAPE OF OPTIMUM PRESSURE

The nominal value of tank wall heat transfer coefficient was chosen on the low side for a 1 g situation, based on correlation studies conducted at NASA Lewis. Figure 33 shows the effect of variations in this value. Lower values, which are likely in low g situations, will result in higher optimum temperatures; higher values, occurring with more turbulent gas flow, will decrease optimum temperatures slightly.

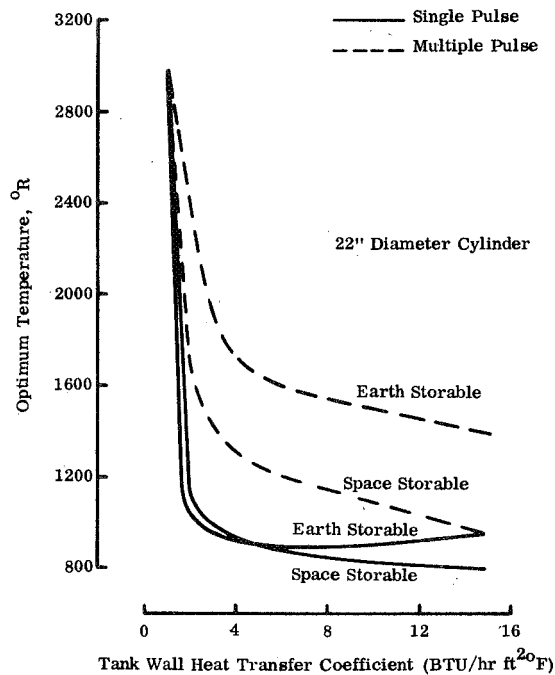


FIGURE 33. EFFECT OF TANK WALL HEAT TRANSFER COEFFICIENT ON OPTIMUM INLET TEMPERATURE

Figure 34a shows the effect of flow duration on optimum temperature of a 30 inch spherical tank under single pulse conditions. It may be seen that there is no significant influence, for earth storable propellant; for space storable propellants, optimum temperature drops 20 percent over the range 200 to 1000 seconds. Values of optimum temperature for earth and space storable propellants both drop approximately 30 percent over the time range for multiple pulse operation, as shown by Figure 34b.

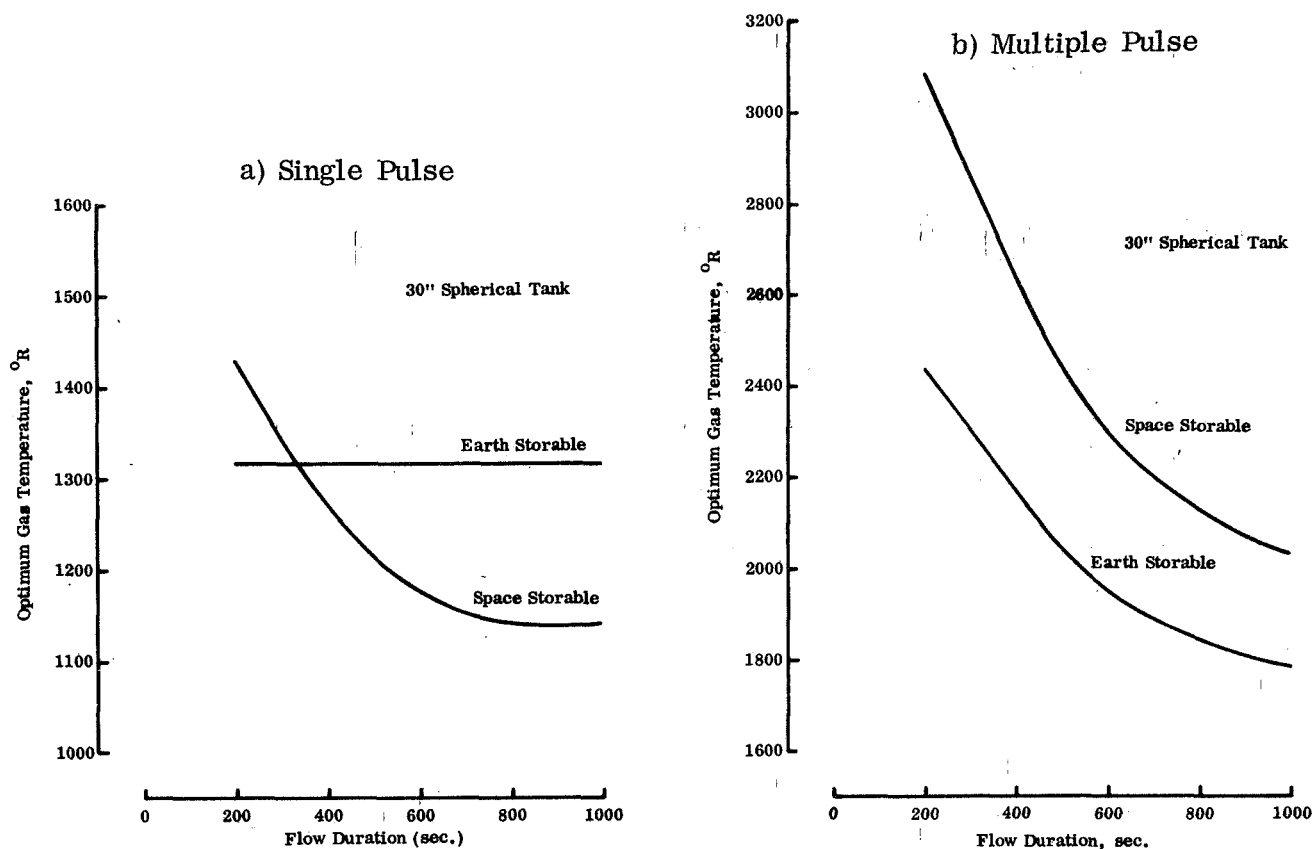


FIGURE 34. INFLUENCE OF FLOW DURATION ON OPTIMUM GAS TEMPERATURE

The thermal model predicted no vaporization of the earth storable propellant (hydrazine) up to the maximum gas inlet temperature considered (3000R). In the case of the space storable propellant (diborane), vaporization began at a gas inlet temperature of 2300R, but amounted to only 0.07 pounds at 3000R. Thus, it may be concluded that propellant vaporization is not a significant factor in system optimization with well diffused gas injection. Along with this fact, analysis indicated that the absence or presence of either a teflon or aluminum bladder (.02 inches thick) had no influence on heat transfer across the gas/propellant interface and thus, does not influence optimum gas temperature.

Figures 35a and 35b present typical plots of the two major component weights versus gas inlet temperature. As noted previously, propellant evaporation does not appear to be a significant influence; therefore, pressurant mass and tankage weight

determine optimum gas inlet temperature.* It may be seen that tankage weight is the most significant influence; addition of inner insulation (with its accompanying weight tradeoff) might be considered to reduce this effect.

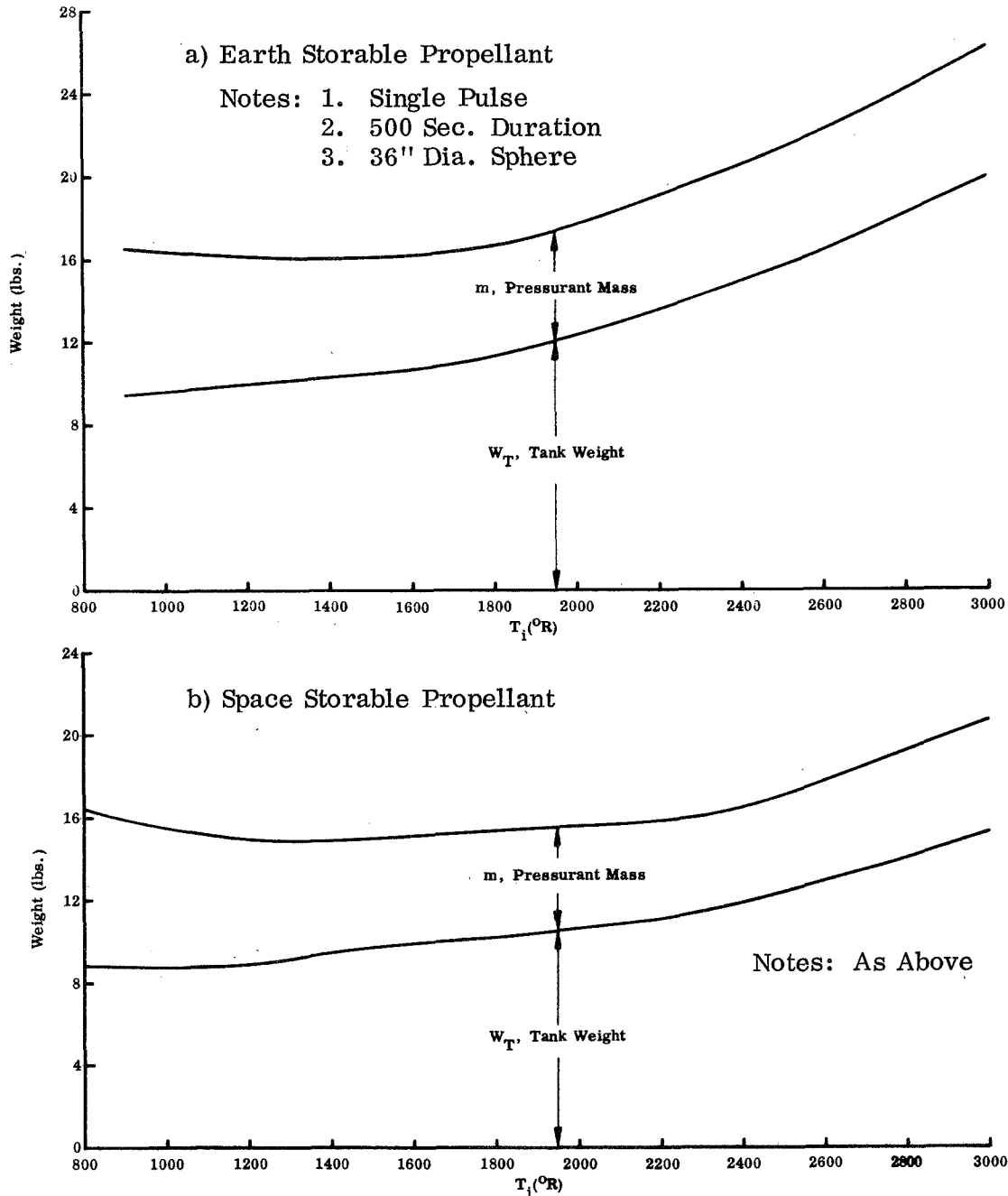


FIGURE 35. VARIATION OF COMPONENT WEIGHTS WITH PRESSURANT INLET TEMPERATURE

* It would perhaps be more rigorous to additionally include gas generator inert weight, which at the present time is some unknown fraction of pressurant mass; a small shift of the optimum to higher values would occur but tankage weight will remain the overriding influence.

SECTION VII

SUMMARY AND CONCLUSIONS

A review of available information in pertinent areas was conducted during which searches of the literature and contacts with fuels researchers were made. The resulting information proved useful to many aspects of the program. A bibliography of the literature reviewed will be found in Appendix I.

Analytical study of acceptable hot gas constituents (those providing theoretical reaction temperatures below 2000F with CTF or NTO) indicated that no hydrogen or methane content is permissible with CTF, and very little is permissible with NTO; acceptable amounts of other constituents were also identified. Theoretical study of a list of potential fuels, treated with various additives to reduce temperature and/or reactivity, showed that none were more suitable than sodium azide.

Experimental studies indicated that CTF/sodium azide was hypergolic; hypergolic ignition was not obtained with NTO/sodium azide, with or without potentially hypergolic additives. This was also true of CTF/teflon.

On the basis of these analytical and experimental studies, the combination chlorine trifluoride/sodium azide was selected as the hybrid liquid oxidizer/solid fuel for the breadboard pressurization system. Theoretical computations, at an oxidizer/fuel ratio of 0.04, indicate a combustion temperature of 1575F and a yield of 62.2 percent nitrogen, with 32.6 percent liquid products and 5.2 percent solids, separable in a Demister/filter.

Dies were manufactured and fuel grains pressed in both 1/4-inch to 1/2-inch diameter pellets and perforated slugs, of various inside and outside diameters, for tests in both pellet bed and shell grain configurations.

Extensive combustion studies were conducted in a 1-1/4-inch diameter chamber with grain lengths varying from 1 inch to 8 inches. All configurations (shell, pellet bed, or mixed) burned stably and at moderate temperatures; combustion ceased upon termination of oxidizer flow. Stable operation was also obtained at extremely low injector ΔP . Shell grains were found to burn in an end plus internal burning mode. As part of this effort, a combination of valve, injector, and combustion chamber was achieved which is capable of operating steady-state with extremely small oxidizer flows (as low as 5×10^{-4} lb/sec). In addition, a capillary flowmeter was successfully developed to measure these low flow rates.

Breadboard system design was based on the results of this previous phase of testing. A shell grain, 7 inches long by 1-1/4-inch OD by 3/8-inch ID was initially selected, but it was later found necessary to modify the design to 1-1/2-inch OD by 5/8-inch ID to obtain the desired weight flow. Previous test equipment was used, with the addition of a longer chamber body, a Demister, and vacuum jacketed expellant tank.

Analytical techniques were derived during this and the previous test phase which provided accurate analysis and correlation of test results. The regression rate was found to conform to "classical" hybrid behavior in the following form:

$$\dot{r} = 1.173 G_{ox}^{.6} \left(\frac{L}{D_p} \right)^{-.61}$$

Optimum gas temperatures were studied theoretically for both earth and space storable propellants, with and without bladders, and for both spherical and cylindrical tankage. The essential tradeoff which was found to occur was between pressurant mass, which decreases with increasing temperature, and tank wall mass, which increases with increasing temperature.

Final demonstrated results of the breadboard system testing were as follows:

- Specified gas weight flow ($.008 \pm .002$ lb/sec) and pressure (200 ± 20 PSIA).
- 60 seconds burning duration with only 10% fuel residuals.
- Specified expulsions of water and liquid nitrogen, including expulsion of liquid nitrogen in three sequential events.
- All sodium trapped by the Demister; no CTF detected in gas samples.
- Pressure feedback loop operates satisfactorily in controlling oxidizer flow and holding pressure within specified limits.

It may be concluded that CTF/sodium azide represents a suitable combination for a hybrid pressurization system, that the concept will generate hot non-reactive nitrogen gas which is pressure controllable, and that the concept is ideal for direct contact pressurization of propellant tanks on restart and/or throttling rocket applications.

SECTION VIII
RECOMMENDATIONS FOR FURTHER STUDY
OF THE HYBRID PRESSURIZATION SYSTEM

The objectives of further study are to expand the usefulness of the concept and to explore design aspects critical to flight-weight system design while learning more about basic thermochemical characteristics of the system. Study is broken up into the following headings; tasks may be conducted totally, individually, or in part.

I - High Hydrogen Hybrid Pressurization Systems

Use of a separate pressurization system for the fuel tank would eliminate the possibility of oxidizer migration through connecting lines and permit design of a Hybrid Pressurization System based on a fuel rich in hydrogen, as well as nitrogen, thus providing a low molecular weight gas and lighter weight system.

A study of this approach would draw upon the knowledge accumulated thus far. For example, fuels rejected during the inert gas study, because of their obviously high hydrogen content, or which were discarded when theoretical computations indicated excessive hydrogen, would provide a starting point for this study. This would include DB-27, TAG (and related compounds), the tetrazoles, dicyandiamide, and hydrazine azide.

Preliminary studies indicate that hot gases having a combined molecular weight of approximately 13-14 (half that of nitrogen) could be obtained; in addition, yield would approach 100 percent of the fuel (as versus 64 percent with sodium azide).

II - Hot Gas Pressurization of Earth and Space Storable Propellants

Review of the literature indicated a severe lack of experimental data to verify theoretical computations regarding hot gas pressurization of both earth and space storable propellants; therefore, the following study effort is recommended.

A. DIFFUSER DESIGN

Effective diffusers need to be developed for both earth and space storable

propellants, with and without positive expulsion devices. Both analytical and experimental studies will be conducted.

B. OXIDIZER EXPULSION SYSTEM

An expulsion system suitable for zero "G" operation is necessary for the hybrid oxidizer on the flight configuration. Experimental study and development of pressurization and propellant orientation components are required. Pressurized nitrogen gas with either a surface tension device or reversing aluminum diaphragm would probably represent the initial approach.

C. DESIGN AND CORRELATION STUDIES

Tests will be conducted, with optimum diffuser designs from Part (A) and various sizes of flight weight tankage, which include the effects of external environment, expellant type and flow rate, gas temperature, and operating duration. The optimum gas temperature computer program, developed during this contract, and/or other programs will be empirically correlated to the test results.

III - Operational/Theoretical Aspects

Studies under this heading represent a natural progression beyond the limitations of the breadboard system, toward the level of flight-weight system performance. In addition, studies are required which, although not contributing directly to a specific point design, will broaden the base of understanding and thus contribute to a more efficient design. The following aspects merit investigation.

A. TRANSPARENT CHAMBER STUDIES

Use of a transparent walled chamber will enable studies to be made of the influence of injector design and location on grain burning behavior, and will permit study of sodium formation and removal. A half-cylinder of metal with a transparent flat side-wall is envisioned.

B. CHAMBER ORIENTATION STUDIES

The breadboard test set-up will be modified to permit rotation of the combustion chamber from horizontal to vertical. By conducting tests at various angles, the influence of acceleration on sodium removal and thus, combustion behavior, can be studied. Some of these studies would also utilize the transparent walled chamber.

C. BURNING DURATION EXTENSION

Studies will be made to extend operating duration to several minutes. Primary emphasis will be on added grain length and its influence on performance.

D. REGRESSION RATE CORRELATIONS

Additional studies will be conducted to fully characterize regression rate with respect to oxidizer flow per unit of port area, chamber pressure, grain length, and port area.

E. INJECTOR DESIGN

A commercial, readily available injector was used on this program. Improvements in design will be studied and tested in the present breadboard, extended length, and transparent walled chambers.

F. COMBUSTION EFFICIENCY IMPROVEMENT

Combustion efficiency should be improved with extended grain length and as a result of information gained from (A), (B), and (E); if necessary, additional study of chamber and grain design, including addition of turbulators, will be included.

G. PELLET BED DESIGN

Since the pellet bed concept was not selected for breadboard design primarily due to the inconvenience of producing pellets manually (good combustion characteristics were exhibited), further study with machine-pressed pellets is warranted.

H. CHAMBER/DEMISTER INSULATION

A non-contaminating insulation will be required to minimize system weight and increase efficiency for extended duration operation. It is believed that either a graphite-based or ceramic-based insulation will meet this requirement.

SECTION IX

COMPARISONS

An analytical comparison study was made to identify potential performance advantages of the hybrid system. The hybrid gas generator and competitive systems were designed for a typical set of requirements and performance calculated and compared on the basis of weight, volume, and reliability. The paragraphs which follow document this effort.

Requirements

The following typical design requirements were assumed:

Tank Pressure	200 psia
Allowable Bulk Gas Temperature	980°R
Propellant Volume	10 ft ³

For a typical application, a final bulk gas temperature of 980°R would result from a theoretical gas combustion temperature of about 1890°R, considering combustion efficiency and heat losses to ducting, tank wall, and propellant.

These requirements were intentionally simplified and did not include advanced performance needs which might favor the hybrid pressurization system. Component redundancy was omitted to obtain a clear-cut comparison. Operating duration was also omitted and reliability judged on the basis of failure rate per 100 hours.

Design and Performance

All reactant, reactant container, and reactant pressurization system weights and volumes were calculated on a uniform basis for fair comparison. The weights and volumes of pressure regulators, valves, and other similar components, were obtained from the Pressurization Systems Design Guide, Aerojet-General Report No. 2736 (July 1966 revision). This reference was also the source of failure rate data; when data was not available, failure rates and weights were estimated on the basis of similar components.

Since some competitive pressurization systems produce a reactive gas, comparisons were made separately between those systems capable of producing nonreactive gas and those producing reactive gas.

NONREACTIVE PRESSURIZATION SYSTEMS

Component weights, volumes, and failure rates of systems producing nonreactive pressurizing gas are listed in Table 1. Screen tension devices are assumed for liquid orientation of both gas generator reactants and expelled propellants--weights, volumes and failure rates are neglected. The systems are described in the paragraphs which follow.

Hybrid - Sodium Azide

Design was based on a nitrogen yield of 0.61 lb/lb of sodium azide, 10 percent residuals, 90 percent volumetric efficiency, and chlorine trifluoride oxidizer. The oxidizer is stored in a container which also contains an equal volume of nitrogen gas under initial pressure of 2000 psia for expulsion. Flow into the chamber, after initial opening of a squib valve, is controlled by a nonmodulating pressure regulator, thus eliminating the need for any major valving.

Since the combustion chamber requires only a simple, single element injector and a minimum of insulation, and the hybrid grain is, by nature, not subject to problems due to cracks or inhibitor failure, a reliability similar to that of a heat exchanger was assigned. Two filters (one oxidizer and one hot gas), two fill valves, and a squib-actuated valve are included under Miscellaneous.

Stored Nitrogen Gas

The stored nitrogen gas design assumes storage at 3000 psi and 520°R in a titanium tank, no heat transfer to the tank during use, and the need for a relief valve (plus a 10 percent gas reserve), due to the possibility of heat transfer from propellant to gas and accompanying overpressurization during intermediate shutdown. A filter, fill valve, and squib-actuated valve are also included under Miscellaneous.

Stored and Heated Nitrogen Gas

This design assumes gas stored under similar conditions, and with similar components as the previous system, but with the gas heated in a nozzle heat exchanger to a final bulk gas temperature similar to the hybrid system (980°R). A weight

penalty was not included for the heat exchanger, but the computed gas weight was increased by 50 percent to allow for cold starts. A 3-position solenoid valve plus a temperature transducer and amplifier were included to regulate flow and temperature of the gas. An active valve, capable of bypassing a portion of flow around the heat exchanger, is necessary to compensate for both changing stored gas temperature and heat exchanger wall temperature.

Bipropellant

Nitrogen tetroxide and a hydrazine-type fuel are assumed to be burned in two chambers, one providing fuel-rich products (with molecular weight of 11) and the other, oxidizer rich (with molecular weight of 28.7). Due to the nature of the concept, two bipropellant valves (listed under major valves) and a separate stored gas pressurization system are necessary. Miscellaneous components include 1 squib-valve, 5 fill valves, and three filters; two pressure transducers with amplifiers are required to maintain delivered gas pressure.

REACTIVE PRESSURIZATION SYSTEMS

Table 2 lists component weights, volumes, and failure rates of those systems producing a reactive pressurizing gas (high in hydrogen or hydrogen-containing compounds). Bladders, required to provide separation of this gas from the expelled propellants, are not included in the table. The failure rate for one bladder is given as 8.5 failures/100 hrs. in the referenced report — a value which would overshadow the remainder of the comparison. The systems are described in the paragraphs which follow.

Hybrid — DB-27

Previous study at Northrop indicated that DB-27, a classified compound high in hydrogen which was developed by Dow, reacted hypergolically and smoothly with CTF. There are also other fuels such as TAG, TAGCY, miscellaneous tetrazoles, etc., which would provide hot gas of low molecular weight. A system was designed assuming a gas molecular weight of 15, and 100 percent gas yield; other assumptions and components are similar to the sodium azide based hybrid design.

Solid Propellant

The solid propellant system was designed on the basis of a gas molecular weight of 21, 100 percent yield and 10 percent residuals. A hot gas relief valve, estimated to weigh 3.0 lbs, is assumed necessary to control pressure. In lieu of an actual estimate, reliability of the chamber was assumed similar to that of an ablative chamber as listed in the referenced design guide.

Monopropellant

The monopropellant system design is based on a hydrazine-type reactant with an assumed hot gas molecular weight of 18.3. A separate stored gas pressurization system is assumed; however, operation of the liquid reactant flow control is assumed similar to that of the hybrid oxidizer (a nonmodulating pressure regulator). A reactor failure rate similar to the hybrid is also assumed, in view of the basic simplicity. Additional components include 2 filters, 1 squib-actuated valve, and 3 fill valves.

COMPARISON

Table 3 summarizes weights, volumes, and reliabilities of all systems studied. Review of the nonreactive systems indicates that the hybrid system is 40 percent lighter than the next lightest system (the bipropellant) and significantly more reliable. Weight savings are even more significant in comparison to stored gas systems and extremely large savings in volume also occur. Reliability appears to fall between that of ambient stored gas and heated gas systems.

As shown in the table, the reactive gas systems, due to their inherently lower molecular weight products, are significantly lighter in weight. Again, a hybrid system shows advantages in weight, volume, and reliability over competing system.

It is important to note that a reactive gas system decreases vehicle reliability and safety. If the system is designed for direct contact between the gas and propellants, and a controlled reaction is planned, there is the danger of higher temperatures and local hot spots. Should the vehicle flight mode require some form of bladder, the problem of an unplanned reaction between the gas and the oxidizer exists. A small propellant leak could result in a near stoichiometric reaction, with accompanying high

temperatures and serious damage to the bladder and/or tank wall. Thus, where failure of the bladder (note the rather high failure rate) with inert gas would only degrade performance, failure with a reactive pressurant could result in total vehicle loss.*

Summary

The results of this comparison are necessarily confined to the requirements assumed, and are presented only to show potential advantages of the hybrid in appropriate applications. Although absolute magnitudes of the differences computed are not large, it should be recalled that where pressurization systems are being considered for final stages of propulsion weight savings are directly translatable into payload; volume and reliability are also at their most critical level in these applications.

The advantages of the hybrid pressurization system may be summarized as follows:

1. Weight and Volume Savings: Significant weight savings are realized over all competitive systems; volume is comparable to the most compact.
2. High Reliability: Large performance improvements are obtained over stored gas systems with small degradation in reliability. Reliability of the hybrid is significantly better than competitive advanced systems.
3. Potential Design and Operating Advantages: Design and operating advantages present to a varying, but significant extent in comparison to all of the competitive advanced systems include:
 - a. Design simplicity
 - b. Compact, modular design
 - c. Nonreactive gas
 - d. Potential for broad storage and operating temperatures
 - e. Desirable delivered gas temperatures
 - f. Controllability
 - g. Repeatability of flow

* An attractive alternative exists in the use of a reactive hybrid for fuel expulsion and a nonreactive hybrid for oxidizer expulsion (with a weight of 15 lbs. and failure of .7169 in the present application).

TABLE 1. TABULATED WEIGHTS, VOLUMES, AND FAILURE RATES - NONREACTIVE SYSTEMS

COMPONENT	HYBRID-AZIDE				STORED N ₂ GAS				STORED AND HEATED N ₂ GAS				BIPROPELLANT			
	QTY	LBS	IN ³	FAIL/ 100 HRS	QTY	LBS	IN ³	FAIL/ 100 HRS	QTY	LBS	IN ³	FAIL/ 100 HRS	QTY	LBS	IN ³	FAIL/ 100 HRS
OXIDIZER/ FUEL	1 EA	9.6	—	—	0	—	—	—	0	—	—	—	1 EA	4.2	—	—
O/F CONTAINER	1 EA	5.0	249	0.1500*	0	—	—	—	0	—	—	—	1 EA	0.8	89.3	<10 ⁻⁴
COMB CHAMBER	INCL IN FUEL CONTAINER				0	—	—	—	0	—	—	—	2	6.5	52.2	1.0000
PRESSURANT AND TANK	INCL IN OX CONTAINER				1	43.6	2230	<10 ⁻⁴	1	25.0	1140	<10 ⁻⁴	1	.3		<10 ⁻⁴
HEAT EXCHANGER	0	—	—	—	0	—	—	—	1	NEGLECTED		0.1500*	0	—	—	—
PRES REGULATOR	1	0.8	8.5	0.1820	1	.8	8.5	0.1820	1	0.8	8.5	0.1820	1	0.8	8.5	0.1820
MAJOR VALVES	0	—	—	—	1	.4	4.0	0.0446	1	3.5	8.5	0.1350*	2	14.0	34.0	0.6720
TRANSD AND AMPLIF	0	—	—	—	0	—	—	—	1	—	—	0.0860*	2	—	—	0.1720*
MISCELLANEOUS	5	3.7	38.5	0.0529	3	3.1	33.5	0.0075	3	3.1	33.5	0.0075	9	5.2	51.5	0.1129
TOTALS	10	19.1	296.0	0.3849	6	47.9	2276.0	0.2341	8	32.4	1190.5	0.5605	21	31.8	247.0	2.1389

*ESTIMATED VALUES

TABLE 2. TABULATED WEIGHTS, VOLUMES AND FAILURE RATES - REACTIVE SYSTEMS

COMPONENT	HYBRID-DB-27				SOLID				MONOPROPELLANT			
	QTY	LBS	IN ³	FAIL/ 100 HRS	QTY	LBS	IN ³	FAIL/ 100 HRS	QTY	LBS	IN ³	FAIL/ 100 HRS
OXIDIZER/ FUEL	1 EA	3.2	—	—	1	4.3	—	—	1	3.8	—	—
O/F CONTAINER	1 EA	2.7	60.0	0.1500*	1	1.9	94.0	0.6560*	1	1.1	105.5	<10 ⁻⁴
COMB CHAMBER	INCL IN FUEL CONTAINER				INCL IN FUEL CONTAINER				1	4.0	38.0	0.1500*
PRESSURANT AND TANK	INCL IN OX CONTAINER				0	—	—	—	1	0.8	12.0	<10 ⁻⁴
IGNITER	0	—	—	—	1	0.4*	8.0*	0.0100	0	—	—	—
PRES REGULATOR	1	0.8	8.5	0.1820	0	—	—	—	2	1.6	17.0	0.3640
MAJOR VALVES	0	—	—	—	1	3.0*	8.0*	0.4460*	0	—	—	—
MISCELLANEOUS	5	3.7	38.5	0.0529	1	2.0	20.0	<10 ⁻⁴	6	4.1	42.5	.0602
TOTALS	10	10.4	107.0	0.3849	5	11.6	130.0	1.1120	12	15.4	215.0	0.5742

*ESTIMATED VALUES

TABLE 3. SUMMARY OF SYSTEM PERFORMANCE

SYSTEM	WEIGHT (LBS)	VOLUME (IN ³)	FAILURES/100 HRS
<u>NONREACTIVE</u>			
HYBRID – CTF/SODIUM AZIDE	19.1	296.0	0.3849
STORED NITROGEN GAS	47.9	2,276.0	0.2341
STORED & HEATED NITROGEN GAS	32.4	1,190.5	0.5605
BIPROPELLANT	31.8	247.0	2.1389
<u>REACTIVE</u>			
HYBRID – CTF/DB-27	10.4	107.0	0.3849
SOLID PROPELLANT	11.6	130.0	1.1120
MONOPROPELLANT (HYDRAZINE)	15.4	215.0	0.5742

APPENDIX I

BIBLIOGRAPHY OF DOCUMENTS PERTINENT TO STUDY OF HYBRID PRESSURIZATION SYSTEMS

The results of the literature searches conducted under the contract are included in the pages which follow. Pertinent documents are annotated and listed under the following headings:

- . Hybrid Systems
- . Fuels
- . Pressurization and Expulsion Systems
- . Injector Design

Documents are listed alphabetically by source or author and chronologically under source. Those documents reviewed, but whose content was not found germane, are referenced without annotation at the end of each group.

Hybrid Systems

1. Aerojet-General Corporation,
HYBRID ROCKET ENGINE FEASIBILITY PROGRAM, Report No. 0382-04F,
April 1962.

A program to demonstrate feasibility of the hybrid rocket engine was conducted by Aerojet-General Corporation.

Theoretical analysis, laboratory investigations, fuel fabrication, component design, full-scale testing, and post firing engine analyses were performed. Four major systems were subjected to full scale testing: Aluminum plus Polyurethane with CTF, Lithium Hydride plus Titanium Hydride with CTF, Lithium Hydride plus Aluminum with CTF, and Lithium Hydride plus Aluminum with CTF plus bromine pentafluoride. The latter system demonstrated the most promise.

2. Chemical Propulsion Information Agency,
CHEMICAL PROPULSION ABSTRACTS, 1965-1968

Provided many of the references obtained and annotated in this report.

3. Liquid Propulsion Information Agency,
PRESENTATIONS OF HYBRID PROPULSION SYSTEMS SYMPOSIUM, Document No. LHS-1
January 1962.

Presents resumes of hybrid studies active at the time of symposium. Provided useful further references.

4. Lockheed Propulsion Company,
HYBRID PROPULSION RESEARCH PROGRAM, Fourth Quarter Report No. 594-2-4
(AD 338 759), 15 July 1963.

Studied NTO and CTF with hydrocarbon and lithium hydride fuels. Found that regression rate behavior followed the relationship

$$r = a(G)^{0.8}$$

5. Lockheed Propulsion Company,
GRAIN DESIGN FOR HYBRID MOTORS, Special Report No. 594-S-1, January
1963, (AD 333 988).

Report summarizes knowledge of hybrid grain design. Presents a somewhat different regression rate law:

$$r = a \frac{(G)^{0.8}}{(L)^{0.2}} + b$$

Where $G = \frac{\dot{W}_t}{A_p} \quad \frac{(\text{Total Weight Flow Through Nozzle})}{(\text{Port Area})}$

L = Length of Port

a, b = Coefficients (Not necessarily constant)

6. Redstone Scientific Information Center,
HYBRID PROPULSION, A BIBLIOGRAPHY, by G. J. Caras, Report RSIC-687,
August 1967 (C).

Report contained annotated references to the published literature and provided several references of potential interest.

7. Rohm and Haas,
HYBRID MOTOR CONCEPTS (II) & (III) - DEV. OF THE TANDEM SOLID-HYBRID
MOTOR FOR ZONING DEMONSTRATION, by W. C. Stone, Report S-82, August 1966,
(AD 374 598 and AD 385867).

Studies conducted with IRNA/hydrocarbon plus Aluminum (not hypergolic). Obtained regression rates in the neighborhood of .02 in/sec.

8. United Technology Corporation,
INVESTIGATION OF FUNDAMENTAL PHENOMENA IN HYBRID PROPULSION, Contract
NOw-63-0737-c, Final Report 2051-FR, July 1964.

Report, extremely academic in part, discusses and verifies fundamentals of hybrid behavior. Verifies the simplified form of regression rate equation for low radiation systems:

$$\dot{r} = a G_o^n$$

More sophisticated equations are difficult to use due to typing errors and multitude of components.

9. Aerojet-General Corporation,
HYBRID ENGINE PERFORMANCE IMPROVEMENT PROGRAM, Contract NOw 63-0666-c,
Report No. 0792-81 (Final), June 1964.

10. Chemical Propulsion Information Agency,
ICRPG/AIAA SOLID PROPULSION CONFERENCE, June 1965-1968.
11. Lockheed Propulsion Company
AN INVESTIGATION OF THE CHARACTERISTICS OF HYBRID PROPULSION SYSTEMS,
Report No. 628-F, Air Force Report No. RTD-TDR-63-1116, Vol. I, II,
December 1963, (AD 346 620).
12. Lockheed Propulsion Company,
HYBRID PROPULSION RESEARCH PROGRAM, Vol. II, Quarterly Tech., Summary
Report No. 6, TP 2990, January 1964.
13. Naval Ordnance Test Station,
PROPULSION TECHNIQUES, SYSTEMS, AND ANALYSIS, TP 2990, July 1961,
(AD 330 265).
14. United Technology Center,
DEMONSTRATION OF A HIGH THRUST HYBRID THRUST CHAMBER ASSEMBLY, by J. R.
Feemster, Air Force Report No. AFRPL-TR-68-56, April 1968.

Fuels

15. Aerojet-General Corporation,
DEVELOPMENT OF SELF-GENERATING PROPELLANT PRESSURIZATION SYSTEMS,
by Hughes, Secchi, Bamesberger, et al, AFFTC TR 60-68, Part I and II, October 1960, June 1961.

The feasibility of using sodium azide and lithium azide as prime gas generants in a viton rubber formulation was demonstrated, A technique for pilot plant production of high purity LiN_3 was developed. LiN_3 was incorporated in various binder matrices. Final feasibility was demonstrated by mini-midget motor firings. (LiN_3 and LiN_3 in matrices functions as a monopropellant).

16. Aerojet-General Corporation,
DEVELOPMENT AND DEMONSTRATION OF INERT GAS PRESSURIZATION SYSTEM,
Vol. 6, Report 8160-01Q-6F, November 1960.

Discusses prototype sodium azide/viton binder solid propellant gas generators which delivered gas in the temperature range, 500-1000°F. Used a solid propellant grain, cooling section (azide pellets), Demister, centrifugal separator, and porous filter element. Burning rate range was $1/16''$ - 1 in/sec at pressures of 20-2000 psia. Also expelled Nitrogen tetroxide/Aerozine 50 successfully without separator or filter.

17. Aerojet-General Corporation,
RESEARCH AND DEVELOPMENT ON HYBRID PROPELLANTS, by Lawrence, R. W., et al, Contract NOW 61-0950-c, Quarterly Progress Report No. 0532-01-3, April 1962.

Report considered performance of several high nitrogen compounds, $(\text{C}_2\text{H}_3\text{N}_5)_n$, $(\text{C}_2\text{H}_3\text{N}_5)_n$, $(\text{C}_5\text{H}_{16}\text{N}_{12})_n$ with CTF (among others) which could be of interest to the HPS study. Heats of formation and densities are provided. Studied burning rates of CaB_6 and AlB_2 .

18. Aerojet-General Corporation,
RESEARCH AND DEVELOPMENT ON HYBRID PROPELLANTS, by Lawrence, R. W., et al, Contract NOW 61-0950-c, Quarterly Progress Report No. 0532-01-4, July 1962.

Reported on preparation of TiB_3 : Found that it decomposes at ambient temperatures. Pressed grains at 10,000 - 40,000 psi with satisfactory properties. Tested reactivity of CaB_6 , BaB_6 (among others) with MDFNA and CTF; none ignited hypergolically with DMFNA, all did so with CTF. Describes use of a 1" I.D. combustor with brass hollow-cone spray injectors. Grains consisted of 4 1" long x 1-1/8" dia. slugs.

19. Aerojet-General Corporation,
INVESTIGATION OF ADVANCED HYBRID PROPELLANTS, Contract N600(19)59367, Quart. Report No. 0722-01-3, July 1963.

Primarily studied LiH/Al/PBDA/PS with CTF but provides useful information on use of small combustors and general hybrid behavior.

20. Aerojet-General Corporation,
INVESTIGATION OF ADV. HYBRID PROPELLANTS, Contract NOW 64-0210-c, Report No. 0722-03-2 (Quart.), July 1964.

Report covers progress in R&D work on a hybrid propellant system, LiH/Al/ PBDA/PS with ClF_3 , ClO_3F , and BrF_5 chosen for study under previous program (Contract N600(19)-59367. While the fuel as such is not appropriate to hybrid pressurization system studies, the report discusses work with small fuel grains and a related oxidizer. Use of aluminum dodecaboride (AlB_{12}) as a regression rate modifier is also discussed and a supply source noted.

21. Aerojet-General Corporation,
RESEARCH AND DEVELOPMENT OF HIGH ENERGY PROPELLANTS FROM NITROGEN-RICH BINDERS, Report 0876-81F, April 1965 (AD 358 894).

INVESTIGATION OF ADV. HYBRID PROPELLANTS (Continued)

The report covers synthesis and evaluation of nitrogen-rich compounds for three different applications: (1) polymeric binder components, (2) solid additives, (3) plasticizers. Reactions of DB-27 are included. The majority of these compounds exhibit relatively high carbon and/or hydrogen content for our immediate purpose.

22. Aerojet-General Corporation,
THEORETICAL AND EXPERIMENTAL STUDY OF EXTINGUISHABLE SOLID PROPELLANTS,
by R. L. Lou, L. C. Landers, and R. L. Lovine, Report TR No. AFRPL-TR-66-128,
July 1966, (AD 374 691).

This report summarizes a theoretical and experimental study of solid propellant extinguishment. A two-part theory of extinguishment was defined; the theory includes a criterion for extinguishment initiation and a criterion for extinguishment permanence.

23. Air Force Rocket Propulsion Laboratory,
FEASIBILITY TESTING OF A NITROGEN-GENERATING SOLID CHARGE (SODIUM AZIDE)
FOR PROPELLANT TANK PRESSURIZATION, by David T. Clift, Report RTD-TDR-63-1080,
August 1963.

Conducted four tests of the solid propellant sodium azide grain (Viton Binder) for pressurization. Tests were unsuccessful due to grain cracking in storage.

24. Air Force, Rocket Propulsion Laboratory,
PROPELLANT HANDBOOK, by P. J. Von Doehren, Report No. AFRPL-TR-66-4,
January 1966, (AD 370 870).

A compilation of data on both liquid and solid propellants is presented with emphasis on liquids. Physical properties of liquids include: boiling point, freezing point, density, heat of formation, vapor pressure, critical properties, heat of vaporization, viscosity and specific heat. A discussion of the preparation method, toxicity, sensitivity, compatibility and availability of liquid propellants is also given.

25. American Cyanamid Company,
SOLID ROCKET PROPELLANT RESEARCH AND DEVELOPMENT, Annual Report
1 January - 31 December 1964 and Final Report January 1959 - December
1964 (AD 357 794).

Reviews research on nitrogen polymers for entire period.

26. American Cyanamid Company,
SOLID ROCKET PROPELLANT RESEARCH AND DEVELOPMENT, Annual Report,
January 1 - December 31, 1963 (AD 349 669).

Discusses research in high amine binders, such as TAF-PVT, as well as NF oxidizers.

27. American Cyanamid Company,
SOLID ROCKET PROPELLANT RESEARCH AND DEVELOPMENT, Annual Report for
1964, Vol. 1 (AD 357 794) February 1965.

Provides thermochemical and physical data on several high nitrogen compounds including TAG, TAG Nitrate, TAG-5AT, TAG-PUT.

28. Armour Research Foundation,
GAS GENERATOR PROPELLANT SYSTEMS, by C. K. Hersch and J. N. Keith,
Final Report ARF 3154-49, May 1961 (AD 324 104).

Report documents laboratory study of solid propellant gas generators based primarily on azides and high nitrogen binders. Lithium Boroazide ($\text{LiB}(\text{N}_3)_4$) was found to offer the greatest improvement over Sodium azide, however, production of neither it nor the binders was fully characterized.

29. Army Engineer Research and Development Laboratory,
HYDRAZOIC ACID AND THE METAL AZIDES, Corps of Engineers Report 1551-TR,
October 1958 (AD 208 892).

This report covers data presented in the unclassified literature on HN_3 and the metal azides since 1924. The chief source of information was Chemical Abstracts. An extensive bibliography is given.

30. Arnold Engineering Development Center,
THE DESIGN AND OPERATION OF A CRYOGENIC ROCKET PROPELLANT SYSTEM
USING OXYGEN DIFLUORIDE AND DIBORANE AS PROPELLANTS, by N. S. Dougherty Jr.,
Report AEDC-TR-66-30 (AD 478 450).

A series of tests using a Thiokol-RMD research and development engine was performed at AEDC to evaluate the performance of the $\text{OF}_2/\text{B}_2\text{H}_6$ propellant combination under simulated altitude conditions (in excess of 100,000-ft equivalent ambient pressure). Discusses performance and design, cleanliness, quality control and safety requirements.

31. Atlantic Research Corporation,
CHEMICAL-KINETIC AND PHYSICAL PROCESSES IN COMPOSITE SOLID PROPELLANT
COMBUSTION, by G. Von Elbe, M. K. King, et al, NASA CR 66307,
January 1967.

The complex inter-relationships of burning velocity, thermal transport, and chemical-kinetic variables are examined. Three combustion regimes are described and analyzed. Several subtopics are reviewed; e.g., heat generation by condensed-phase reactions, gas phase kinetics, and analog burner studies.

32. AVCO Corporation,
HIGH TEMPERATURE BEHAVIOR OF TEFLON, by T. Wentink, Air Force Report
AFBMD-TN-59-15, July 1959.

Reviews properties and behavior of tetrafluoroethylene polymer in the temperature range 300-800°K.

33. Battelle Memorial Institute,
ICRPG PROPELLANT INGREDIENT SYNTHESIS CONFERENCE, October 1967.

A paper by Morton and Rosher describes a family of nitramine azides that have been synthesized and studied as ingredients in double-base propellants. The compounds are 2-nitrazapropyl azide (NPA), 1,5-diazido-2,4-dinitrazapentane (DADZP), 1,6-diazido-2,5-dinitrazahexane (DADNH), 1-azido-2,4,6-trinitrazahexane (ATAH), and 1,7-diazido-2,4,6-trinitrazahexane (DATH).

34. Boeing Company,
PROPERTIES OF SELECTED ROCKET PROPELLANTS, by Harry George, Volume I,
DND 2-11677 (AD 450 926), 21 January 1963.
A comprehensive compilation of data on beryllium, fluorine, hydrogen, lithium, oxygen, oxygen difluoride, and pentaborane. No other propellants are covered. The material presented contains the chemical, physical and thermodynamic properties as well as methods of production, handling and safety characteristics, availability and cost of the above named propellants.
35. Dow Chemical,
QUARTERLY PROGRESS REPORTS AR-2Q-64 and AR-3Q-64, August and November, 1964.
Provides thermochemical and physical data on DB-27, a high nitrogen compound.
36. Dow Chemical,
ANNUAL TECHNICAL SUMMARY REPORT (JAN-DEC 1964), by R. S. Karpuk,
Report AR-4Q-64, AFRPL-TR-65-31, February 1965.
Includes a discussion of Dow's research in nitrogen chemistry. Provides data on behavior and properties of DB-27 polymer. Also references previous quarterly reports numbers AR-2Q and AR-3Q-64.
37. Dow Chemical,
THE HEAT OF FORMATION OF PROPELLANT INGREDIENTS, Report No. AF-T0009-67, December 1967, (AD 387 455).
A tabulation of selected heats of formation and densities of propellant ingredients is given for state-of-the-art and new compounds. December 1967.
38. Experiment Incorporated,
SUPERIOR HYBRID ROCKET SYSTEMS, Final Report EI TP-170, Contract NOrd-18330, April 1961.
On the basis of a 2-1/2 year study, recommends the combination elemental Boron plus Hyrazine azide fuel/Chlorine trifluoride plus Bromide pentafluoride oxidizer.

39. Gary, P., and Waddington, T. C.,
THERMOCHEMISTRY AND REACTIVITY OF THE AZIDES I. THERMOCHEMISTRY OF
THE INORGANIC AZIDES, Proc. of Royal Soc., P. 106, A, 235, 1956.

This paper deals with the thermochemical relations of the azides and their application to reactivity. The experimental determination of consistent enthalphy data for hydrazoic acid, the aqueous azide ion, the alkali metal, the alkaline-earth and heavy metal azides is described.

40. Gray, P., and Waddington, T. C.,
THERMOCHEMISTRY AND REACTIVITY OF THE AZIDES II. LATTICE ENERGIES
OF IONIC AZIDES, ELECTRON AFFINITY AND HEAT OF FORMATION OF THE
AZIDE RADICAL AND RELATED PROPERTIES, Proc. of Royal Soc., P. 481,
A, 235, 1956.

The thermochemical data of part I, the heats of formation and solution of the alkali-metal (group 1a) azides, are used in conjunction with other data to derive values for the lattice energies of alkali-metal azides, the heat of formation of the azide radical, for the electron affinity and hydration heat of the azide ion.

41. Illinois Institute of Technology,
BULLETIN OF THE CONFERENCE ON HIGH NITROGEN CONTENT COMPOUNDS,
September 11-13, 1950.

Contained information on the preparation and properties of nitrotriazoles and nitroaminoguanidine.

42. JPL/Cal Tech,
STERILIZED SOLID-PROPELLANT ROCKET MOTORS FOR MARS LANDING MISSIONS,
by L. C. Montgomery and H. E. Marsh, Jr., Technical Report No. 32-725,
20 June 1965 (AD 620 161).

Current requirements for heat sterilizability are 3 cycles of exposure to 145°C for 36 hours. Off the shelf propellants from seven U.S. sources were subjected to this process. Four propellants passed the slump test and were evaluated for physical and ballistic changes. The chemical approach to sterilization was investigated. A state-of-the-art propellant was sterilized successfully with ethylene oxide.

43. Martin Company,
STERILIZABLE LIQUID PROPULSION SYSTEM, by C. Holt, Prepared for JPL (JPL-951709), NASA CR 88020, (N67-35988), April 1967.

This is the first quarterly report of a program designed to evaluate the effects of ETO sterilization techniques on a loaded bipropellant propulsion system. The first quarterly report covers system design and materials investigation phases.

44. Midwest Resrarch Institute,
A CRITICAL REVIEW OF THE CHEMISTRY OF ADVANCED OXIDIZERS, Program 2620-C, December 1965 (AD 370 190).

The review covers the period 1955-1965. The source material includes over 1,200 technical reports and all pertinent literature and patents. The chemistry of fluorine-containing oxidizers comprises the major portion of the review, but other oxidizers are also described. Tabulations included in the Appendices cover: toxicity, spectral information, physical and thermodynamic properties, and the reactions of perfluoroguanidine.

45. Midwest Research Institute,
A CRITICAL REVIEW OF THE CHEMISTRY OF ADVANCED FUELS, Project No. 2620, March 1966, (AD 370 189).

Summarized the chemistry discovered since about 1957 on the intense government-supported research program directed toward the development of light metal hydrides for use in fuels for advanced rockets. The chemistry of beryllium and aluminum hydrides comprises most of the review, but a chapter on compounds of very high-nitrogen content is included.

46. NASA,
COMPATIBILITY OF POLYMERIC MATERIALS WITH FLUORINE AND FLUORINE-OXYGEN MIXTURES, by L. M. Russell, H. W. Schmidt and L. H. Gordon, TN D-3392, June 1966.

COMPATIBILITY OF POLYMERIC MATERIALS WITH FLUORINE AND FLUORINE-OXYGEN MIXTURES (Continued)

Compatibility tests were performed on a number of polymeric materials with the use of various mixtures of fluorine and oxygen in both gaseous and liquid states.

47. Picatinny Arsenal,
DUAL GRAIN SYSTEMS FOR GAS GENERATORS APPLICATION, by B. D. Strauss,
Technical Memo No. 1201, March 1963.

Studied use of a second (tubular) grain containing oxamide, nitro-cellulose and triacetin downstream of a conventional double base solid. Endothermic decomposition occurred causing significant cooling. Exhaust products were not analyzed but smoke was noted.

48. Rocketdyne,
FINAL REPORT ASPEN PROPULSION SYSTEM, PART II (SUPPLEMENT: SODIUM AZIDE) GRAIN EVALUATION, Report R-2640Pa, December 1960 (AD 321 154).

A technical presentation on the experimental evaluation of sodium azide gas generators is presented. Sodium azide was compounded with Viton, a binder in approximately 9:1 ratio. Decomposition efficiencies of 92-95% were achieved. This corresponds to a 57% combustion efficiency. The most serious problem was containment of liquid sodium droplets.

49. Rocket Research Corporation,
DEVELOPMENT OF LOW TEMPERATURE GAS GENERATOR TECHNOLOGY, by R. Poole,
April, July 1967, AFTPL-TR-67-103, AFRPL-TR-67-220.

The objective of this program was to characterize hydrazine-based monopropellants which, by the use of ammonia and ammonia-water diluents, are capable of producing clean, low temperature gases when passed through a catalytic decomposition chamber.

50. Stanford Research Institute,
SYNTHESIS AND EVALUATION OF POLYCYANO COMPOUNDS AS HIGH ENERGY FUELS FOR PROPELLANT SYSTEMS, by M. B. Frankel, et al., Final Report SRI-65-0223, January 1965 (AD 357 042).

Discusses synthesis and properties and evaluates performance of polycyano compounds. Recommends TAGCY as solid propellant gas generator.

51. Stanford Research Institute,
SYNTHESIS AND EVALUATION OF POLYCYANO COMPOUNDS AS HIGH ENERGY FUELS
FOR PROPELLANT SYSTEMS, Final Report (AD 357 042), January 1965.

Report describes TAGCY (Tranimoguanidine Cyanoformate) and recommends it for use in gas generators. Indicates that TAGCY is a thermally stable, insensitive solid with high heat of formation (the latter property plus a significant amount of hydrogen in the combustion products may preclude its consideration for the hybrid pressurization system).

52. United Aircraft Corporation,
EXPERIMENTAL EVALUATION OF THE HEATS OF FORMATION OF C-H-O-N-F-B
COMPOUNDS, Report D910257-4, September 1965 (AD 367 056).

Heats of formation were determined for ten compounds formed from carbon, hydrogen, oxygen, nitrogen, fluorine, boron and chlorine. The experimental apparatus and techniques used for the determination are described.

53. United Technology Corporation.
INTEGRATED RESEARCH EFFORT ON HIGH-ENERGY HYBRID PROPELLANTS, Annual
Tech. Summary No. 2, Report 2029-AT2 (AD 351 678) July 1964.

Studies conducted with Lithium/Hydrocarbon Binder with OF_2 .
Regression Rate Given by

$$r = 0.17 G_0^{0.5}$$

Found that hollow spray cone injectors gave uneven regression (higher at head end).

54. United Technology Corporation,
AN INTEGRATED RESEARCH EFFORT ON HIGH ENERGY HYBRID PROPELLANTS,
9th Quarter Progress Report No. 2098-QPR9, (AD 359 984) January 1965.

Studies concerned with OF_2 and CTF oxidizers, lithium, lithium hydride/hydrocarbon binder and THA/Hydrocarbon binder fuels. Found that THA (double salt of triaminoguanidine azide and hydrazine azide) provided a pressure sensitive regression rate. Also studied injectors and found that hollow cone spray angles existed at which uneven length-wise grain regression did not occur.

55. United Technology Corporation,
AN INTEGRATED RESEARCH EFFORT ON HIGH-ENERGY HYBRID PROPELLANTS,
10th Quarter Progress Report No. 2098-QPR10, (AD 359 985) April 1965.
- Suggests aluminum boride (AlB_{12}) as substitute for Boron (S.G.=2.75).
A continuation of effort described in Reference 54.
56. United Technology Center,
FUNDAMENTAL INVESTIGATION OF HYPERGOLIC IGNITION OF SOLID PROPELLANTS,
(AD 363 114) January 1966 (C).
- Specific conclusions regarding operating parameters for hypergolic ignition are derived on a theoretical and empirical basis. Limiting physical conditions that must exist for hypergolic ignition are presented. A new ignition aid is described.
57. United Technology Center,
FUNDAMENTAL INVESTIGATION OF HYPERGOLIC IGNITION OF SOLID PROPELLANTS
VOL I, Report 2074-FR Contract NOW 64-0209-c (AD 372 183), April 1966 (C).
- Referenced a chemical, tetramethylammonium hydrotriborate (QMB-3) and indicated that it was very reactive with liquid CTF, IRFNA, and gaseous F_2 .
58. Aerojet-General Corporation,
HYBRID ENGINE PERFORMANCE IMPROVEMENT PROGRAM, Contract NOW 63-0666-c, Report No. 0792-81 (Final), June 1964.
59. Aerojet-General Corporation,
INVESTIGATIONS OF HYDRIDES AND COMBUSTION, Quarterly Report No. 0870-01-2, December 1964 (AD 355 919) and 0870-01-1, September 1964 (AD 355 857).
60. Lockheed Propulsion Company,
PHASE 1 REPORT - HYBRID GAS GENERATORS FOR AIR-AUGMENTED ROCKET APPLICATIONS, Report No. 847 (AFRPL-TR-67-306), November 1967.
61. NASA,
HIGH ENERGY PROPELLANTS, A continuing bibliography, April 1967. SP-7002(03).

62. Naval Weapons Center,
SOLID BORON PROPELLANTS FOR AIR-AUGMENTED PROPULSION, by J. R. Sims,
B. Y. S. Lee, and J. Gonzales, TP 4438 (AD 390 987) April 1968.
63. Rohm and Haas,
PROPELLANT TECHNOLOGY, Quarterly Progress Report P-67-4, May 1968
(AD 390 105).
64. Stanford Research Institute,
SYNTHESIS OF NOVEL BINDER SYSTEMS, Final Report No. 6636-3, June 1968
(AD 390 757).
65. Thiokol Chemical Corporation,
FIELD TESTING OF PROPELLANTS, by S. Griff, and F. Hoffman,
RMD 5087/5112-F, March-April 1968.
66. Thiokol Chemical Corporation,
MONOPROPELLANT GAS GENERATOR, by B. M. Speyer, RMD 5810-F.
67. Unidynamics,
NEW METHODS OF CHEMICAL AGENT DISSEMINATION BY THERMAL MEANS, by H. R. Spragg,
Report D66-928, (AD 378312), August 1966.

Pressurization and Expulsion Systems

68. Aerojet-General Corporation,
PRESSURIZATION SYSTEM DESIGN GUIDE, VOLUME I, SYSTEM ANALYSIS AND
SELECTION, Report No. 2736, prepared for NASA under Contract NAS7-169.

Comprehensive reference list and good exposition of problems
associated with tank pressurization analysis.

69. Aerojet-General Corporation,
DESIGN GUIDE FOR PRESSURIZATION SYSTEM EVALUATION, Liquid Propulsion
Rocket Engines, Volume 1, Report No. 2334, September 1962.

Indicates that teflon bladders will operate at temperatures up
to 500°F.

70. Arpaci, V. S., Clark, J. A. and Winer, W. O.,
DYNAMIC RESPONSE OF FLUID AND WALL TEMPERATURES DURING PRESSURIZED
DISCHARGE OF A LIQUID FROM A CONTAINER, Advances in Cryogenic Engineering,
K. D. Timmerhaus (Ed.), Vol. 6, pp. 310-321, Plenum Press, N.Y. (1961).

Exact Analytical Solution for Idealized Problem.

71. Arpaci, V. S., Clark, J. A.,
DYNAMIC RESPONSE OF FLUID AND WALL TEMPERATURES DURING PRESSURIZED
DISCHARGE FOR SIMULTANEOUS TIME-DEPENDENT INLET GAS TEMPERATURE, AMBIENT
TEMPERATURE, AND/OR AMBIENT HEAT FLUX, Advances in Cryogenic Engineering,
K. D. Timmerhaus (Ed.), Vol. 7, pp. 419-432, Plenum Press, N.Y. (1962).

Continuation of exact solution of Reference (70). Can handle more
general conditions.

72. Beech Aircraft Corporation,
DEVELOPMENT OF CRYOGENIC POSITIVE EXPULSION BLADDERS, by D. H. Pipe,
et al, 20 January 1968.

73. Clark, J. A., Van Wylen, G. J. and Fenster, S. K.,
TRANSIENT PHENOMENA ASSOCIATED WITH THE PRESSURIZED DISCHARGE OF A
CRYOGENIC LIQUID FROM A CLOSED VESSEL, Advances in Cryogenic Engineering,
K. D. Timmerhaus (Ed.), Vol. 5, pp. 467-480, Plenum Press, N.Y. (1960).

Analysis for heat transfer to wall of propellant tank during discharge.
Exact solution for idealized case.

74. Clark, J. A.,
A REVIEW OF PRESSURIZATION, STRATIFICATION AND INTERFACIAL PHENOMENA, International Advances in Cryogenic Engineering, pp. 259-283, K. D. Timmerhaus (Ed.), Plenum Press, N.Y. (1965).

Excellent review article. A "must" for any study on pressurization problems.

75. Cox, E. F., Tatom, J. W.,
ANALYSIS OF THE PRESSURIZED GAS REQUIREMENTS FOR AN EVAPORATED PROPELLANT PRESSURIZATION SYSTEM, Advances in Cryogenic Engineering, K. D. Timmerhaus (Ed.), Vol. 7, pp. 234-243, Plenum Press, N.Y., (1962).

Lumped parameters analysis.

76. Epstein, M., Georgins, H. K., and Anderson, R. E.,
A GENERALIZED PROPELLANT TANK-PRESSURIZATION ANALYSIS, International Advances in Cryogenic Engineering, pp. 290-302, K. D. Timmerhaus (Ed.), Plenum Press, N.Y. (1965).

Presents the analysis behind a generalized computer program dealing with pressurization problems (Rocketdyne-Marshall Spacecraft Center program). This program is very sophisticated, but suffers from a requirement of a fairly large semi-empirical input.

77. Epstein, M.,
PREDICTION OF LH_2 AND LO_2 PRESSURANT REQUIREMENTS, International Advances in Cryogenic Engineering, pp. 303-307, K. D. Timmerhaus (Ed.), Plenum Press, N.Y. (1965).

The author has used the Rocketdyne-MSFC computer program to carry out a parametric study of LO_2 and LH_2 pressurization during liquid expulsion, using the liquid vapor or helium as pressurant. An equation is presented which correlates the collapse factor as a function of other variables over a very wide range of parameters.

78. Gluck, D. F., Kline, J. F.,
GAS REQUIREMENTS IN PRESSURIZED TRANSFER OF LIQUID HYDROGEN, Advances in Cryogenic Engineering, K. D. Timmerhaus (Ed.), Vol. 7, pp. 219-233, Plenum Press, N.Y. (1962).

Lumped parameter analysis of pressurant mass requirements.

79. JPL,
PROPELLANT EXPULSION IN UNMANNED SPACECRAFT, by R. N. Porter, and
H. D. Stwanord, Technical Report No. 32-899, July 1966.

Presents an excellent review of the state-of-the-art in expulsion systems including design details on metallic and non-metallic bladders.

80. Martin Company,
DEVELOPMENT AND DEMONSTRATION OF MAIN TANK INJECTION (MTI) PRESSURIZATION SYSTEM, Final Report, RTD-TDR-63-1123, AFFTC, Edwards AFB, (1963).

Not very relevant to tank pressurization problems.

81. Martin-Marietta Corporation,
PRESSURIZATION SYSTEM FOR USE IN THE APOLLO SERVICE PROPULSION SYSTEM, by D. N. Gorman, and G. R. Page, Phase I Interm Report No. CR-65-50, (1965).

82. NASA,
AN ANALYSIS OF THE PROBLEM OF TANK PRESSURIZATION DURING OUTFLOW, by W. H. Roudebush, TN D-2585, 1965.

Results analysis behind the Lewis Computer program. The relevant partial differential equations are shown by finite differences. Theory is compared with experiment.

83. NASA,
PARAMETRIC INVESTIGATION OF LIQUID HYDROGEN TANK PRESSURIZATION DURING OUTFLOW, by D. A. Mandell, and W. H. Roudebush, TN D-2797, 1965.

Conclusions are derived based on dimensional analysis and results from "numerical experiments" with the Lewis Computer program. A comparison of the results with those obtained from actual tests is made.

84. NASA,
EXPERIMENTAL AND ANALYTICAL INVESTIGATION OF INTERFACIAL HEAT AND MASS TRANSFER IN A PRESSURIZED TANK CONTAINING LIQUID HYDROGEN, by W. A. Olsen, TN D-3219, 1966.

An elementary analysis (the same as that of Reference (92)) is compared with results of tests.

85. NASA,
EXPERIMENTAL AND ANALYTICAL STUDIES OF CRYOGENIC PROPELLANT TANK
PRESSURANT REQUIREMENTS, by M. E. Nein, and J. F. Thompson, TN D-3177,
1966.

Discussion of the Rocketdyne - MSFC Computer program (essentially
that presented in Reference (76)) and comparison with experiments.

86. NASA,
EXPERIMENTAL EVALUATION OF PRESSURANT GAS INJECTORS DURING THE PRESSURIZED
DISCHARGE OF LIQUID HYDROGEN, by R. J. DeWitt, R. J. Stochl, and
W. R. Johnson, TN D-3458, 1966.

Presentation and discussion of results obtained with various
injectors for the pressurant.

87. NASA,
PREDICTION OF PROPELLANT TANK PRESSURIZATION REQUIREMENTS BY DIMENSIONAL
ANALYSIS, by T. F. Thompson, and M. E. Nein, TN D-3451.

Dimensional analysis is used to derive various non-dimensional groups
which are used to correlate the results of "numerical experiments"
carried out with the Rocketdyne-MSFC Computer program. Some comparison
with actual test results.

88. Northrop Corporation,
PRELIMINARY INVESTIGATION OF ADVANCED PRESSURIZATION SYSTEMS, by W. F.
Keller, Report NOR 65-27, March 1965.

Provides results of a preliminary investigation which identified
as analytically promising a sodium azide based hybrid pressurization
system.

89. Northrop Corporation,
A HYBRID HOT GAS PRESSURIZATION SYSTEM FOR LIQUID PROPELLANT MISSILES,
Report NB 66-119, April 1966.

A Technical Brief containing the results of initial Northrop
research showing the feasibility of a gaseous fluorine/sodium azide
hot gas pressurization system. Also contains applications studies
and preliminary design data.

90. Prentice-Hall Incorporated,
ROCKET PROPELLANT AND PRESSURIZATION SYSTEM, by E. Ring, Englewood Cliffs, N. J. (1964).

Contains useful section on "Tank Gas Thermodynamics," which should be a good introduction to the subject.

91. Thikol,
INVESTIGATION OF ADV. POSITIVE EXPUL. TECHNIQUES FOR GELLED METALIZED PROP., Quarterly Report RMD 6-54-Q-1, October 1967, CPIA 68-296 (AD 386 650L).

Abstract states that heat transfer analysis conducted on Rolldex Expulsion Design indicates that calculated metal temperature not excessive and thus does not require insul. protection from hot gas.

92. Thomas, P. D., and Morse, F. H.,
ANALYTIC SOLUTION FOR THE PHASE CHANGE IN A SUDDENLY PRESSURIZED LIQUID VAPOR SYSTEM, Advances in Cryogenic Engineering, K. D. Timmerhaus (Ed.), Vol. 8, pp. 550-562, Plenum Press, N.Y. (1963).

Analytical investigation of phase-change phenomenon in a suddenly pressurized liquid-vapor system as a function of the initial and final ullage pressure, and the temperature existing in the vapor after the introduction of the propellant.

93. Wein, M. E., and Head, R. R.,
EXPERIENCES WITH PRESSURIZED DISCHARGE OF LIQUID OXYGEN FROM LARGE FLIGHT VEHICLE PROPELLANT TANKS, Advances in Cryogenic Engineering, K. D. Timmerhaus (Ed.), Vol. 7, pp. 245-250, Plenum Press, N.Y. (1962).

Presentation and discussion of test results obtained during static findings of Saturn Vehicle and tests on large single tanks.

94. Yang, W. J., and Clark, J. A.,
ON THE APPLICATION OF THE SOURCE THEORY TO THE SOLUTION OF PROBLEMS INVOLVING PHASE CHANGE, PART 2: TRANSIENT HEAT AND MASS TRANSFER IN A MULTI-COMPONENT LIQUID-VAPOR SYSTEM, ASME Paper 63-WA-116, (1963).

Relevant to the problem of computing heat and mass transfer at the liquid-vapor interface.

95. Yang, W. J., Larsen, P. S., and Clark, J. A.,
INTERFACIAL HEAT AND MASS TRANSFER IN A SUDDENLY PRESSURIZED, BINARY
LIQUID-VAPOR SYSTEM, ASME Transactions, J. Engineering for Industry,
pp. 413-418, November 1965.

Relevant to the problem of computing heat and mass transfer at
the liquid-vapor interface.

Injector Design

96. Air Force Foreign Technology Division,
DESIGN AND CONSTRUCTION OF MECHANICAL INJECTORS, by V. A. Pavlov, and
Y. P. Stroozhuk, Report FTD-MT-67-28 (AD670 089) September 1967.

Provides methods of determining geometric and fluid dynamic design characteristics for hollow-cone spray nozzles.

97. JPL,
ON THE DYNAMIC CHARACTERISTICS OF FREE-LIQUID JETS AND A PARTIAL
CORRELATION WITH ORIFICE GEOMETRY, by J. H. Rupe, Technical Report
No. 32-207, January 1962.

Report provides a good literature review and experimental categorization of free jets.

98. JPL,
CUP AND PLUG INJECTOR INVESTIGATIONS, by W. B. Powell, Space Programs
Summary 37-31, Vol. IV, P. 203, January 1965.

Describes a cup and plug type injector and test results.

99. JPL,
INJECTOR DEVELOPMENT, by R. W. Riebling, Space Programs Summary 37-44,
Volume V, May 1967.

Provides experimental results of tests on a 2000-4000 lb. thrust bi-propellant rocket utilizing impinging sheet type injectors.

100. JPL,
THE FORMATION AND PROPERTIES OF LIQUID SHEETS SUITABLE FOR USE IN
ROCKET ENGINE INJECTORS, by R. W. Riebling, Technical Report 32-112,
June 1967.

Describes a research program in which both geometrical and fluid dynamic characteristics of flowing liquid sheets, suitable for liquid rocket injectors, were defined.

101. Physics International Company,
PIEZOELECTRIC INJECTION SYSTEM FOR VERNIER IMPULSE THRUSTERS, Final
Report AFPRL-TR-67-201, June 1967.

Reports the design and technical evaluation of a reciprocating-piston injection pump capable of delivering accurate, small quantities of propellants.

APPENDIX II

OPTIMUM GAS TEMPERATURES STUDY

PREPARED BY

DR. D. B. ADARKAR and L. B. HARTSOOK

1. Introduction

In gas pressurization, the efflux of gas from a container or generator is fed into the propellant tank under pressure, thereby forcing out the propellant. It is necessary that the tank pressure be maintained within certain limits during this process and that enough pressurant be supplied to expel the required volume of the propellant.

An order of magnitude estimate of the pressurant mass requirement might be made by assuming that the gas remains at its inlet temperature. If tank pressure and volume are known along with the equation of state for the gas, the mass required may be easily obtained. However, during the pressurization process, the gas bulk temperature must fall below its inlet value because of energy losses due to heat transfer to the tank walls and propellant as well as work done in expelling the latter. As a consequence, the pressurant mass required would be greater than suggested by the crude estimate above. Thus it might seem that the way to minimize final gas weight would be to maximize final gas temperature by making the inlet gas temperature as high as technologically possible. However, two factors militate against this.

Firstly, high gas temperatures could cause significant evaporation of the propellant in the absence of a bladder. This evaporated propellant would no longer be available as fuel and its mass would have to be allocated to pressurization system weight. When propellant molecular weights are greater than pressurant molecular weights, evaporation could cause an increase in system weight. Secondly, increased inlet gas temperatures would cause the tanks to run hotter, thereby requiring greater tank thicknesses (and hence weights) to contain the internal pressures.

The following sections present the analysis used in estimating the important components of system weight, i. e., the weights of pressurant, tank and evaporated propellant. The analysis assumes cylindrical tanks with negligible end effects, perfect gas behavior for the pressurant and propellant vapor and either a "thin" bladder or a stable liquid gas interface.

2. The Thermodynamics of Pressurization

The mass of pressurant needed to occupy a given tank volume depends on the various energy losses suffered by the pressurant during the duty cycle. Various analyses have been developed to predict pressurant mass requirements, and an excellent review of these methods has been given by Clark⁽¹⁾.

The fluid dynamic and thermodynamic problems posed by the pressurization process are very difficult, but an apparently successful phenomenological model has been evolved which makes these problems tractable. It is assumed that the pressurant gas flow in the tank, as well as the liquid flow, is quasi one-dimensional. The more sophisticated solutions then involve the derivation of the relevant partial differential equations for mass and energy conservation and their numerical solution. A very few exact solutions are available for idealized cases. Another method of solving the problem is to perform a "lumped system" analysis, rather than the distributed system analysis of the partial differential equations.

The lumped system approach is taken in this study. The thermodynamic analysis closely follows the work of Gluck and Kline⁽²⁾. The cited authors, along with others⁽³⁾, have shown that a lumped parameter approach can yield results of satisfactory accuracy, particularly for preliminary design estimates.

Consider the "control mass" enclosed within the dotted line denoting the system boundary in Figure 1. During the time interval between t and $t + dt$, a plug of gas, mass dm , enters the tank, some liquid leaves the tank and a mass of liquid dm_t is vaporized. It is assumed that the pressurant gas is perfect, with an equation of state given by

$$p v = \frac{GT}{\mu_p} \quad (2.1)$$

where μ_p is the molecular weight of the pressurant, v is the specific volume and G the universal gas constant. The specific enthalpy (h) is assumed to be given by

$$h = h_r + c_p (T - T_r) \quad (2.2)$$

where the specific heat at constant pressure, c_p , is constant and h_r and T_r are reference enthalpy and temperature respectively. From an application of the First Law of Thermodynamics to the control mass of Figure 1, it may readily be shown⁽²⁾ that if the tank pressure remains constant at p , then

$$dm = \frac{dQ_w + dQ_l + dm_t h_{fg} + \frac{\gamma}{\gamma-1} p dV}{h_i + C_p T_r - h_r} \quad (2.3)$$

Here dQ_w and dQ_l represent heat transfer to the wall and liquid, h_{fg} is the enthalpy of phase change, γ is the ratio of gas specific heats, h_i is the inlet pressurant enthalpy and dV is the change in ullage volume. It should be noted that given the above assumptions, Equation (2.3) is "exact" and does not involve any approximation.

Obviously, any "difficulties" in the analysis must arise from the lack of knowledge of dQ_w , dQ_l and dm_t . The more sophisticated approaches to the problem essentially solve for these quantities implicitly during the finite difference solutions of the relevant partial differential equations. It was not possible to use a similar approach here, within the scope of this program effort. Accordingly, an approximate solution has been derived for dQ_w and some known solutions applicable to idealized models have been adapted for dQ_l and dm_t . These analyses will be presented in following sections.

The analysis leading to Equation (2.3) applies to the problem of expulsion, i. e., when $dV \neq 0$. During the duty cycle there is another operation of interest, viz., pressurization. Thus, some pressurant is admitted before expulsion to bring up the tank pressure to the specified value during expulsion. There does not appear to be much discussion of this problem in the literature. However, NASA personnel have compared the results of their computer program (based on the analysis of Roudebush⁽⁴⁾) with experiment for the pressurization process. After much discussion with NASA personnel, their basic model has been adapted to the needs of this approximate analysis. This is the element of analysis most subject to possible errors. However, pressurization is often much shorter than the expulsion, which would tend to lessen these errors.

The model of pressurization used assumes that the "old" ullage gas acts as a spring, which is compressed isentropically by the incoming gas. The only energy transfers from the incoming pressurant are, then, the heat transfer to the portion of the wall cleared of the old gas and the work done in compressing the old gas. If these assumptions are introduced into the basic analysis of Reference (2), the resulting equation for the pressurant mass requirement is

$$dm = \frac{dQ_w + \frac{1}{-1} (p - p_{cold}) V}{h_i + c_p (T_r - h_r)} \quad (2.4)$$

where p_{cold} is the "cold" ullage pressure (i. e., before pressurization) p is the final pressure and V is the ullage volume (which, of course, stays constant during the process).

The mass transfer is assumed negligible during this process. Also, the heat transfer to the wall (dQ_w) is evaluated more conservatively, for reasons discussed further below.

3. Heat Transfer to the Wall

This section is essentially concerned with the computation of dQ_w , to be used in Equations 2.3 and 2.4. If the problem of pressurization thermodynamics is stated in the form of the partial differential equations which require solution, it is found that the terms in Equations (2.3) and (2.4) (such as dQ_w , dQ_ℓ , etc.), do not have to be explicitly computed. Rather the various energy transfers are allowed for implicitly in the solution to the partial differential equations. However, because of the limited scope of this analytical effort, it becomes necessary to use a lumped system analysis, which has led as shown above, to the need for determining various energy transfers explicitly. Gluck and Kline⁽²⁾, on whose analysis the present work is based, used empirical correlations of experimental data to obtain the heat transfer terms. As empirical data of a similar nature do not exist for the materials and temperatures to be considered here, an analysis has to be developed.

It has been observed in numerous experiments and computations that the temperature distribution in the pressurant gas may be assumed to vary only in the axial direction. Models which assume negligible heat transfer in the axial direction and one dimensional (space) variation of temperature have been

successful in predicting pressurant thermodynamics almost universally, provided that gas injection into the tank is relatively "gentle." This analysis assumes such a model. It is further assumed that heat flux between gas and wall at any axial position does not vary circumferentially and is given by the difference between gas and wall temperature times a convective heat transfer coefficient.

The analysis for dQ_w during the expulsion process makes a further key assumption, based on empirical knowledge. It is assumed that at any instant the gas temperature varies linearly from its inlet value at the hot end to the saturation temperature of the liquid at the gas/liquid interface. This assumption should slightly overestimate the actual gas temperatures, resulting in a somewhat high (but conservative) estimate for dQ_w and hence for dm . It should be pointed out that this assumption regarding temperature variation in the gas enters the analysis only in the computation of dQ_w . This assumption is further discussed at the end of the section.

Consider the idealized circular cylindrical tank indicated in Figure 2. It is assumed that the gas/liquid interface is initially at the origin of x . At time zero, the interface starts moving with a constant velocity $\dot{\ell}$. So at time, t ,

$$\ell(t) = \dot{\ell} t \quad (3.1)$$

It is assumed that the wall temperature θ , is a function of x and t alone.

$$\theta = \theta(x, t) \quad (3.2)$$

The gas temperature $T(x, t)$ is assumed to be, as discussed above,

$$T(x, t) = T_i - (T_i - T_s) \frac{x}{\ell} \quad (3.3)$$

where T_s is put equal to the liquid saturation temperature. It is assumed that the heat loss to the surroundings can be represented by a specified constant heat flux. Note that this heat flux only leaves that portion of the wall not wetted by the liquid. This is basically because the high thermal capability of the liquid prevents the wetted wall from attaining high enough temperatures to emit significant heat fluxes. This assumption has been shown to be valid by Clark⁽¹⁾.

If the thermal capacity of the wall per unit length is σ , the wall temperature is given by,

$$\sigma \frac{\partial \theta}{\partial t} = \lambda \left[T_i - (T_i - T_s) \frac{x}{\ell} - \theta \right] - \dot{q}'' \quad 2\pi r \quad (3.4)$$

where λ is the heat transfer coefficient and the other symbols in the above equation are defined in Figure 2. The initial wall temperature is

$$\theta(0, t) = T_\ell \quad (3.5)$$

The boundary condition on wall temperature is

$$\theta(x, t) = T_\ell, \quad x \geq \ell \quad (3.6)$$

The following dimensionless variables are now defined

$$\phi = \frac{\theta - T_\ell}{T_i - T_\ell}, \quad \tau = \frac{\ell}{2\pi r} t, \quad \xi = \frac{x}{2\pi r}$$

$$\Gamma = \frac{4\pi^2 r^2 \lambda}{\sigma \ell}, \quad \hat{q} = \frac{\dot{q}''}{\lambda(T_i - T_\ell)}, \quad \Delta = \frac{T_i - T_s}{T_i - T_\ell}$$

Substituting in Equation (3.4)

$$\frac{\partial \phi}{\partial \tau} + \Gamma \phi = \Gamma(1 - \hat{q}) - \Gamma \Delta \frac{\xi}{\tau} \quad (3.7)$$

Equations (3.5) and (3.6) imply the condition

$$\dot{\phi} = 0, \quad \tau \leq \xi \quad (3.8)$$

The solution to 3.7 which satisfies 3.8 is next obtained. The net energy increase of the wall cleared of liquid in time t is

$$E_w(t) = (T_i - T_\ell) \int_0^{\dot{\ell}t} \phi \sigma \, dx \quad (3.9)$$

$$\Xi = E^* \left[2\pi r \sigma (T_i - T_\ell) \right] \quad (3.10)$$

where E^* is given by

$$E^* = \int_0^{\xi} \phi \, d\xi \quad (3.11)$$

$$\xi = \frac{\dot{\ell}t}{2\pi r} = \tau \quad (3.12)$$

The solution of $E^*(\tau)$ may be shown to be

$$E^*(\tau) = (1 - \hat{q}) \left[\tau + \frac{1}{F} (e^{-F\tau} - 1) \right] - \frac{1}{2} \Delta\tau \left[\left(\frac{e^{-F\tau} - 1}{F\tau} \right) + 1 \right] \quad (3.13)$$

Hence $E_w(t)$ follows directly by substitution. The above analysis is applicable to the first expulsion, i. e. , when initial ullage volume is zero. When the initial ullage volume is significant, it becomes necessary to take into account the thermodynamics of the pressurization process as well. It will be recalled that this led to different expressions for pressurant mass [Equation (2.4) instead of Equation (2.3).] In the model for heat transfer to the wall during this period, it will be assumed that the incoming gas exchanges heat with the wall that is cleared of the "old gas," which is compressed adiabatically. Also, it will be assumed

that the "new gas" temperatures during this process are constant with x , the value being equal to T_i from the inlet to the interface between the new and the old gas.

If the tank pressure before pressurization is known and if it is assumed that the ullage gas behaves like a pressurant gas with a ratio of specific heats still equal to γ (i.e., the value not significantly changed by any propellant vapor present), then the final compressed volume of the old gas follows (from $pV^\gamma = \text{constant}$). Thus the volume (or tank length) occupied by the pressurant gas is known. It is further assumed that the rate of movement of the interface (old gas/new gas) is a known constant times the rate of movement of the liquid/gas interface during expulsion. The assumption on gas temperature implies $\Delta = 0$ in Equation (3.13). With this modification, Equations (3.13) and (3.9) may be used to estimate E_w . Of course, because an upper bound has been assumed as the value of gas temperature, the value of E_w will be conservative, i.e., high.

The remaining problem of wall heating is that of an expulsion with non-zero initial ullage. That is, the problem of heat transfer for the post pressurization expulsion. This is a difficult problem to solve, particularly without a finite difference solution. However, a reasonable model, again conservative on wall heating, is to assume that at the start of expulsion, the wall is uniformly at the liquid temperature and the gas temperature drops linearly from T_i at the inlet to the liquid saturation temperature at the interface. This problem is similar to the first problem solved in this section except that now l is given by

$$l = l_0 + \dot{l} t \quad (3.14)$$

where l_0 is the value of l at the start of expulsion. Because of the linearity of Equation 3.4 in θ , the solution to the present problem may be made by

"starting" the solution at $\ell = 0$, with the entering gas heating the walls in parallel with a fictitious cold gas at temperature $T_\ell - T_i$. This heating plus cooling would take place until $\ell = \ell_o$, with Equation (3.3) being applicable because the initial value of ℓ is again 0. Consideration shows that when $\ell = \ell_o$, the net result of heating with gas at temperature T_i and cooling with a gas at temperature $T_\ell - T_i$ would be $E_w = 0$, with wall temperatures remaining at T_ℓ . The cooling process may now be mathematically "stopped" but the heating process allowed to continue, with ℓ increasing past ℓ_o . This is equivalent to starting with the initial conditions described above as being appropriate to post pressurization expulsion. Thus the process required is obtained by a heating process starting at $\ell = 0$ and continuing until ℓ is the required value, combined with a cooling process starting at $\ell = 0$ and stopping at $\ell = \ell_o$.

By means of a simple energy balance it may be shown that:

$$\text{Heat transfer to wall } (Q_w) = E_w - \text{Heat loss to surroundings } (\dot{q}'') \quad (3.15)$$

If E_w and q'' are known, Q_w follows from Equation (3.15).

The exact value of \dot{q}'' is so dependent upon actual configuration and ambient conditions, that within the scope of this study it was decided to use various values of q'' which would cover a typical range. The values of \dot{q}'' assumed in this study are:

$$\begin{aligned}
\dot{q}'' &= \sigma \epsilon \left(\frac{T_i + T_\ell}{4} \right)^4 & \dots \dots \text{Nominal (a)} \\
\dot{q}'' &= \sigma \epsilon \left(\frac{T_i + T_\ell}{2} \right)^4 & \dots \dots \text{High Perturbation (b)} \\
\dot{q}'' &= \sigma \epsilon T_\ell^4 & \dots \dots \text{Low Perturbation (c)}
\end{aligned}
\quad \left. \vphantom{\begin{aligned} \dot{q}'' &= \sigma \epsilon \left(\frac{T_i + T_\ell}{4} \right)^4 \\ \dot{q}'' &= \sigma \epsilon \left(\frac{T_i + T_\ell}{2} \right)^4 \\ \dot{q}'' &= \sigma \epsilon T_\ell^4 \end{aligned}} \right\} \quad (3.16)$$

The above analyses have been used to determine the value of dQ_w to be used in Equations (2.3) and (2.4). These analyses are conservative and should hence overpredict dQ_w , resulting in a high estimate for pressurant mass. This positive error would be cumulative, increasing with the number of pulses in the duty cycle.

4. Heat and Mass Transfer at the Gas/ Liquid Interface

As mentioned in the introduction, it is important to have estimates of heat and mass transfer between liquid and gas. However, as might be expected, the interfacial transfers depend strongly on the nature of the interface, i.e., whether it is steady and continuous or unsteady and broken. An important determinant is the type of gas injection used. If injection of the pressurant gas with the tank is via an energetic jet, the interfacial transfers could be high. Unfortunately, this is the case for which pure analysis becomes very difficult. However, it has been found that when injection is "gentle" resulting in slug flow in the tank, analytical predictions can be reasonably good.

A complete analytical solution would of course require the consideration of the diffusion equation in addition to the mass (and species) conservation and energy equations. The model used here assumes negligible "mass transfer resistance" at the interface, which implies that the energy equation alone can be

used to compute mass transfer. Because of the neglect of the mass transfer resistance, the computed mass transfer should be less than would actually exist for the idealized flow model. However, for reasons mentioned above the idealized flow model probably provides only a lower bound on the mass transfer.

The analysis used here is that recommended by Olsen⁽⁵⁾. The mass transfer, m_t , is given by

$$m_t = -2\pi r^2 \left(\frac{k_g \rho_g}{c_{p,g}} \right)^{1/2} \mu t^{1/2} \quad (4.1)$$

where k_g , ρ_g and $c_{p,g}$ are gas thermal conductivity, density and specific heat, and μ is given by the solution of the transcendental equation

$$\frac{\theta_b e^{-n^2 \mu^2}}{n[1 + \operatorname{erf}(n\mu)]} + \frac{\theta_r e^{-\mu^2}}{\operatorname{erfc}(\mu)} + \pi^{1/2} \mu = 0 \quad (4.2)$$

where

$$\theta_b = \frac{-c_\ell(T_s - T_\ell)}{L}, \quad \theta_r = \frac{c_{p,g}(T_i - T_s)}{L},$$

$$L = h_{fg}, \quad n = \sqrt{\frac{k_g \rho_g c_\ell}{k_\ell \rho_\ell c_{p,g}}}.$$

The subscript ℓ refers to liquid properties. The interfacial heat transfer Q_ℓ is given by,

$$Q_\ell = 2\sqrt{\pi} r^2 \frac{e^{-\mu^2}}{\operatorname{erfc}(\mu)} \left(\frac{\rho_g k_g}{c_{p,g}} \right)^{1/2} (T_i - T_s) t^{1/2} - L m_t \quad (4.3)$$

The analysis on which the above equations are based applies strictly to a one component system. The analysis is valid for either condensation or evaporation. However, in the present case, the saturation temperatures of the propellants will be much higher than saturation temperature of the pressurant (N_2 here). As a result, condensation will never take place within the range of temperatures to be

considered in the problem. The boundary between evaporation and no evaporation occurs at $\mu = 0$ [Equations (4.1) and (4.2)], i.e., at

$$T_i = T_s + \frac{1}{n} \frac{c_\ell}{c_{p,g}} (T_s - T_\ell) \quad (4.4)$$

At gas inlet temperatures below those given by Equation (4.4), a different model has to be used for the interfacial heat transfer in the absence of mass transfer. A pure conduction model consistent with the assumptions of the mass transfer model is used in this analysis. However, because this model is a limiting case of the model for heat transfer from the gas in the presence of the bladder, it is presented in the next section, which deals with that subject.

5. Heat Transfer to Liquid with a Bladder Present

The model for heat transfer used here is consistent with the mass transfer model. The presence of a bladder will prevent liquid propellant evaporation. If the bladder is thin (which it should be for low weight because it is only a separation device which is not pressure stressed), a valid idealization is that the bladder may represent a thermal contact resistance between the pressurant and the propellant.

An estimate of the heat transfer from pressurant to propellant may be made by assuming that heat transfer is by conduction alone, that the conduction is one (space) dimensional and that the two media are each semi-infinite. The appropriate conservative conditions appear to be that both media are initially at T_ℓ until time $t = 0$, when the pressurant temperature is uniformly raised to T_i . The system is then allowed to move towards equilibrium by heat conduction lessening temperature differences. The solution to this problem has been presented by Carslaw and Jaeger⁽⁶⁾, and Q_ℓ is readily obtained from their solution as being

$$Q_{\ell} = \pi r^2 \frac{k_g}{\alpha_g} B \left\{ \frac{1}{J} \operatorname{erfc} (J \sqrt{\alpha_g t})_{\ell} J^2 \alpha_g t - \frac{1}{J} + \frac{2}{\sqrt{\pi}} \sqrt{\alpha_g t} \right\} \quad (5.1)$$

where

$$\alpha = \text{Thermal Diffusivity} = \left(\frac{k}{c\rho} \right)$$

$$B = \frac{T_i - T_{\ell}}{\frac{k_g}{k_{\ell}} \left(\frac{\alpha_{\ell}}{\alpha_g} \right)^{1/2} + 1}$$

$$J = \frac{k_{\text{bladder}}}{s_{\text{bladder}}} \left\{ \frac{k_g \alpha_g^{-1/2} + k_{\ell} \alpha_{\ell}^{-1/2}}{k_g k_{\ell} \alpha_{\ell}^{-1/2}} \right\}$$

The subscript ℓ refers to liquid properties and g refers to pressurant gas properties.

s_{bladder} is bladder thickness

Note that Equation (5.1) contains implicitly the solution for Q_{ℓ} with no bladder and no evaporation. This solution is the limiting one for $s_{\text{bladder}} \rightarrow 0$, i. e.,

$$Q_{\ell} = \frac{\pi r^2 k_g}{\alpha_g} \left(\frac{2}{\sqrt{\pi}} \sqrt{\alpha_g t} \right) \quad (5.2)$$

6. Cooldown Between Expulsion Pulses

In a pulsed propulsion system, the contents of the tank will in general come to some sort of thermodynamic equilibrium between pulses. What this equilibrium will be depends entirely on the ambient conditions "seen" by the tank as well as the configuration of the tank. In this study, the very simple assumption is made that all the contents of the tank return to the original liquid temperature during

the inter-pulse equilibrium stage. This assumption should be reasonable when heat transfer exchanges with the surroundings are low and if liquid mass between pulses always remain significantly greater than the mass of the gas and tank.

It is useful to know what the equilibrium pressure will be in the tank, between pulses. If it is assumed that the propellant vapor mass is small, so that the vapor behaves as a perfect gas, then the equilibrium pressure, p_{cold} , is given by

$$p_{\text{cold}} = \left(\frac{m}{\mu_p} + \frac{m_t}{\mu_t} \right) \frac{GT_\ell}{V} \quad (6.1)$$

where

- m = Mass of pressurant
- m_t = Mass of propellant vapor
- μ_p = Pressurant molecular weight
- μ_t = Propellant molecular weight
- Q = Universal gas constant
- V = Ullage volume

7. Tank Weight

The weight of the tank will depend on the pressurization thermodynamics because the stress that the tank can stand will depend on its temperature. A reasonable estimate of the allowable ultimate tensile stress in the tank material is that corresponding to the bulk temperature of the tank wall at the end of the last expulsion.

The tank material considered in this study is titanium. Its curve of ultimate tensile strength (UTS) versus temperature has been approximated by a series of linear relationships of the sort

$$UTS = a - bt \quad (7.1)$$

where a and b are constants.

The bulk wall temperature at the end of the last pulse is defined as

$$T_f = E_w / (\sigma L) \quad (7.2)$$

where E_w is the energy increase of the wall during the last pressurization-expulsion process and L is the tank length.

The wall thickness, d, is then given by

$$d = f \left[pr / (a - b T_f) \right] \quad (7.3)$$

where f is a safety factor. Equations (7.2) and (7.3) have to be solved iteratively to determine the "design value" of d. Once d is known, along with other tank dimensions and the density of titanium, tank weight follows immediately.

8. Determination of the Optimum Inlet Temperature for the Pressurant

The above sections have presented the analysis necessary to compute the weights of the important components of the pressurization system, viz., the pressurant and evaporated propellant masses and the tank weights.

A typical cycle of calculations starts with the pressurization analysis (Equation 2.4) followed by the expulsion analysis (Equation 2.3). During each process the energy and mass transfers are computed as outlined. After expulsion, the equilibrium pressure is computed by using Equation (6.1). The stage is then set for computation of another cycle if necessary.

The computer program starts the solution for a particular value of T_i by assuming the value of wall thickness to be the minimum allowable (i. e. , 0.02 inch, set by fabrication constraints). The computer program then runs through the specified duty cycle, at the end of which a value of T_f is computed. If the value of T_f results in a design thickness less than or equal to 0.02 inch, the calculation is over and thickness is set equal to the latter value. Otherwise, the program guesses a higher value of wall thickness and runs through the duty cycle again, producing a new value of T_f . If this leads to a wall thickness negligibly different from the previous guess, the calculation stops. Otherwise, the program continues until the latest guess of wall thickness is insignificantly different from the one previous. This determines the design thickness of the wall for the particular T_i considered. At this stage the program determines the individual weights of all three components and stores the total along with T_i . This is done for a number of values of T_i over the specified range. Finally, the program scans the stored weights, determines the lowest and prints out the details of the solution for that value of T_i , i. e. , the optimal inlet temperature.

9. Results

Perturbation Analysis

A study was carried out using the computerized analysis discussed above, to investigate the effects of perturbations in various parameters on the optimum gas inlet temperature. The pressurant considered was N_2 and the propellants were Hydrazine and Diborane. The operating pressure during expulsion was taken to be 200 psi. Two duty cycles were considered, a single pulse and a triple pulse defined by 10% - 80% - 10% expulsion.

A standard case was first analyzed and subsequently the effects of perturbing each of several parameters independently was investigated. The standard tank considered was 36 inches in length and 12 inches in radius. The heat transfer coefficient between gas and tank wall was assumed to be 8.0 BTU/hour feet²°F, which is felt to be a reasonable figure for less than 1 g conditions. The expulsion time for both the single and triple pulses was taken to be 500 seconds, with uniform propellant flow rate throughout. The nominal formula for \dot{q}'' was used (Equation 3.16a). The safety factor f (Equation 7.1) was taken to be 2.0. The pressurant was taken to impinge directly on the propellant without a bladder intervening. The optimum inlet temperatures were determined for the standard case for both Hydrazine and Diborane (assumed representative of earth and space storable propellants) for both single and triple pulse operation. Table 9.1 summarizes the specification for the standard case.

TABLE 9.1 SPECIFICATIONS FOR STANDARD CASE

Length of Cylindrical Tank	L	36 inches
Radius	r	12 inches
Heat Transfer Coefficient		8.0 BTU/hour feet ² °F
Safety Factor	f	2.0
Expulsion Time	t	500 seconds
Heat Transfer to Ambient	\dot{q}''	Nominal (Equation 3.16a)
Bladder		No
Propellants		Hydrazine Diborane
Duty Cycles		Single Pulse 10% - 80% - 10%

The consequences of parameter perturbation are described in order as follows.

1. Length Perturbation

Figure 3 shows the effect of tank length perturbation ($L = 60$ inches, 24 inches) on the optimum temperatures. It may be seen that there is almost no change.

2. Radius Perturbation

Figure 4 shows the effect of tank radius perturbation ($r = 6$ inches, 18 inches). It appears that for the cases considered there is a minimum value of optimum temperature, which occurs at a tank radius of about 14 inches.

3. Heat Transfer Coefficient Perturbation

In the literature on tank pressurization, the most popular method of estimating heat transfer to the wall involves using a natural convection heat transfer coefficient with some (at times arbitrarily defined) temperature difference. Although this method appears to give reasonable results in a 1 g environment it does not have a completely rigorous justification. Thus it is difficult to conclude that the present means of estimating heat transfer coefficients may be extrapolated to low g situations. Therefore the value of λ chosen for the standard case was on the low side for 1 g situations. It is felt that the perturbations chosen on λ ($\lambda = 1.0, 2.0, 5.0, \text{ and } 15.0 \text{ BTU/hour feet}^2\text{ }^\circ\text{F}$) should cover the applicable range even for low g situations.

The results of the perturbation analysis bear out the importance of λ as a parameter. Figure 5 shows the very strong effect of λ on optimum

temperature, at low values of λ . This points out the importance of further research on the effects of low g on λ .

4. Safety Factor Perturbation

Although f is not strictly a variable of the problem, it is interesting to study the effect of varying it. Figure 6 shows that the optimum inlet temperature can be significantly affected by the value assumed for f . This fact is worth notice, because it is possible that the designer might be willing to change safety factors slightly if the corresponding optimum inlet temperature thereby becomes more conveniently attainable.

5. Expulsion Time Perturbation

Figure 7 shows that optimum temperature tends to drop with increasing expulsion times.

6. Perturbation of Heat Transfer to Ambient

Table 9.2 shows the effect of perturbing the ambient heat transfer formulation.

TABLE 9.2 OPTIMUM TEMPERATURES FOR VARYING AMBIENT HEAT TRANSFER

	OPTIMUM TEMPERATURES			
	HYDRAZINE		DIBORANE	
	Single Pulse	Triple Pulse	Single Pulse	Triple Pulse
High Perturbation (Equation 3.16b)	3000°F	- - -	3000°R	1000°F
Standard (Equation 3.16a)	900°F	1550°F	850°F	1150°R
Low Perturbation (Equation 3.16c)	900°R	1000°R	850°R	1150°R

7. Bladder Effects

In the context of the present analysis, the only term that could be affected by the presence of the bladder would be Q_ℓ . In addition there would also be a prevention of mass transfer.

The analysis of Section 4 was carried out for the standard case (but with $f = 1$ rather than $f = 2$, at the request of W. Keller), for both propellants for the single-pulse duty cycle. Two bladders were considered, Aluminum and Teflon -- both 0.02-inch thick.

Table 9.3 shows the results. As may be seen, the bladder has almost no effect on Q_ℓ .

TABLE 9.3 EFFECT OF BLADDER ON Q_ℓ

	Q_ℓ (BTU)*	
	DIBORANE	HYDRAZINE
No Bladder	58.74	57.12
Teflon Bladder	58.65	57.03
Aluminum Bladder	58.74	57.12
*Standard Case (except that $f = 1$)		

Dependence of Weights on Inlet Temperature

Figures 8 and 9 show the effects of pressurant inlet temperature on the components of system weight for the standard cases. In the case of Hydrazine, the interface model used predicts no vaporization even up to 3000°R . In the case of Diborane, although vaporization does begin (at $T_i \approx 2300^\circ\text{R}$), the amounts are too small to depict on the figure. Thus at 3000°R , the amount of Diborane vaporized is only 0.07 pound.

Time History

Figures 10, 11, 12, and 13 show the time history of the pressurant mass, average exposed wall temperature, and bulk pressurant gas temperature for the standard cases for both the propellants. As may be seen, equilibrium is attained very soon in the case of T_f and T_b . The pressurant mass, of course, continues to grow with time, linearly as it appears. As mentioned above, the vapor mass increase is insignificant and is accordingly not shown on the graph. The wall temperatures are artificially high (should approach, but not exceed, bulk gas temperature) due to the conservative assumptions made in estimating heat transfer to the wall.

10. References

1. Clark, J.A., "A Review of Pressurization, Stratification, and Interfacial Phenomena," International Advances in Cryogenic Engineering (Ed. K.D. Timmerhaus), pp 259-283, Plenum Press, New York (1965).
2. Gluck, D.F., and Kline, J.F., "Gas Requirements in Pressurized Transfer of Liquid Hydrogen," Advances in Cryogenic Engineering (Ed. K.D. Timmerhaus), Vol. 7, pp 219-233, Plenum Press, New York (1962).
3. Coxe, E.F., and Tatom, J.W., "Analysis of the Pressurizing Gas Requirements for an Evaporated Propellant Pressurization System," Advances in Cryogenic Engineering (Ed. K.D. Timmerhaus), Vol. 7, pp 234-243, Plenum Press, New York (1962).
4. Roudebush, W.H., "An Analysis of the Problem of Tank Pressurization During Outflow," NASA TN D-2585 (1965).
5. Olsen, W.A., "Experimental and Analytical Investigation of Interfacial Heat and Mass Transfer in a Pressurized Tank Containing Liquid Hydrogen," NASA TN D-3219 (1966).
6. Carslaw, H.S., and Jaeger, J.C., Conduction of Heat in Solids, 2.15 (iii), pp 87-89, Second Edition, Clarendon Press, Oxford (1959).

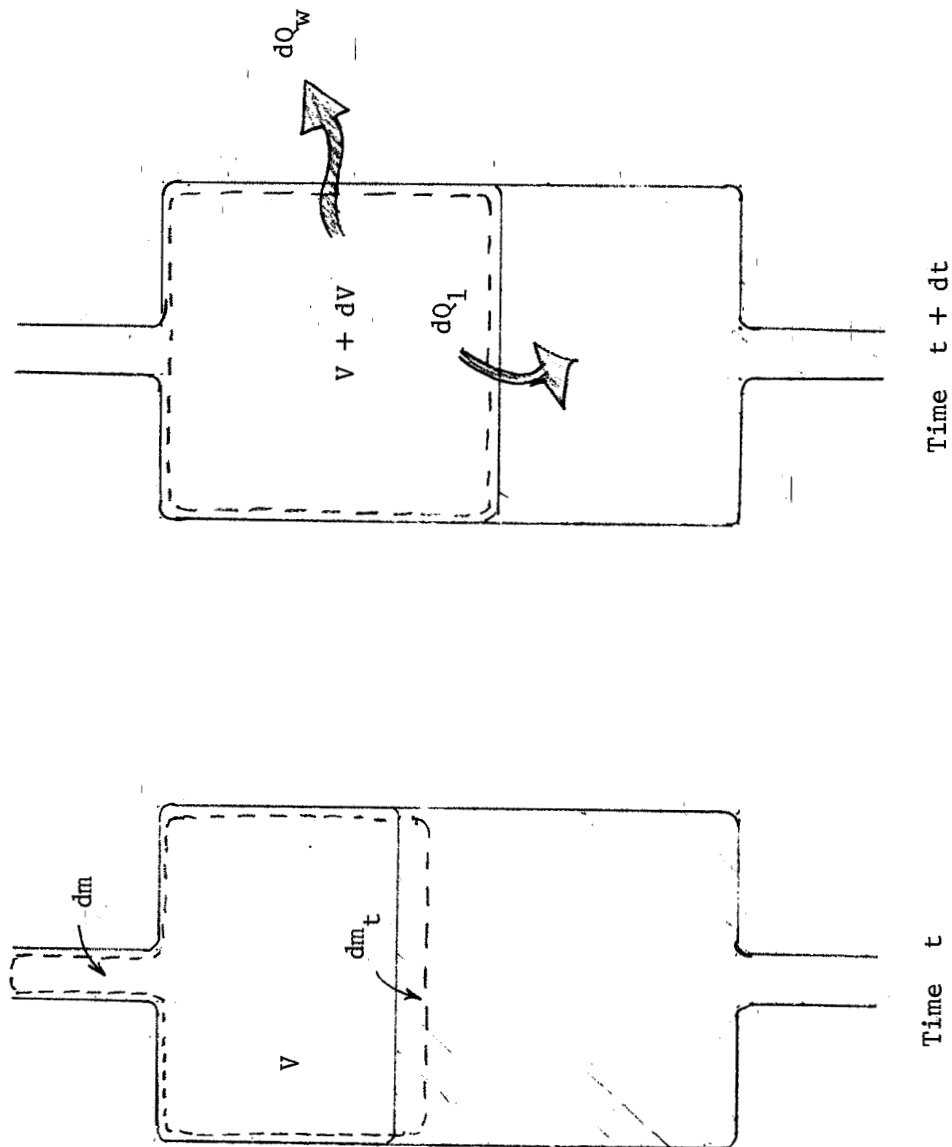


FIGURE 1 Definition of Control Mass for Thermodynamic Analysis

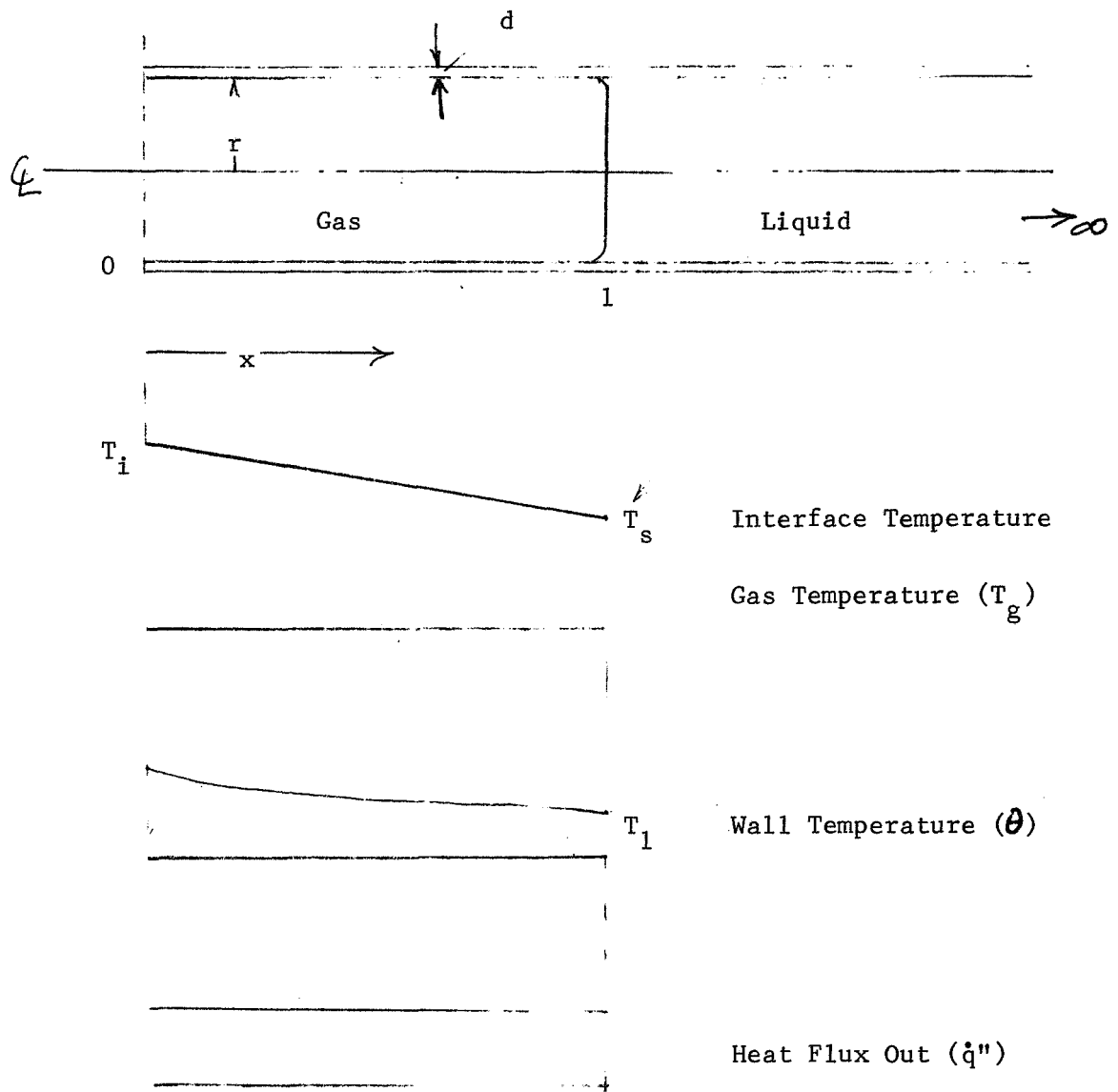


FIGURE 2 Model for Analysis of Q_w

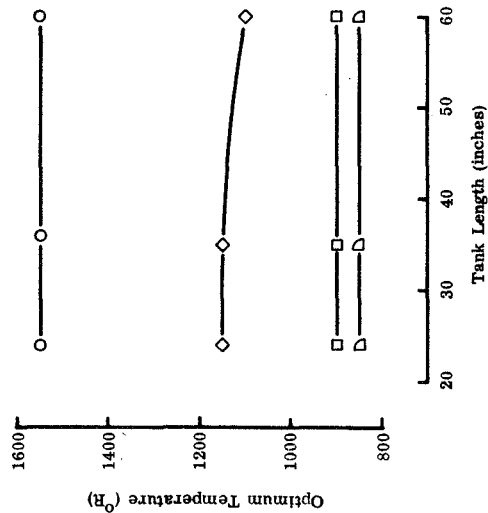


FIGURE 3. THE EFFECT OF TANK LENGTH (L) ON OPTIMUM INLET TEMPERATURE

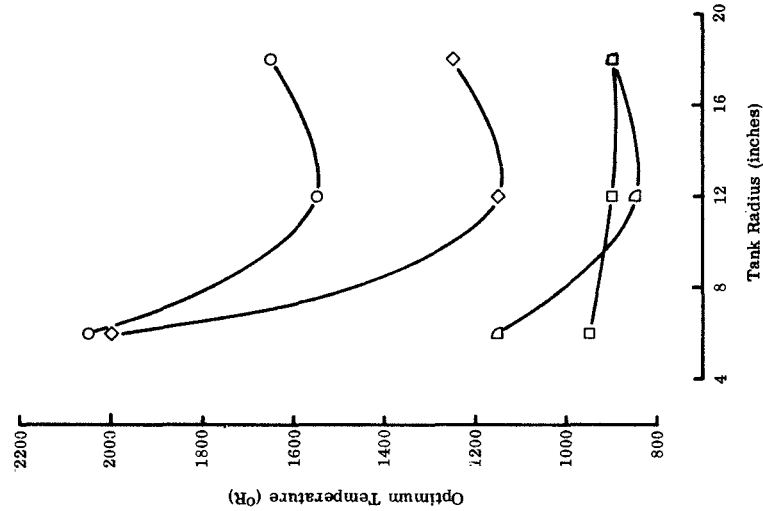


FIGURE 4. THE EFFECT OF TANK RADIUS (r) ON OPTIMUM INLET TEMPERATURE

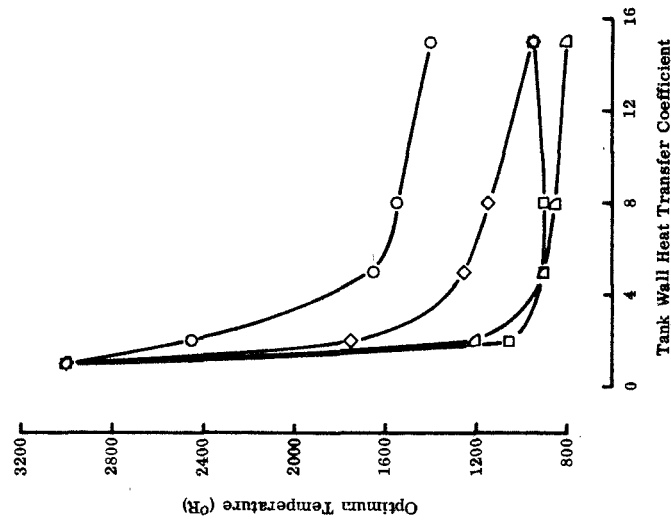


FIGURE 5. THE EFFECT OF TANK WALL HEAT TRANSFER COEFFICIENT (λ) ON OPTIMUM INLET TEMPERATURE

- Hydrazine (N_2H_4) Multiple Pulse
- Hydrazine (N_2H_4) Single Pulse
- ◇ Diborane (B_2H_6) Multiple Pulse
- ▷ Diborane (B_2H_6) Single Pulse

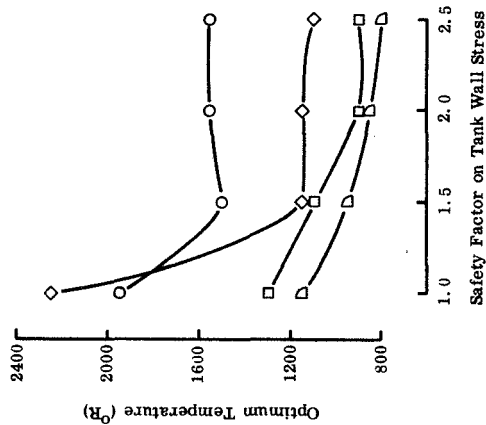


FIGURE 6. THE EFFECT OF SAFETY FACTOR
ON TANK WALL STRESS ON
OPTIMUM INLET TEMPERATURE

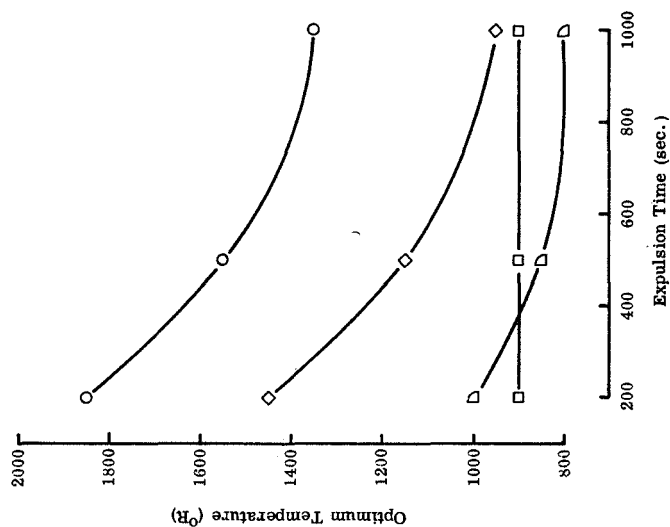


FIGURE 7. THE EFFECT OF EXPULSION TIME
ON OPTIMUM INLET TEMPERATURE

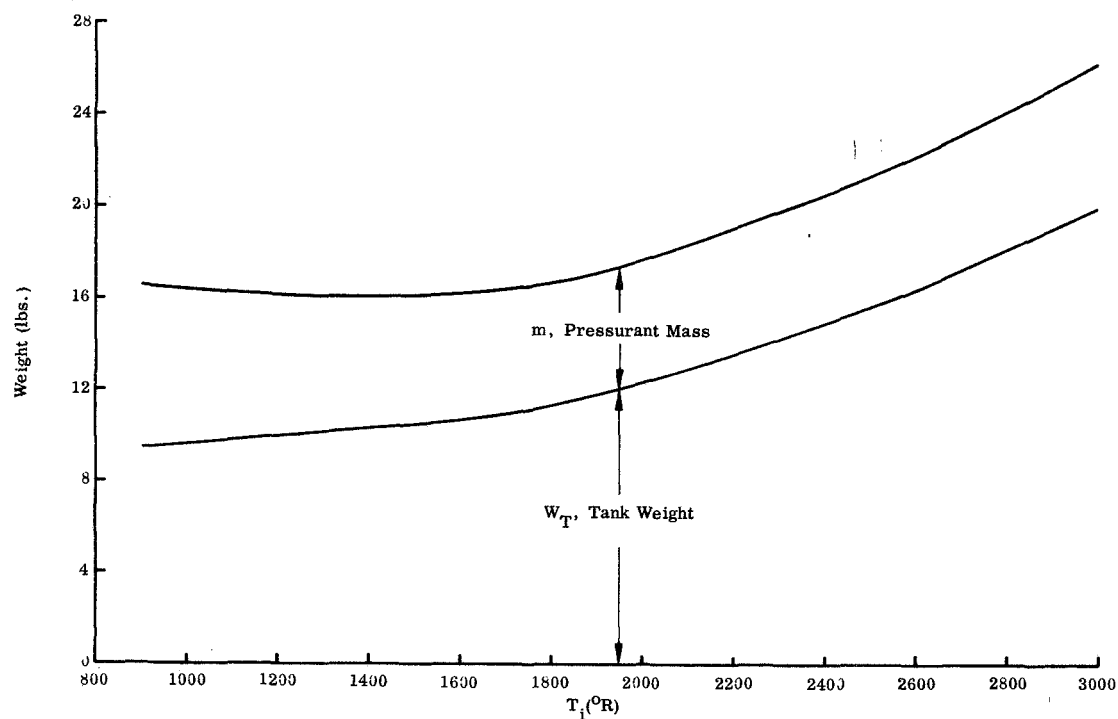


FIGURE 8. VARIATION OF COMPONENT WEIGHTS WITH PRESSURANT INLET TEMPERATURE (PROPELLANT - HYDRAZINE)

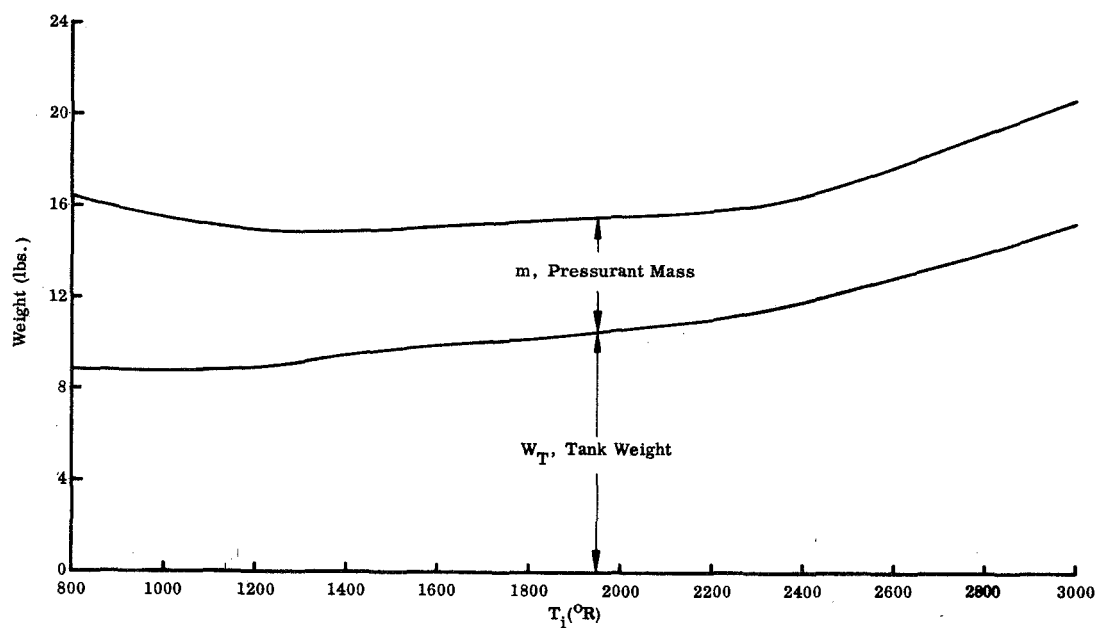


FIGURE 9. VARIATION OF COMPONENT WEIGHTS WITH PRESSURANT INLET TEMPERATURE (PROPELLANT - DIBORANE)

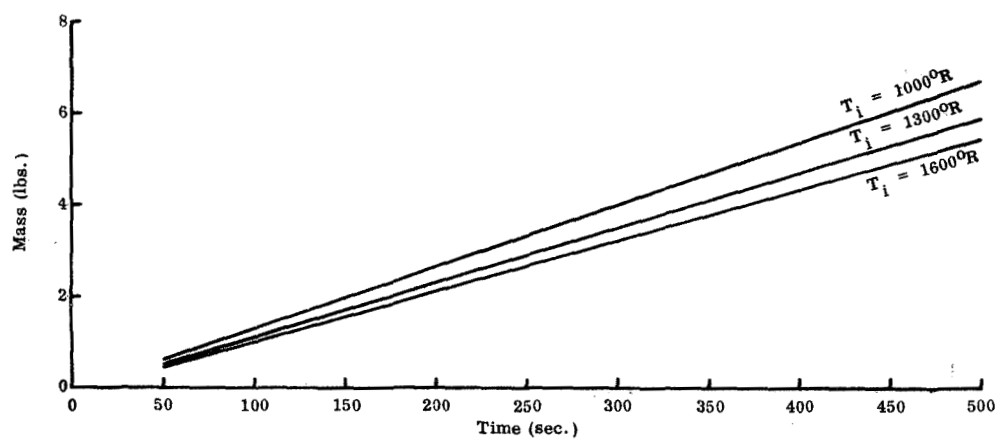


FIGURE 10. PRESSURANT MASS VS. TIME (HYDRAZINE - SINGLE PULSE)

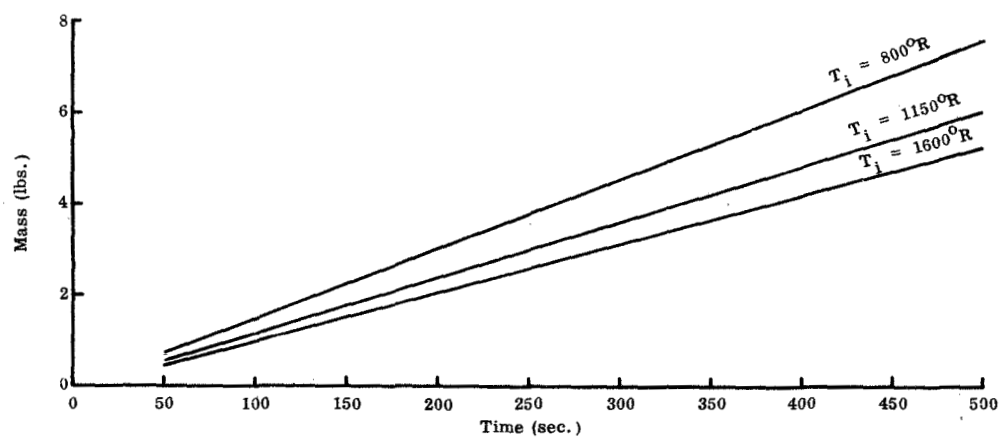


FIGURE 11. PRESSURANT MASS VS. TIME (DIBORANE - SINGLE PULSE)

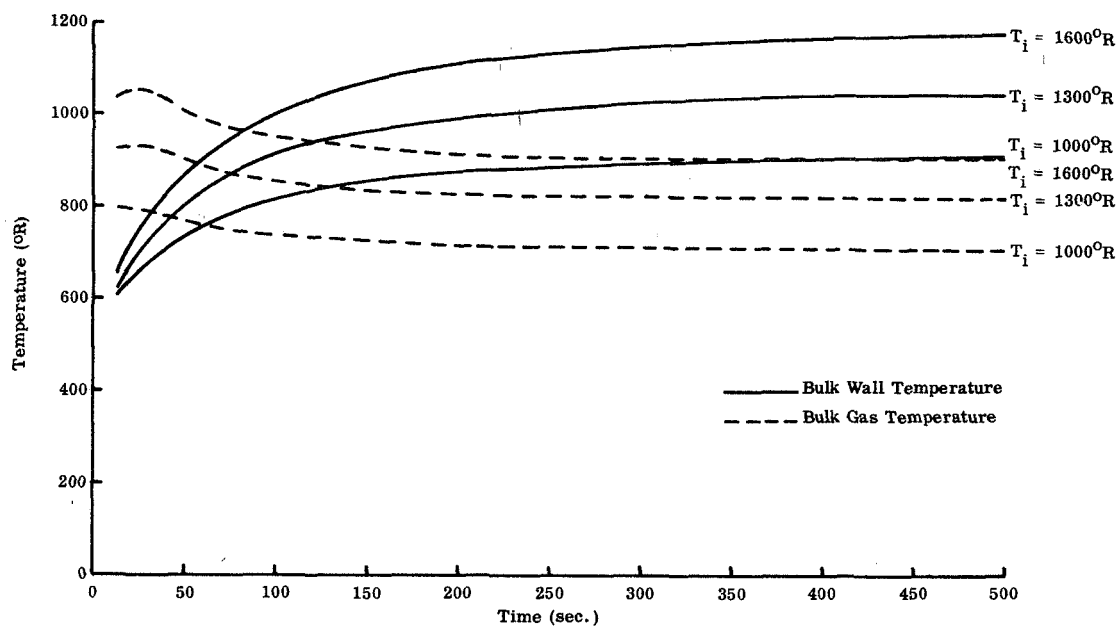


FIGURE 12. WALL AND PRESSURANT BULK TEMPERATURES VS. TIME
(HYDRAZINE - SINGLE PULSE)

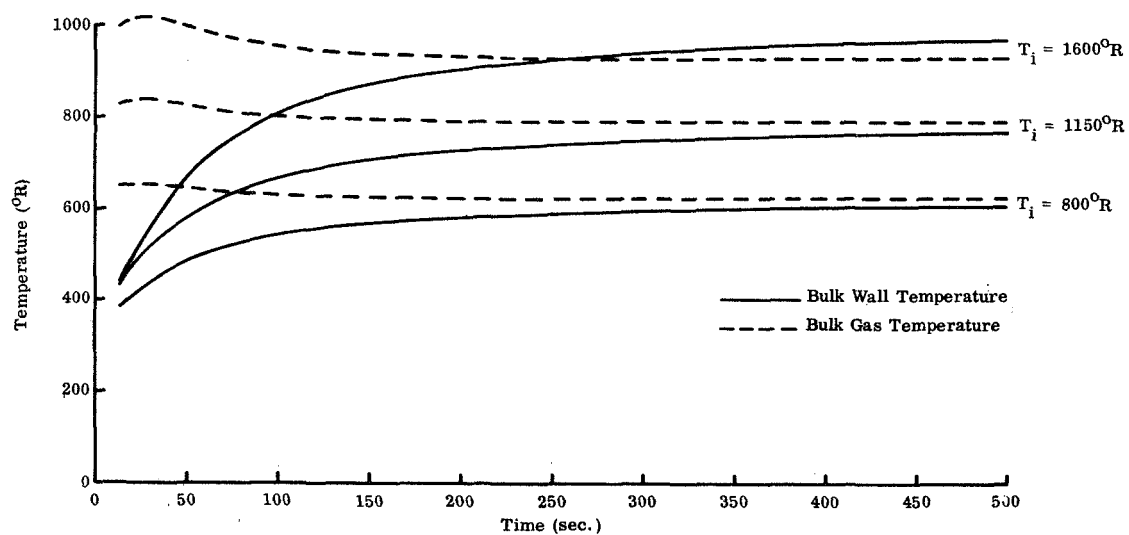


FIGURE 13. WALL AND PRESSURANT BULK TEMPERATURES VS. TIME
(DIBORANE - SINGLE PULSE)

APPENDIX III
DISTRIBUTION LIST FOR FINAL REPORT

COPIES	RECIPIENT
1	NASA Pasadena Office 4800 Oak Grove Drive Pasadena, Ca. 91103 Patents and Contracts Management
10	Jet Propulsion Laboratory 4800 Oak Grove Drive Pasadena, Ca. 91103 Wolfgang Simon
3	Chief, Liquid Propulsion Technology RPL Office of Advanced Research and Technology NASA Headquarters Washington, D.C. 20546
1	Director, Technology Utilization Division Office of Technology Utilization NASA Headquarters Washington, D.C. 20546
25	NASA Scientific and Technical Information Facility P.O. Box 33 College Park, Md. 20740
1	Director, Launch Vehicles and Propulsion, SV Office of Space Science and Applications NASA Headquarters Washington, D.C. 20546
1	Director, Advanced Manned Missions, MT Office of Manned Space Flight NASA Headquarters Washington, D.C. 20546
1	Mission Analysis Division NASA Ames Research Center Moffett Field, Ca. 24035
2	Ames Research Center Moffett Field, Ca. 94035

COPIES

RECIPIENT

1	Goddard Space Flight Center Greenbelt, Md. 20771
2	Jet Propulsion Laboratory California Institute of Technology 4800 Oak Grove Drive Pasadena, Ca. 91103
2	Langley Research Center Langley Station Hampton, Va. 23365
2	Lewis Research Center 21000 Brookpark Road Cleveland, Oh. 44135
2	Marshall Space Flight Center Huntsville, Al. 35812
2	Manned Spacecraft Center Houston, Tx. 77001
2	John F. Kennedy Space Center, NASA Cocoa Beach, Fl. 32931
1	Aeronautical Systems Division Air Force Systems Command Wright-Patterson Air Force Base Dayton, Oh. 45433
1	Air Force Missile Development Center Holloman Air Force Base NM. 88330
1	Air Force Missile Test Center Patrick Air Force Base, Fl. 32925
1	Space and Missile Systems Organization Air Force Unit Post Office Los Angeles, Ca. 90045
1	Arnold Engineering Development Center Arnold Air Force Station Tullahoma, Tn. 37388
1	Bureau of Naval Weapons Department of the Navy Washington, D.C. 20546

COPIES

RECIPIENT

1	Defense Documentation Center Headquarters Cameron Station, Building 5 5010 Duke Street Alexandria, Va. 22314 Attn: TISIA
1	Headquarters, U.S. Air Force Washington, D.C. 20546
1	Picatinny Arsenal Dover, NJ. 07801
2	Air Force Rocket Propulsion Laboratory Research and Technology Division Air Force Systems Command Edwards, Ca. 93523
1	U.S. Army Missile Command Redstone Arsenal Al. 35809
1	U.S. Naval Ordnance Test Station China Lake Ca. 93557
1	Chemical Propulsion Information Agency Applied Physics Laboratory 8621 Georgia Avenue Silver Springs, Md. 20910
1	Aerojet-General Corporation P.O. Box 296 Azusa, Ca. 91703
1	Aerojet-General Corporation P.O. Box 1947 Technical Library, Bldg. 2015, Dept. 2410 Sacramento, Ca. 95809
1	Space Division Aerojet-General Corporation 9200 East Flair Drive El Monte, Ca. 91734
1	Aerospace Corporation 2400 East El Segundo Boulevard P.O. Box 95085 Los Angeles, Ca. 90045

COPIES

RECIPIENT

1	Astrosystems International, Inc. 1275 Bloomfield Avenue Fairfield, NJ. 07007
1	Atlantic Research Corporation Edsall Road and Shirley Highway Alexandria, Va. 22314
1	Avco Systems Division Wilmington, Ma. 01887
1	Beech Aircraft Corporation Boulder Division Box 631 Boulder, Co. 80302
1	Bell Aerosystems Company P.O. Box 1 Buffalo, NY. 14240
1	Bellcomm 955 L'Enfant Plaza, S.W. Washington, D.C. 20020
1	Bendix Systems Division Bendix Corporation 3300 Plymouth Road Ann Arbor, Mi. 48105
1	Boeing Company P.O. Box 3707 Seattle, Wa. 98124
1	Boeing Company 1625 K Street, N.W. Washington, D.C. 20006
1	Boeing Company P.O. Box 1680 Huntsville, Al. 35801
1	Missile Division Chrysler Corporation P.O. Box 2628 Detroit, Mi. 48231
1	Wright Aeronautical Division Curtiss-Wright Corporation Wood-Ridge, NJ. 07075

COPIES

RECIPIENT

1	Research Center Fairchild Hiller Corporation Germantown, Md. 21401
1	Republic Aviation Corporation Fairchild Hiller Corporation Farmingdale, Long Island, NY. 11735
1	General Dynamics, Convair Division Library & Information Services (128-00) P.O. Box 1128 San Diego, Ca. 92402
1	Missile & Space Systems Center General Electric Company Valley Forge Space Technology Center P.O. Box 8555 Philadelphia, Pa. 19101
1	Grumman Aircraft Engineering Corporation Bethpage, Long Island NY. 11714
1	Honeywell, Inc. Aerospace Division 2600 Ridgeway Road Minneapolis, Mn. 55413
1	Hughes Aircraft Company Aerospace Group Centinela and Teale Streets Culver City, Ca. 90230
1	Walter Kidde and Company, Inc. Aerospace Operations 567 Main Street Belleville, NJ. 07109
1	Ling-Temco-Vought Corporation P.O. Box 5907 Dallas, Tx. 75222
1	Arthur D. Little, Inc. 20 Acorn Park Cambridge, Ma. 01240
1	Lockheed Missiles and Space Company Attn: Technical Information Center P.O. Box 504 Sunnyvale, Ca. 94088

COPIES

RECIPIENT

1	Lockheed Propulsion Company P.O. Box 111 Redlands, Ca. 92374
1	The Marquardt Corporation 16555 Saticoy Street Van Nuys, Ca. 91409
1	Baltimore Division Martin Marietta Corporation Baltimore, Md. 21203
1	Denver Division Martin Marietta Corporation P.O. Box 179 Denver, Co. 80201
1	Orlando Division Martin Marietta Corporation Box 5837 Orlando, Fl. 32805
1	Astropower Laboratory McDonnell-Douglas Aircraft Company 2121 Paularino Newport Beach, Ca. 92663
1	McDonnell-Douglas Aircraft Corporation P.O. Box 516 Municipal Airport St. Louis, Mo. 63166
1	Missile and Space Systems Division McDonnell-Douglas Aircraft Company 3000 Ocean Park Boulevard Santa Monica, Ca. 90406
1	Space & Information Systems Division North American Rockwell 12214 Lakewood Boulevard Downey, Ca. 90241
1	Rocketdyne (Library 586-306) 6633 Canoga Avenue Canoga Park, Ca. 91304
1	Northrop Corporate Laboratories 3401 West Broadway Hawthorne, Ca. 90250

COPIES

RECIPIENT

1	Aeronutronic Division Philco Corporation Ford Road Newport Beach, Ca. 92663
1	Astro-Electronics Division Radio Corporation of America Princeton, NJ. 08540
1	Rocket Research Corporation 520 South Portland Street Seattle, Wa. 98108
1	Sunstrand Aviation 2421 11th Street Rockford, IL. 61101
1	Stanford Research Institute 333 Ravenswood Avenue Menlo Park, Ca. 94025
1	TRW Systems Group TRW Incorporated One Space Park Redondo Beach, Ca. 90278
1	Tapco Division TRW Incorporated 23555 Euclid Avenue Cleveland, Oh. 44117
1	Thiokol Chemical Corporation Huntsville Division Huntsville, Al. 35807
1	Research Laboratories United Aircraft Corporation 400 Main Street East Hartford, Ct. 06108
1	Hamilton Standard Division United Aircraft Corporation Windsor Locks, Ct. 06096
1	United Technology Center 587 Methilda Avenue P.O. Box 358 Sunnyvale, Ca. 94088

COPIES

RECIPIENT

1

Florida Research and Development
Pratt and Whitney Aircraft
United Aircraft Corporation
P.O. Box 2691
West Palm Beach, Fl. 33402

1

Vickers, Incorporated
Box 302
Troy, Mi. 48084